

Updates to the Saltstone Disposal Facility Stochastic Fate and Transport Model

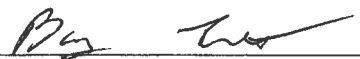
June 2013

Prepared by: Savannah River Remediation LLC
Closure and Waste Disposal Authority
Aiken, SC 29808



APPROVALS

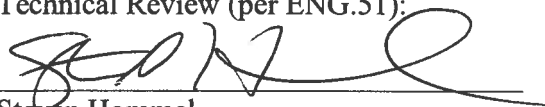
Author:



Barry Lester
Savannah River Remediation LLC
Closure & Waste Disposal Authority

6/6/2013
Date

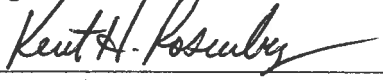
Technical Review (per ENG.51):



Steven Hommel
Savannah River Remediation LLC
Closure & Waste Disposal Authority

6/6/2013
Date

Management Review:



Kent Rosenberger
Savannah River Remediation LLC
Closure & Waste Disposal Authority

6/6/2013
Date

TABLE OF CONTENTS

APPROVALS	2
TABLE OF CONTENTS.....	3
LIST OF FIGURES	5
LIST OF TABLES	8
ACRONYMS	9
1.0 EXECUTIVE SUMMARY	10
2.0 PURPOSE	12
2.1 <i>Advective-Dispersive Transport Simulation</i>	14
2.2 <i>Dose Calculator Model</i>	15
3.0 SDF GOLDSIM MODEL UPDATES	16
3.1 <i>Special Analysis Specific Updates</i>	16
3.1.1 Linear Sorption Coefficients and Tc-99 Solubility Limits	16
3.1.2 Floor Joints.....	22
3.1.3 Wall-to-Floor Joints	22
3.1.4 Segmented Columns	22
3.2 <i>Improvements to Computational Efficiency</i>	22
3.3 <i>Sampling of Data from External Files</i>	24
3.3.1 Methodology	24
3.3.2 Data	25
3.3.3 IHI Scenario	29
3.3.4 Floor Discretization	31
4.0 STRUCTURE OF THE SDF GOLDSIM MODEL	32
4.1 <i>Model Organization</i>	32
4.1.1 Radionuclide Transport Modeling	34
4.2 <i>New Model Capabilities</i>	54
4.2.1 Importing PORFLOW Files.....	54
4.2.2 Evaluating FDCs by Group.....	61
5.0 MODEL BENCHMARKING.....	65
5.1 <i>Benchmarking Results</i>	65
5.1.1 Mass Releases to the Saturated Zone.....	66
5.1.2 Radionuclide Concentrations at the 100-Meter Boundary.....	77
5.1.3 MOP Dose Time Histories.....	84
5.1.4 IHI Well Dose Time Histories	92

5.2	<i>Benchmarking Conclusion</i>	96
6.0	REFERENCES	98

LIST OF FIGURES

Figure 2.0-1: Sectors Along the 100-Meter Boundary	13
Figure 3.3-1: Tc-99 Total Release from SDU 4 for the Twelve Flow Cases to Be Analyzed (Technetium Solubility Value of 1.0E-08 mol/L for Saltstone and SDU 4 Concrete)	28
Figure 3.3-2: Tc-99 Total Release from SDU 2 for the Twelve Flow Cases to Be Analyzed (Technetium Solubility Value of 1.0E-08 mol/L for Saltstone and SDU 4 Concrete)	28
Figure 3.3-3: IHI Well Locations.....	30
Figure 4.1-1: SDF GoldSim Model Organization.....	34
Figure 4.1-2: Contents of Container <i>DisposalUnits</i>	35
Figure 4.1-3: Contents of Container <i>FDCs</i>	36
Figure 4.1-4: Contents of Container <i>OuterLoop</i>	37
Figure 4.1-5: Contents of Container <i>InnerLoop</i>	37
Figure 4.1-6: External Element Controlling <i>TSProc1.dll</i>	38
Figure 4.1-7: Contents of <i>FDC_TransportSubmodel</i>	39
Figure 4.1-8: Typical GoldSim Time Series Element Used in <i>FDC_Transport_Results</i>	40
Figure 4.1-9: <i>FDC_TransportSubmodel</i> Submodel-Interface	41
Figure 4.1-10: Contents of the <i>Vault_4</i> Container.....	42
Figure 4.1-11: Contents of the <i>FDCs</i> Container.....	42
Figure 4.1-12: Contents of the <i>VaultCells</i> Container for FDCs.....	46
Figure 4.1-13: Contents of the <i>VaultCells</i> Container for FDCs.....	47
Figure 4.1-14: Contents of the <i>Grout</i> Container for FDCs.....	47
Figure 4.1-15: Contents of the <i>InnerZone</i> Container for FDCs.....	48
Figure 4.1-16: Contents of the <i>OuterZone</i> Container for FDCs	48
Figure 4.1-17: Contents of the <i>FastZone</i> Container for FDCs	49
Figure 4.1-18: Contents of the <i>SheetDrain</i> Container for FDCs	49
Figure 4.1-19: Contents of the <i>Wall</i> Container for FDCs.....	50
Figure 4.1-20: Contents of the <i>HDPE</i> Container for FDCs.....	50
Figure 4.1-21: Contents of the <i>Fill</i> Container for FDCs.....	51
Figure 4.1-22: Contents of the <i>VaultFloor1</i> Container for FDCs.....	51
Figure 4.1-23: Contents of the <i>FastZone</i> Container for FDCs	52
Figure 4.1-24: Contents of the <i>Joint</i> Container for FDCs	52
Figure 4.1-25: Contents of the <i>UnsatZone</i> Container for FDCs.....	53

Figure 4.1-26: Contents of the <i>WasteFootprint</i> Container for FDCs	53
Figure 4.1-27: Contents of the <i>NearWell</i> Container for FDCs	54
Figure 4.2-1: GoldSim External Element Used for Reading in Flow Data	56
Figure 4.2-2: <i>ReadPORFLOWData.dll</i> Control File <i>ReadPFData4.in</i>	57
Figure 4.2-3: Contents of the GoldSim Container <i>DLLData</i>	57
Figure 4.2-4: GoldSim External Element Used for Reading in Flow Data	57
Figure 4.2-5: GoldSim Time-Series Elements Used for capturing Darcy Velocities.....	58
Figure 4.2-6: GoldSim Expression Elements Used to Capture Transition Times	59
Figure 4.2-7: GoldSim Scalar and Vector Data Feeds.....	60
Figure 4.2-8: FDC Grouping Structure Module	62
Figure 4.2-9: Contents of Looping Container <i>SetGroupsInventory</i>	63
Figure 4.2-10: User Input Controls for FDC Grouping	63
Figure 4.2-11: SDF Anticipated FDC Layout (from SRR-CWDA-2009-00017, Rev. 0).....	64
Figure 4.2-12: SDF Anticipated FDC Layout (present)	64
Figure 5.1-1: SDU 1 I-129 Release to the Saturated Zone	67
Figure 5.1-2: SDU 1 Ra-226 Release to the Saturated Zone	68
Figure 5.1-3: SDU 1 Np-237 Release to the Saturated Zone.....	68
Figure 5.1-4: Semi-Log Plot of SDU 1 Np-237 Release to the Saturated Zone.....	69
Figure 5.1-5: SDU 4 I-129 Release to the Saturated Zone	71
Figure 5.1-6: SDU 4 Cs-135 Release to the Saturated Zone	71
Figure 5.1-7: SDU 4 Ra-226 Release to the Saturated Zone	72
Figure 5.1-8: Semi-Log Plot of SDU 4 Ra-226 Release to the Saturated Zone	73
Figure 5.1-9: SDU 4 Np-237 Release to the Saturated Zone.....	73
Figure 5.1-10: Semi-Log Plot of SDU 4 Np-237 Release to the Saturated Zone.....	74
Figure 5.1-11: FDC I-129 Release to the Saturated Zone	75
Figure 5.1-12: FDC Cs-135 Release to the Saturated Zone.....	76
Figure 5.1-13: FDC Ra-226 Release to the Saturated Zone	76
Figure 5.1-14: FDC Np-237 Release to the Saturated Zone.....	77
Figure 5.1-15: Maximum Radionuclide Concentrations at 100-Meter Boundary for Sector B ..	79
Figure 5.1-16: Semi-Log Plot of the SDU 4 Cs-135 Release to the Saturated Zone.....	80
Figure 5.1-17: Maximum Radionuclide Concentrations at 100-Meter Boundary for Sector G ..	81
Figure 5.1-18: Semi-Log Plot of an SDU 2 Ra-226 Release to the Saturated Zone.....	82

Figure 5.1-19: Maximum Radionuclide Concentrations at 100-Meter Boundary for Sector H..	83
Figure 5.1-20: Maximum Radionuclide Concentrations at 100-Meter Boundary for Sector I....	84
Figure 5.1-21: GoldSim Total Maximum MOP Dose Evaluation Case Results by Sector over 20,000 years	86
Figure 5.1-22: PORFLOW Total Maximum MOP Dose Evaluation Case Results by Sector over 20,000 years	86
Figure 5.1-23: Comparison of Maximum MOP Dose Evaluation Case Results over 20,000 years	87
Figure 5.1-23: Individual Radionuclide Contributions to the GoldSim Sector B 100-meter Peak Groundwater Pathway Dose Results at 20,000 Years	88
Figure 5.1-24 Individual Radionuclide Contributions to the PORFLOW Sector B 100-meter Peak Groundwater Pathway Dose Results at 20,000 Years	88
Figure 5.1-25: Individual Radionuclide Contributions to the GoldSim Sector G 100-meter Peak Groundwater Pathway Dose Results at 20,000 Years	89
Figure 5.1-26 Individual Radionuclide Contributions to the PORFLOW Sector G 100-meter Peak Groundwater Pathway Dose Results at 20,000 Years	90
Figure 5.1-27: Individual Radionuclide Contributions to the GoldSim Sector H 100-meter Peak Groundwater Pathway Dose Results at 20,000 Years	91
Figure 5.1-28 Individual Radionuclide Contributions to the PORFLOW Sector H 100-meter Peak Groundwater Pathway Dose Results at 20,000 Years	91
Figure 5.1-29: GoldSim Model IHI Well Dose Time Histories	93
Figure 5.1-30: PORFLOW Model IHI Well Dose Time Histories.....	93
Figure 5.1-31: GoldSim Model IHI Well Dose Time Histories for the Northern Wells	94
Figure 5.1-32: PORFLOW Model IHI Well Dose Time Histories for the Northern Wells	94
Figure 5.1-33: GoldSim Model IHI Well Dose Time Histories for the Southern Wells	95
Figure 5.1-34: PORFLOW Model IHI Well Dose Time Histories for the Southern Wells	95
Figure 5.1-35: GoldSim and PORFLOW Model Maximum IHI Well Dose Time Histories.....	96

LIST OF TABLES

Table 3.1-1: Distribution Coefficients (K_d Values) for Elements in Soils	18
Table 3.1-2: Distribution Coefficients (K_d Values) for Elements in Cementitious Material.....	20
Table 3.2-1: FDC Groups	23
Table 3.3-1: Data Extracted from the PORFLOW Data Files	25
Table 3.3-2: Summary of Flow Cases.....	26
Table 3.3-3: Summary of Evaluation Flow Cases	27
Table 4.2-1: Instruction Data Passed to <i>ReadPORFLOWData.dll</i>	55
Table 5.1-1: SDF GoldSim and PORFLOW Model Peak Unsaturated Zone Release Comparisons for SDU 1	67
Table 5.1-2: SDF GoldSim and PORFLOW Model Peak Unsaturated Zone Release Comparisons for SDU 4.....	70
Table 5.1-3: SDF GoldSim and PORFLOW Model Peak Unsaturated Zone Release Comparisons for FDCs	75

ACRONYMS

CZ	Contamination Zone
DLL	Dynamic Link Library
FDC	Future Disposal Cell
GTG	GoldSim Technology Group LLC
HDPE	High-Density Polyethylene
IHI	Inadvertent Human Intruder
LHS	Latin Hypercube Sampling
MCL	Maximum Contaminant Level
MOP	Member of Public
NRC	U.S. Nuclear Regulatory Commission
PA	Performance Assessment
SA	Special Analysis
SDF	Saltstone Disposal Facility
SDU	Saltstone Disposal Unit
SRS	Savannah River Site
UZ	Unsaturated Zone

1.0 EXECUTIVE SUMMARY

This report documents the revision (Version 4.101) of the Saltstone Disposal Facility (SDF) Stochastic Fate and Transport Model (referred to herein as the SDF GoldSim Model or the GoldSim model). The SDF GoldSim Model is an object-oriented, probabilistic model designed to evaluate parameter sensitivity and the influence of parameter uncertainty on the potential for migration, of radionuclides stored at the SDF, to the accessible environment. For each realization of a Monte Carlo or Latin Hypercube Sampling (LHS) of data, the model calculates radionuclide concentrations along a 100-meter boundary surrounding the Saltstone Disposal Units (SDUs). Based on these concentrations the model then calculates doses along the boundary for use in the Member of Public (MOP) dose analysis. In addition, the model calculates concentrations and associated doses at possible well locations at the down gradient edge of seven SDUs for use in the Inadvertent Human Intruder (IHI) analysis and doses from drill cuttings for the Acute Intruder analysis. The dose-calculation module within the SDF GoldSim Model can calculate doses from radionuclide concentrations generated by the SDF GoldSim Model or from concentrations generated by the SDF PORFLOW Model. Note that the IHI doses, generated from the SDF PORFLOW Model results are based on concentrations derived along a 1-meter boundary surrounding the SDUs in addition to the seven aforementioned locations. The radionuclide transport module of the SDF GoldSim Model is a one-dimensional (1-D) abstraction of the three-dimensional (3-D) SDF PORFLOW Model, allowing for a computationally efficient solution to the contaminant transport process, which is necessary for multi-realization runs.

This report describes the updates implemented within the SDF GoldSim Model Version 4.101, relative to Version 3.02, to support future special analyses and the rationale for the changes. The differences between the previous special analysis SDF GoldSim Model (i.e., Version 3.02) and the performance assessment (PA) SDF GoldSim Model are documented in SRR-CWDA-2011-000178. In general, the updates to the SDF GoldSim Model were added to allow the model to consider additional information regarding the degradation of cementitious material, the release of technetium from reducing cementitious materials, distribution coefficients (K_d values), flow through joints, and dose pathway exposure methodology. Changes were also made to improve the computational efficiency of the model, and to allow for a probabilistic evaluation of the influence of the flow fields on the results. In addition, the IHI scenario analysis was updated to allow for a more rigorous evaluation of exposure levels. The major differences between SDF GoldSim Model, Version 4.101 and SDF GoldSim Model, Version 3.02 include:

- The replacement of K_{ds} by the latest Savannah River Site (SRS) K_d data
- The use of leachate impacted K_{ds} in Version 4.101
- The implementation of solubility controls for Tc-99
- The inclusion of an explicit flow paths in the SDU 1 and SDU 4 models to represent floor joints which may act as fast flow paths through the floor
- The inclusion of an explicit flow path in the modeled future disposal cells (FDCs) to represent a wall-to-floor joint
- The inclusion of an explicit flow path in the SDU 4 and FDC models to represent segmented concrete columns that are subject to separate time-dependent deformation histories in each segment

- The updating of the model to allow for the importing (and sampling) of flow-field data and time-dependent diffusion coefficients from PORFLOW output files
- The updating of the model to allow for the importing (and sampling) of Tc-99 release data from PORFLOW output files
- The updating of the model to allow for user identified grouping of FDCs to reduce the number of individual FDCs that have to be simulated
- The addition of a set of seven wells to be used in the IHI analysis.
- The splitting of the floor into explicit floor, upper mud mat, and lower mud mat zones

Section 2 of this report defines the purpose of Version 4.101 of the SDF GoldSim Model. Section 3 of this report discusses the changes implemented in the radionuclide transport modules of Version 4.101, and Section 4 of this report discusses the general structure of Version 4.101 of the SDF GoldSim Model, and the structural changes associated with the enhanced capabilities.

The final section (Section 5.0) of this report documents the benchmark testing performed to show that this abstraction of the SDF GoldSim Model is a valid surrogate for the 3-D SDF PORFLOW Model. During the testing, results from the SDF GoldSim Model and the SDF PORFLOW Model were compared, showing that the abstraction can adequately approximate the trends and results produced by the SDF PORFLOW Model.

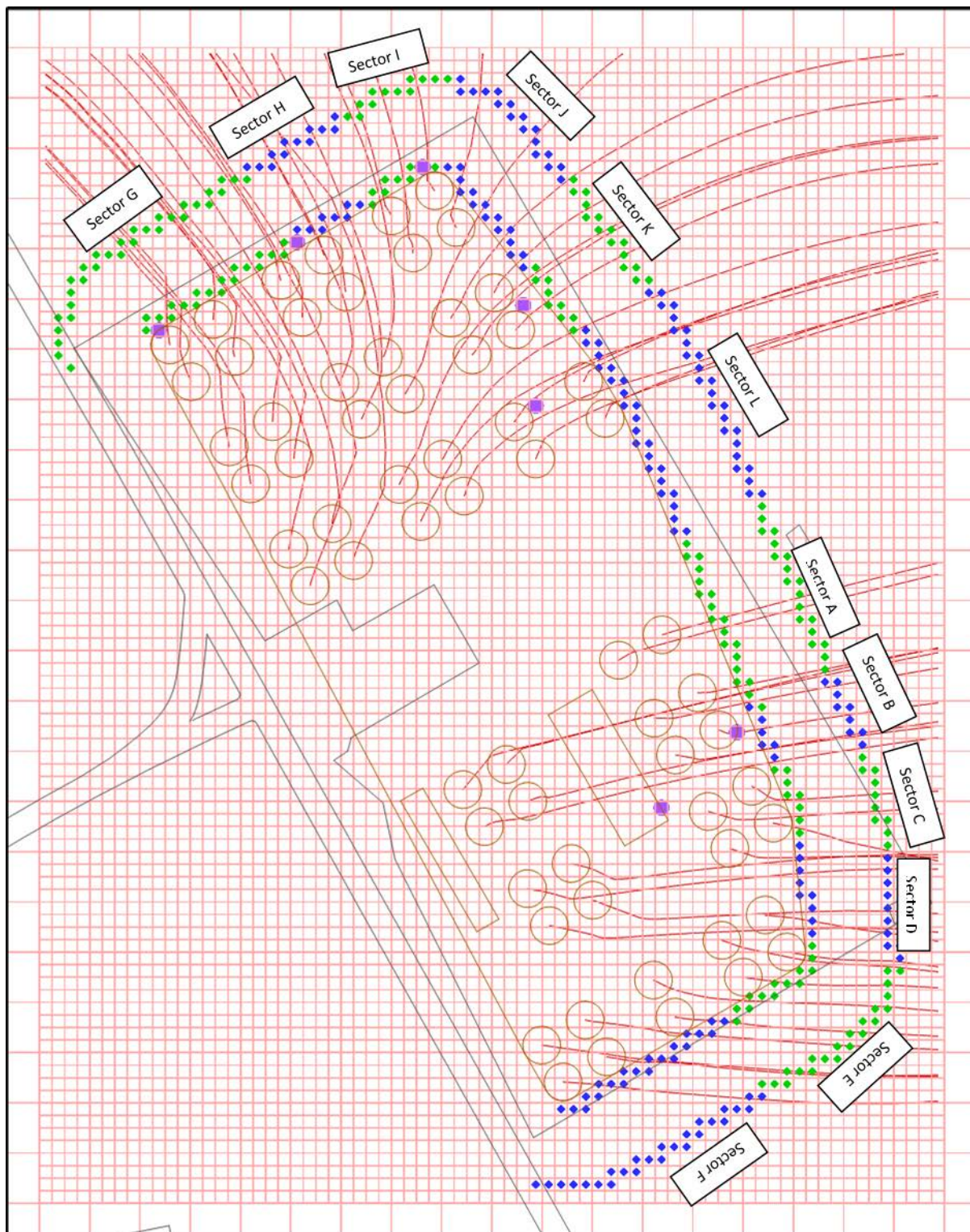
2.0 PURPOSE

The SDF GoldSim Model is an object-oriented, probabilistic model designed to evaluate parameter sensitivity and the influence of parameter uncertainty on the potential for migration of radionuclides in the SDF to the accessible environment. For the purpose of compliance, the accessible environment is defined by a 100-meter perimeter surrounding the Saltstone disposal units (represented by the outer ring of diamonds shown in Figure 2.0-1). The SDF GoldSim Model is comprised of two main modules; 1) an abstraction of the SDF PORFLOW model, and 2) a dose calculator. The abstraction is specifically designed to approximate the process of radionuclide transport from disposal units in a manner that would allow for uncertainty and sensitivity analyses to be performed in a time-efficient manner, while still allowing the influence of parameters on the transport processes to be examined. The model also includes a dose calculator, which can be used to evaluate dose at points of compliance based on the concentrations generated by the transport abstraction module or generated by the SDF PORFLOW model. This volume serves mainly as a documentation of the abstraction of the PORFLOW radionuclide transport model found in Version 4.101 of the SDF GoldSim Model, as provided in the SDF GoldSim Model file: *SRS Saltstone v4.101.gsm*. The dose module is documented elsewhere as noted in Section 2.2.

This version (Version 4.101) of the SDF GoldSim Model was specifically developed to be used in conjunction with the SDF PORFLOW Model in a Special Analysis to help respond to questions asked by the U.S. Nuclear Regulatory Commission (NRC). The updates allow the Model to consider additional information regarding the degradation of cementitious material, the release of technetium from reducing cementitious materials, distribution coefficients (K_d values), flow through joints, and dose pathway exposure methodology.

This version of the SDF GoldSim Model was developed using the GoldSim© software (B-SQP-C-00005).

Figure 2.0-1: Sectors Along the 100-Meter Boundary



2.1 Advective-Dispersive Transport Simulation

The SDF GoldSim Model solves the general equations for transport of dissolved radionuclides within the engineered barriers (the disposal units) and the natural barriers (the unsaturated zone and saturated zone). The SDF GoldSim Model takes advantage of the GoldSim mixing cell-network elements and the 1-D analytical solution-based pipe elements to evaluate the advective-dispersive transport of contaminants through the engineered and natural barriers (GTG-2010e).

The abstraction of the SDF PORFLOW Model included in the SDF GoldSim Model to simulate radionuclide transport in the SDUs and unsaturated zone beneath, is based on the simplifying assumption that vertical flow controls the radionuclide release from the SDUs and unsaturated zone (UZ) except relatively early in simulations when matrix diffusion as a release mechanism may be important. Molecular diffusion in the horizontal direction, is also modeled explicitly in the SDF GoldSim Model because diffusion into and through the walls to the backfill can be relatively important at early times when flow rates are low. The transport module of the SDF GoldSim Model simulates the transport of non-conservative species subject to sorption and either simple decay or ingrowth along decay chains. Other processes controlling the mass release from the disposal units include time-dependent physical and chemical degradation of saltstone and concrete zones (floors, columns, and walls and for the FDCs, the high-density polyethylene (HDPE) liners). The influence of mechanical dispersion is not explicitly considered in the disposal unit structure, backfill, or unsaturated zone although a certain degree of numerical dispersion is inherent in the use of mixing cells.

In the saturated zone, the abstraction of the SDF PORFLOW Model assumes that 1-D transport along streamlines emanating from center of each SDU dominates the transport of radionuclides released by the SDUs. As noted earlier, the 1-D transport along streamlines is modeled using the GoldSim pipe elements. The governing equation for 1-D advective-dispersive transport of a dissolved species in a unidirectional flow field, as solved for in the pipe elements, can be written as follows:

$$\frac{\partial(\phi RC)}{\partial t} = D \frac{\partial^2 C}{\partial l^2} - v \frac{\partial C}{\partial l} - \phi R \lambda C + \sum_{i=1}^{Np} \phi R \lambda_{pi} C_{pi} \quad (2-1)$$

where:

C	=	solute concentration (M/L ³)
R	=	retardation coefficient
ϕ	=	effective porosity
t	=	time (T)
D	=	dispersion coefficient = $v\alpha + \phi D_{eff}$ (L ² /T)
v	=	Darcy velocity (L/T)
α	=	dispersivity (L)
D_{eff}	=	effective diffusion coefficient (L ² /T)
λ	=	decay coefficient (T ⁻¹)

λ_{pi}	=	decay coefficient of the i^{th} parent (T^{-1})
Np	=	number of parent species
l	=	transport pathway coordinate (L)

Horizontal and vertical transverse dispersion may also be important contributors to plume attenuation and therefore also are explicitly modeled in the SDF GoldSim Model. The influence of transverse horizontal and vertical dispersion are included through the use of the GoldSim plume function (GTG-2010e), a built-in function based on Green's function solutions, that can be used to superimpose the influence of transverse (horizontal and vertical) dispersion on the results generated by the 1-D transport analysis. Equation 2-1 can be rewritten to include the effects of horizontal and vertical transverse dispersion as follows:

$$\frac{\partial(\phi RC)}{\partial t} = D_l \frac{\partial^2 C}{\partial s_l^2} + D_{th} \frac{\partial^2 C}{\partial s_{th}^2} + D_{tv} \frac{\partial^2 C}{\partial s_{tv}^2} - v_l \frac{\partial C}{\partial s_l} - \phi R \lambda C + \sum_{i=1}^{Np} \phi R \lambda_{pi} C_{pi} \quad (2-2)$$

where:

D_l	=	longitudinal dispersion coefficient = $v_l \alpha_l + \phi D_{\text{eff}} (L^2/T)$
D_{th}	=	horizontal transverse dispersion coefficient = $v_l \alpha_{th} + \phi D_{\text{eff}} (L^2/T)$
D_{tv}	=	vertical transverse dispersion coefficient = $v_{latv} + \phi D_{\text{eff}} (L^2/T)$
s_l	=	direction of the flow line
s_{th}	=	direction normal to the flow line and horizontal
s_{tv}	=	direction normal to the flow line and vertical

As in the SDU release model, the saturated zone transport module of the SDF GoldSim Model simulates the transport of non-conservative species subject to sorption and either simple decay or ingrowth along decay chains.

2.2 Dose Calculator Model

In addition to simulating radionuclide transport, the SDF GoldSim Model contains a dose calculator designed to calculate MOP or IHI exposure levels, at specified points of assessment based on 1) the results from the transport abstraction module, or 2) output from the SDF PORFLOW Model. The dose calculations are abstracted from conceptualizations of possible exposure pathways. The SDF GoldSim Model implements dose calculations according to the dose methodology described within SRR-CWDA-2013-00058, Rev0.

3.0 SDF GOLDSIM MODEL UPDATES

In response to the questions asked by the NRC, the SDF PORFLOW Model was updated to consider additional information regarding the degradation of cementitious material, the release of technetium from reducing cementitious materials, distribution coefficients (K_d values), flow through joints, and dose pathway exposure methodology. In a parallel effort, Version 3.02 of the SDF probabilistic GoldSim model was updated to allow for consideration of the influence of the additional information on parameter sensitivity and parameter uncertainty analyses. Additional updates to the GoldSim model were also made: (1) to improve the computational efficiency of the model, (2) to allow for a probabilistic evaluation of the influence of the flow fields on the results, and (3) to allow for a more rigorous evaluation of exposure levels for the IHI scenario.

This section describes the updates implemented within the SDF GoldSim Model Version 4.101, relative to Version 3.02, to support this and future special analyses. The major differences between SDF GoldSim Model Version 4.101 and the prior version, Version 3.02, include:

- The replacement of K_{ds} by the latest SRS K_d data
- The use of leachate impacted K_{ds} in Version 4.101
- The implementation of solubility controls for Tc-99
- The inclusion of an explicit flow paths in the SDU 1 and SDU 4 models to represent floor joints which may act as fast flow paths through the floor
- The inclusion of an explicit flow path in the FDC model to represent a wall-to-floor joint which may act as a fast pathway from under the wall to the backfill
- The inclusion of an explicit flow path in the SDU 4 and FDC models to represent segmented concrete columns that are subject to separate time-dependent deformation time-histories in each segment
- The updating of the model to allow for the importing (and sampling) of flow-field data and time-dependent diffusion coefficients from PORFLOW output files
- The updating of the model to allow for the importing (and sampling) of time-histories of Tc-99 releases to the saturated zone from PORFLOW output files
- The updating of the model to allow for user identified grouping of FDCs to reduce the number of individual FDCs that have to be simulated
- The addition of a set of seven wells to be used in the IHI analysis.
- The splitting of the floor into explicit floor, upper mud mat, and lower mud mat zones

3.1 Special Analysis Specific Updates

This section describes the updates to the GoldSim model that were made to evaluate the influence of additional information regarding the degradation of cementitious material, the release of technetium from reducing cementitious materials, distribution coefficients (K_d values), flow through joints, and dose pathway exposure methodology on the model.

3.1.1 Linear Sorption Coefficients and Tc-99 Solubility Limits

Three changes pertaining to the process of the linear sorption were implemented in Version 4.101 of the SDF GoldSim Model. First, the distribution coefficient (K_d) data in the model was updated to reflect the present SRS K_d database used in the SDF PORFLOW modeling

studies. These updated values for both soils and cementitious materials are presented in Tables 3.1-1 and 3.1-2, respectively.

The second change is concerned with the influence of leachate from the saltstone on the sorptive processes in the unsaturated zone. In the updated model, the leachate impacted soil K_d values presented in Tables 3.1-1, are utilized in the unsaturated zone until pH transition occurs. After transition, non-leachate-impacted values are used.

The third model update is the implementation of solubility controls for Tc-99 in the modeling approach. The release of Tc-99, from the saltstone grout and transport through the SDU concrete is presently modeled as a shrinking core where the release of Tc-99 in a reducing environment is controlled by solubility rather than by a K_d value. In the shrinking core model, oxygen is set to a specified concentration (1.06E-3 meq e-/g (SRNL-STI-2013-00280, Rev. 0) in all zones except for the grout (clean grout, saltstone, and sheet drain) and the Vault (floor, roof, wall, upper mud mat, and HDPE). In addition, the backfill and unsaturated zones are defined as oxygen sources with a constant concentration of 1.06E-3 meq e-/g. This causes the oxygen to be transported, by advection and diffusion, into the grout and vault. Within the grout and vault, the oxygen reacts with the slag in the grout and vault until the reducing capacity of the slag in the grout becomes negligible. When the slag reduction capacity in an element becomes negligible, the cementitious material transitions to oxidizing conditions and the Tc-99 transport is controlled by the K_d value. Under reducing conditions, the solubility value for technetium has been estimated to be 1.0E-08 moles/L for saltstone and for SDU concrete containing slag [SRNL-STI-2012-00769]. Because the evaluation of Tc-99 transport in a coupled (oxygen/slag/Tc-99) shrinking core model is computationally intensive, a set of Tc-99 releases to the saturated zone are derived outside the GoldSim model using the SDF PORFLOW Model.

In Version 4.101, of the SDF GoldSim Model, time histories for Tc-99 releases, are sampled from the results of a set of coupled PORFLOW oxygen/slag/Tc-99 simulations. For each realization, a time-history for Tc-99 release from each SDU type (SDU 1, SDU 4, and FDC) is randomly selected, and imported into the GoldSim model. Note that in the Saltstone PA SDU 1 and SDU 4 are referred to as Vault 1 and Vault 4, respectively. [SRR-CWDA-2009-00017] Since this terminology has been updated in the FY13 SA, Vault 1 and Vault 4 will be referred to as SDU 1 and SDU 4 in the text that follows. Additionally note that the model element names were not changed in the updating of the GoldSim model so reference to specific GoldSim model elements will still use Vault 1 and Vault 4. The sampling and importing processes are discussed below in Section 3.3.

Table 3.1-1: Distribution Coefficients (K_d Values) for Elements in Soils

Element	Clayey Soil (Backfill) (mL/g)				Sandy Soil (Vadose) (mL/g)			
	Without Leachate	Ref.	Leachate Impacted	Ref.	Without Leachate	Ref.	Leachate Impacted	Ref.
Ac	8,500	a	12,750	a	1,100	a	1,650	a
Ag	30	b	96	g	10	b	32	g
Al	1,300	a	1,950	a	1,300	a	1,950	a
Am	8,500	a	12,750	a	1,100	a	1,650	a
As	200	a	280	a	100	a	140	a
At	0.9	a	0.1	a	0.3	a	0	a
Ba	101	c	303	g	15	c	45	g
Bk	8,500	a	12,750	a	1,100	a	1,650	a
C	400	a	2,000	a	10	a	50	a
Cd	30	a	90	a	15	a	45	a
Ce	8,500	a	12,750	a	1,100	a	1,650	a
Cf	8,500	a	12,750	a	1,100	a	1,650	a
Cl	8	b	0.8	g	1	b	0.1	g
Cm	8,500	a	12,750	a	1,100	a	1,650	a
Co	100	a	320	a	40	a	128	a
Cr	400	b	560	g	1,000	b	1,400	g
Cs	50	a	50	a	10	a	10	a
Cu	70	a	224	a	50	a	160	a
Eu	8,500	a	12,750	a	1,100	a	1,650	a
Fe	400	a	600	a	200	a	300	a
Fr	50	a	50	a	10	a	10	a
Gd	8,500	a	12,750	a	1,100	a	1,650	a
H	0	a	0	a	0	a	0	a
Hg	1,000	a	3,200	a	800	a	2,560	a
I	0.9	a	0.1	a	0.3	a	0	a
K	25	a	25	a	5	a	5	a
Mn	200	a	280	a	15	a	21	a
N	0	a	0	a	0	a	0	a
Na	25	a	25	a	5	a	5	a
Nb	900	e	1260	g	160	e	224	g
Ni	30	a	96	a	7	a	22	a
Np	9	a	180	c	3	a	60	c
Pa	9	a	180	c	3	a	60	c
Pb	5,000	a	16,000	a	2,000	a	6,400	a
Pd	30	a	96	a	7	a	22	a
Pm	0	f	0	f	0	f	0	f
Po	5,000	a	10,000	a	2,000	a	4,000	a
Pr	0	f	0	f	0	f	0	f
Pt	30	a	96	a	7	a	22	a

Table 3.1-1: Distribution Coefficients (K_d Values) for Elements in Soils (cont.)

Element	Clayey Soil (Backfill) (mL/g)				Sandy Soil (Vadose) (mL/g)			
	Without Leachate	Ref.	Leachate Impacted	Ref.	Without Leachate	Ref.	Leachate Impacted	Ref.
Pu	5,950	a	11,900	a	650	d	1,300	g
Ra	185	c	555	c	25	c	75	c
Rb	50	a	50	a	10	a	10	a
Re	1.8	a	0.2	a	0.6	a	0.1	a
Rh	0	f	0	f	0	f	0	f
Rn	0	a	0	a	0	a	0	a
Ru	0	f	0	f	0	f	0	f
Sb	2,500	a	3,500	a	2,500	a	3,500	a
Se	1,000	a	1,400	a	1,000	a	1,400	a
Sm	8,500	a	12,750	a	1,100	a	1,650	a
Sn	5,000	a	15,000	a	2,000	a	6,000	a
Sr	17	c	51	c	5	c	15	c
Tc	1.8	a	0.2	a	0.6	a	0.1	a
Te	1,000	a	1,400	a	1,000	a	1,400	a
Th	2,000	a	4,000	a	900	a	1,800	a
U	400	b	1,200	a	300	b	900	b
V	0	f	0	f	0	f	0	f
Y	8,500	a	12,750	a	1,100	a	1,650	a
Zn	30	a	90	a	15	a	45	a
Zr	2,000	a	4,000	a	900	a	1,800	a

a. SRNL-STI-2009-00473

b. SRNL-STI-2010-00493

c. SRNL-STI-2011-00011

d. SRNL-STI-2011-00672

e. ML073510127

f. Assigned a value of zero

g. Multiplied the “cement leachate impact factor” from SRNL-STI-2009-00473 to the “without leachate” value

Table 3.1-2: Distribution Coefficients (K_d Values) for Elements in Cementitious Material

Element	Reduced Region II (mL/g)	Ref.	Oxidized Region II (mL/g)	Ref.	Oxidized Region III (mL/g)	Ref.
Ac	7,000	a	6,000	a	600	a
Ag	5,000	a	4,000	a	400	a
Al	7,000	a	6,000	a	600	a
Am	7,000	a	6,000	a	600	a
As	200	b	320	b	100	a
At	9	a	15	a	4	a
Ba	100	b	100	b	70	a
Bk	7,000	a	6,000	a	600	a
C	3,000	a	3,000	a	300	a
Cd	5,000	a	4,000	a	400	a
Ce	7,000	a	6,000	a	600	a
Cf	7,000	a	6,000	a	600	a
Cl	10	a	10	a	1	a
Cm	7,000	a	6,000	a	600	a
Co	5,000	a	4,000	a	400	a
Cr	1,000	a	10	a	1	a
Cs	20	a	20	a	10	a
Cu	5,000	a	4,000	a	400	a
Eu	7,000	a	6,000	a	600	a
F	10	a	10	a	1	a
Fe	7,000	a	6,000	a	600	a
Fr	20	a	20	a	10	a
Gd	7,000	a	6,000	a	600	a
H	0	a	0	a	0	a
Hg	5,000	a	300	a	100	a
I	9	a	15	a	4	a
K	20	a	20	a	10	a
Mn	100	a	100	a	10	a
N	10	a	10	a	1	a
Na	1	a	1	a	0.5	a
Nb	1,000	a	1,000	a	500	a
Ni	4,000	a	4,000	a	400	a
Np	10,000	a	10,000	a	5,000	a
Pa	10,000	a	10,000	a	5,000	a
Pb	5,000	a	300	a	100	a
Pd	5,000	a	4,000	a	400	a
Pm	0	d	0	d	0	d
Po	5,000	a	300	a	100	a

**Table 3.1-2: Distribution Coefficients (K_d Values) for Elements in Cementitious Material
(cont.)**

Element	Reduced Region II (mL/g)	Ref.	Oxidized Region II (mL/g)	Ref.	Oxidized Region III (mL/g)	Ref.
Pr	0	d	0	d	0	d
Pt	5,000	a	4,000	a	400	a
Pu	10,000	a	10,000	a	2,000	a
Ra	100	a	100	a	70	a
Rb	20	a	20	a	10	a
Re	5,000	a	0.8	a	0.5	a
Rh	0	d	0	d	0	d
Rn	0	a	0	a	0	a
Ru	0	d	0	d	0	d
Sb	1,000	a	1,000	a	100	a
Se	300	a	300	a	150	a
Sm	7,000	a	6,000	a	600	a
Sn	5,000	a	4,000	a	2,000	a
Sr	15	a	15	a	5	a
Tc	Note 1	-	0.8	a	0.5	a
Te	300	a	300	a	150	a
Th	5,000	a	10,000	a	2,000	a
U	2,500	a	1,000	c	100	c
V	0	d	0	d	0	d
Y	7,000	a	6,000	a	600	a
Zn	5,000	a	4,000	a	400	a
Zr	5,000	a	10,000	a	2,000	a

Note 1: In reducing cementitious materials technetium release is via solubility controls and for this
SA the K_d value of 0.5 is used in all oxidized regions

- a. SRNL-STI-2009-00473
- b. SRNL-STI-2010-00667
- c. SRNL-STI-2010-00493
- d. Assigned a value of zero

3.1.2 Floor Joints

In the SDF GoldSim Model, a single column of six mixing-cells linked in series now represents the floor joints, found in SDU 1 and SDU 4. The use of six mixing-cells is consistent with the vertical discretization used in the PORFLOW model. The vertical component of Darcy velocity used as the flow rate in the column of cells is the average of the vertical components of Darcy velocities for the all floor joints in the PORFLOW model. Mass Flux to the floor joint mixing-cell column, from each saltstone mixing-cell above the floor is based on flow across a cross-sectional area defined as the product of the cell-bottom area and a joint-area factor. The joint-area factor is the ratio of the total cross-sectional area of all joints in the PORFLOW model to the total cross-sectional area of all the floor and joints combined.

3.1.3 Wall-to-Floor Joints

In the SDF GoldSim Model, wall-to-floor joints found in the FDCs are now explicitly modeled. The horizontal wall-to-floor joint, which separates the wall from the floor, is approximated using a single row of six mixing cells linked in series. The choice of six mixing cells is consistent with the discretization used in the PORFLOW model. In the wall-to-floor joint mixing cells, horizontal flow is modeled to account for leakage into to the backfill surrounding the FDC in addition to vertical leakage from the joint into the floor. The horizontal component of Darcy velocity used as the flow rate in the row of cells is the arithmetic average of the horizontal components of Darcy velocities for all wall-to-floor joint elements in the PORFLOW model

3.1.4 Segmented Columns

For this special analysis, the PORFLOW model concrete column structure is divided from top to bottom into segments, and the model input was updated to reflect individual degradation time-histories within each segment of the column. The GoldSim model was also updated to consider the influence of the segmented column approach on radionuclide transport in SDU 4 and the FDCs. Because the cement columns in SDU 4 and the FDCs represent a potential fast-flow path, they were already included in Version 3.02 of the SDF GoldSim (and PORFLOW) model. The changes implemented in GoldSim model Version 4.101, allow the model to consider the effects of segment specific degradation patterns. These changes include: (1) the application of individual spatially averaged vertical flow rates for each segment of the column, and (2) the application of segment specific chemical transition times.

3.2 Improvements to Computational Efficiency

In order to reduce the computational time needed for stochastic simulations using the SDF GoldSim Model, the model was updated to allow for assembling FDCs into groups which can be evaluated by solving the transport equations for a representative FDC, only. In other words, for each group, radionuclide releases from a representative FDC and saturated zone transport from that FDC to the 100-meter boundary, would be evaluated. The resultant 100-meter boundary concentration from the representative FDC is then used in conjunction with the FDC specific plume functions for individual FDCs to generate concentrations for each FDC in a group to be used in dose calculations. When using the grouping option, the model automatically determines

an average saturated zone path-length for each group, an average saturated zone Darcy velocity along stream traces and an average inventory. The grouping process is also applied to the IHI analysis. The FDC groups to be used in the Special Analysis are listed in Table 3.2-1

Table 3.2-1: FDC Groups

FDC Name	FDC Number	Group Representative	FDC Name	FDC Number	Group Representative
V2A	1	1	V12C	33	31
V2B	2	1	V12D	34	31
V5A	3	3	V3A	35	35
V5B	4	3	V3B	36	35
V5C	5	3	V13A	37	37
V5D	6	3	V13B	38	37
V6A	7	7	V13C	39	37
V6B	8	7	V13D	40	37
V6C	9	7	V14A	41	41
V6D	10	7	V14B	42	41
V7A	11	11	V15A	43	43
V7B	12	11	V15B	44	43
V7C	13	11	V15C	45	43
V7D	14	11	V15D	46	43
V8A	15	15	V16A	47	47
V8B	16	15	V16B	48	47
V8C	17	15	V16C	49	47
V8D	18	15	V16D	50	47
V9A	19	19	V17A	51	51
V9B	20	19	V17B	52	51
V9C	21	19	V17C	53	51
V9D	22	19	V17D	54	51
V10A	23	23	V18A	55	55
V10B	24	23	V18B	56	55
V10C	25	23	V18C	57	55
V10D	26	23	V18D	58	55
V11A	27	27	V19A	59	59
V11B	28	27	V19B	60	59
V11C	29	27	V20A	61	59
V11D	30	27	V20B	62	59
V12A	31	31	V20C	63	59
V12B	32	31	V20D	64	59

3.3 Sampling of Data from External Files

Although the previous SDF GoldSim Model versions allowed for consideration of uncertainty in most parameters controlling the transport of radionuclides within the engineered barrier and UZ beneath it, the model did not explicitly account for changes in flow fields within the engineered barrier and UZ. To enhance the probabilistic capabilities of the GoldSim model, the model was updated to allow it to read in flow rates and other data from external files containing time series assembled in table form. For use with the SDF GoldSim Model, a set of flow fields and associated data for 36 possible flow scenarios (for each SDU type) was generated using the SDF PORFLOW Model. The SDF GoldSim Model randomly selects a flow scenario from the set of scenarios, then reads the data associated with the selection. The GoldSim model also reads a correlated scenario specific file containing time histories of time-dependent diffusion coefficients. The diffusion-coefficient time histories reflect the influence of degradation on the diffusion coefficient. In addition, a subset of the flow fields have had time histories of Tc-99 releases to the saturated zone generated for three different solubility limits, to be used for sensitivity or uncertainty analyses. The methodology implemented to read the data is discussed in Section 3.3.1 and the data used with this new implementation is discussed in Section 3.3.2.

3.3.1 Methodology

For this Special Analysis and future ones, the updated SDF GoldSim Model (Version 4.101) was restructured to allow flow rates and other associated data to be imported from external files as opposed to having the data reside in GoldSim data elements, where the data remains until it is updated and replaced. This change allows the model to sample from sets of data files that have been generated using PORFLOW (or another process model). The process of reading in the data is performed using a DLL containing a FORTRAN based function that accepts instructions from the SDF GoldSim Model, reads from an external file as per the instructions, and returns the data needed to the GoldSim model. The DLL, “*ReadPORFLOWData.dll*” (B-SQP-C-00003, Rev. 2), is integrated into the SDF GoldSim Model using GoldSim external elements. Instructions pertaining to the file to be read and the locations of the data needed within the file are passed to the DLL through the external element interface.

The data passed back from the DLL to the SDF GoldSim Model (as listed in Table 3.3-1) include time series of zone-based Darcy velocities, saturations, infiltration rates, time-dependent diffusion coefficients, and Tc-99 mass flux rates, as well as scalar values of pH-based transition times, E_h -based transition times.

Table 3.3-1: Data Extracted from the PORFLOW Data Files

Data	Form	Units
Darcy Velocities ¹	1-D Table	cm/yr
Saturations ¹	1-D Table	N/A
pH Transition Times ¹	Scalar	yr
Eh Transition Times ¹	Scalar	yr
Infiltration Rate ¹	1-D Table	cm/yr
Diffusion Coefficients ²	1-D Table	cm ² /s
Tc-99 Release Mass-Flux Rates ³	1-D Table	mol/yr

¹ from flow data file(s)

² from diffusion coefficient data file(s)

³ from radionuclide release rate data file(s)

3.3.2 Data

The 36 flow cases (for each SDU type) generated by the SDF PORFLOW Model to be used in the upcoming SA are based on flow parameters for an Evaluation Case (Case F1 as listed below in Table 3.3-2), with the following attributes varied:

- 3 infiltration cases (minimum, average, maximum)
- 2 degradation rates (nominal, expected)
- 2 joint moisture conductivity curve (gravel, relative permeability (K_{rel}) = 1))
- 3 initial grout hydraulic conductivity (6.4E-09 cm/s, 4.5E-07 cm/s, 3.9E-10 cm/s)

The parametric cases from which the flow fields were sampled, are listed in Table 3.3-2.

3.3.2.1 Selection of Flow Cases for Tc-99 Sensitivity and Uncertainty Analyses

A subset of 12 of the flow cases (as denoted by the superscript ¹ in Table 3.3-2) for each SDU type have been simulated using the SDF PORFLOW Model to generate Tc-99 releases to the saturated zone. These Tc-99 release time histories are then sampled during SDF GoldSim Model runs to provide Tc-99 input to the saturated zone transport model. Specifically, flow cases F1, F4, F5, F14, F15, F16, F17, F25, F26, F28, F29, and F30 were selected as cases to be sampled from.

The 12 flow fields were chosen as representative of the 36 flow cases, because they reflect major differences in the volumetric flow rates found in the 36 cases. Of the 36 flow cases, 18 were screened out from further analysis based on the MCCs of the joints. The preliminary SDF PORFLOW Model simulation results indicated that varying the MCCs of the joints provided a negligible impact with respect Tc-99 release. As such, the following flow cases were screened out: F7-F12, F19-F24, and F31-F36.

Of the 18 remaining flow cases:

- F2 was screened out as being very similar to F5;
- F3 was screened out as being very similar to F1;
- F6 and F18 were screened out as both being very similar to F30 during the first 15,000 years and similar to F4 after 15,000 years;
- F13 was screened out as being very similar to F15; and
- F27 was screened out as being very similar to F25.

Table 3.3-2: Summary of Flow Cases

Case	Infiltration Rate	Cementitious Degradation Rate	Initial Saltstone Saturated Hydraulic Conductivity (cm/sec)	Joint Material for MCC
F1 ¹	Average	Nominal	6.4E-09	Gravel
F2	Average	Nominal	4.5E-07	Gravel
F3	Average	Nominal	3.9E-10	Gravel
F4 ¹	Average	Expected	6.4E-09	Gravel
F5 ¹	Average	Expected	4.5E-07	Gravel
F6	Average	Expected	3.9E-10	Gravel
F7	Average	Nominal	6.4E-09	K _{rel} =1
F8	Average	Nominal	4.5E-07	K _{rel} =1
F9	Average	Nominal	3.9E-10	K _{rel} =1
F10	Average	Expected	6.4E-09	K _{rel} =1
F11	Average	Expected	4.5E-07	K _{rel} =1
F12	Average	Expected	3.9E-10	K _{rel} =1
F13	Maximum	Nominal	6.4E-09	Gravel
F14 ¹	Maximum	Nominal	4.5E-07	Gravel
F15 ¹	Maximum	Nominal	3.9E-10	Gravel
F16 ¹	Maximum	Expected	6.4E-09	Gravel
F17 ¹	Maximum	Expected	4.5E-07	Gravel
F18	Maximum	Expected	3.9E-10	Gravel
F19	Maximum	Nominal	6.4E-09	K _{rel} =1
F20	Maximum	Nominal	4.5E-07	K _{rel} =1
F21	Maximum	Nominal	3.9E-10	K _{rel} =1
F22	Maximum	Expected	6.4E-09	K _{rel} =1
F23	Maximum	Expected	4.5E-07	K _{rel} =1
F24	Maximum	Expected	3.9E-10	K _{rel} =1
F25 ¹	Minimum	Nominal	6.4E-09	Gravel
F26 ¹	Minimum	Nominal	4.5E-07	Gravel
F27	Minimum	Nominal	3.9E-10	Gravel
F28 ¹	Minimum	Expected	6.4E-09	Gravel
F29 ¹	Minimum	Expected	4.5E-07	Gravel
F30 ¹	Minimum	Expected	3.9E-10	Gravel
F31	Minimum	Nominal	6.4E-09	K _{rel} =1
F32	Minimum	Nominal	4.5E-07	K _{rel} =1
F33	Minimum	Nominal	3.9E-10	K _{rel} =1
F34	Minimum	Expected	6.4E-09	K _{rel} =1
F35	Minimum	Expected	4.5E-07	K _{rel} =1
F36	Minimum	Expected	3.9E-10	K _{rel} =1

¹ Used for solubility limit sampling

Adapted from SRNL-STI-2013-00280 Rev. 0, Table 4-1

This screening process left 12 flow cases to be used in conjunction with three solubility limits, to generate a set of Tc-99 releases to be used as input to the SDF GoldSim Model. Table 3.3-3 summarizes the 12 remaining flow cases to be used for subsequent evaluation. Figures 3.3-1 and 3.3-2 present the Tc-99 release from SDU 4 and SDU 2, respectively, for the twelve flow cases based on the conditions described in Table 3.3-3 and using the nominal saltstone technetium solubility value of 1.0E-8 mol/L in conjunction with the SDU concrete also having the same technetium solubility value as saltstone. The legend in each figure is ranked from high to low based on the Tc-99 total release at 10,000 years.

Table 3.3-3: Summary of Evaluation Flow Cases

Case	Infiltration Rate	Cementitious Degradation Rate	Initial Saltstone Saturated Hydraulic Conductivity (cm/sec)
F1	Average	Nominal	6.4E-09
F4	Average	BE ^a	6.4E-09
F5	Average	BE ^a	4.5E-07
F14	Maximum	Nominal	4.5E-07
F15	Maximum	Nominal	3.9E-10
F16	Maximum	BE ^a	6.4E-09
F17	Maximum	BE ^a	4.5E-07
F25	Minimum	Nominal	6.4E-09
F26	Minimum	Nominal	4.5E-07
F28	Minimum	BE ^a	6.4E-09
F29	Minimum	BE ^a	4.5E-07
F30	Minimum	BE ^a	3.9E-10

^a “BE” refers to best estimate values for cementitious material degradation

Figure 3.3-1: Tc-99 Total Release from SDU 4 for the Twelve Flow Cases to Be Analyzed (Technetium Solubility Value of 1.0E-08 mol/L for Saltstone and SDU 4 Concrete)

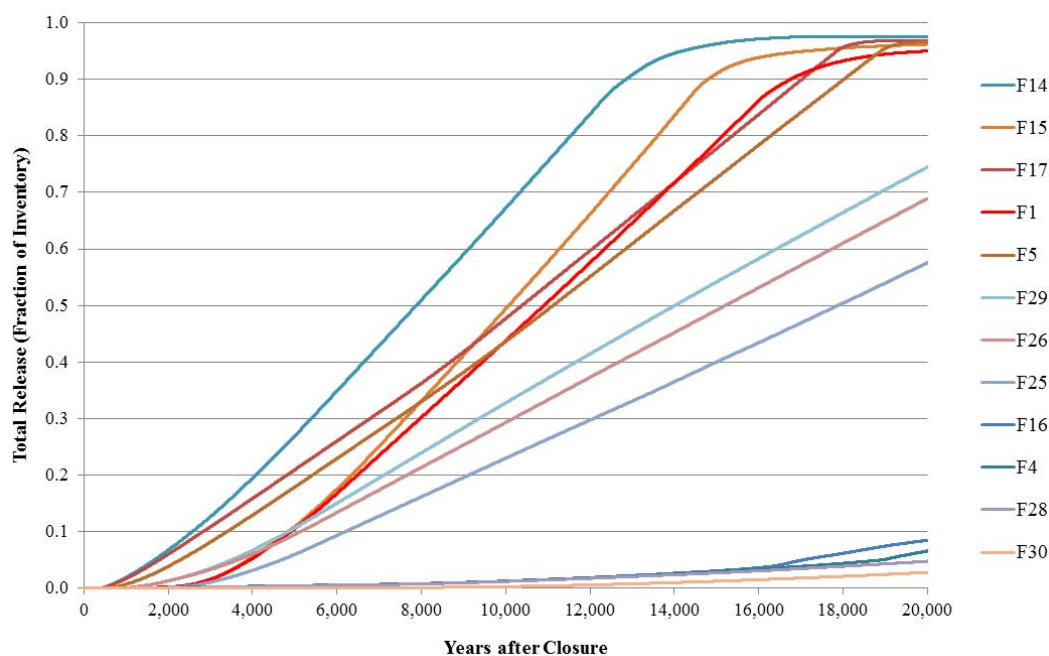
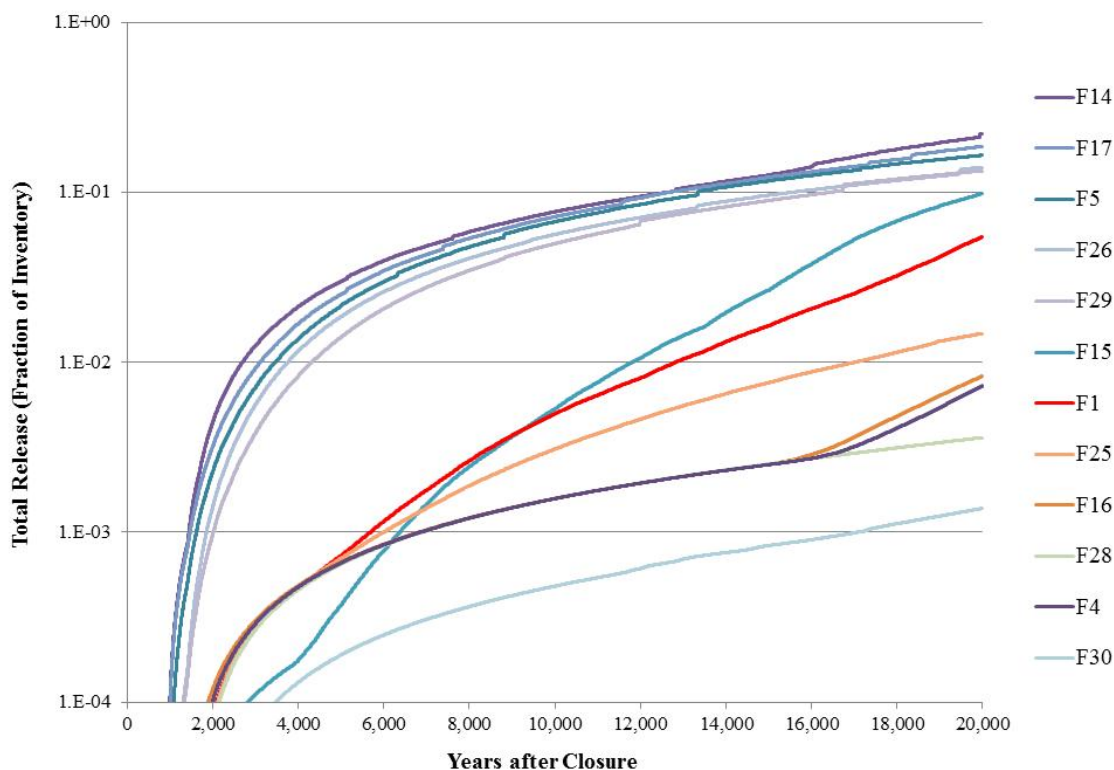


Figure 3.3-2: Tc-99 Total Release from SDU 2 for the Twelve Flow Cases to Be Analyzed (Technetium Solubility Value of 1.0E-08 mol/L for Saltstone and SDU 4 Concrete)



Note that the modeling results shown in the above figures indicate that the selection of the flow cases illustrates:

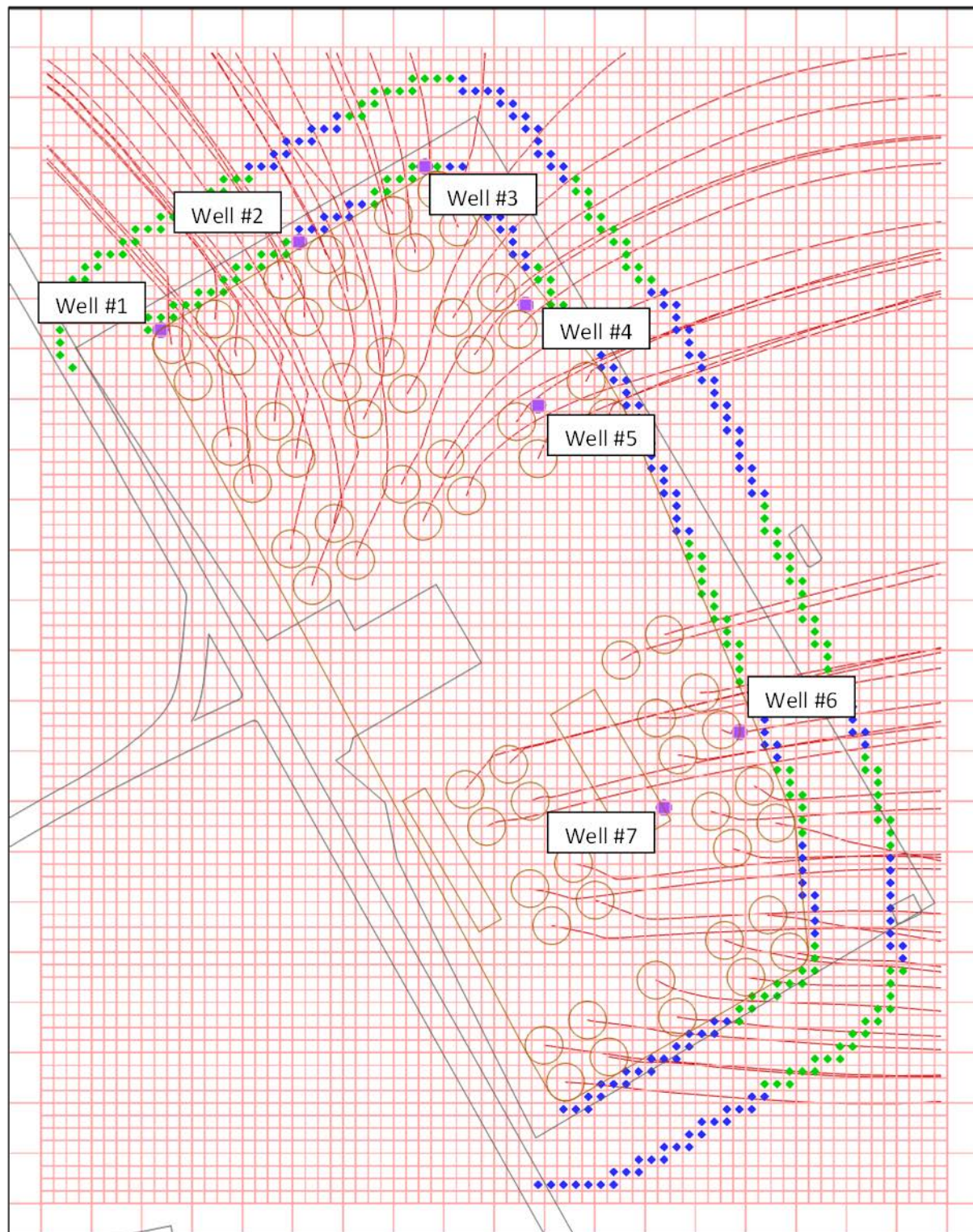
- (1) the probabilistic modeling results will demonstrate a wide range of potential future outcomes to provide greater insights into the sensitivities of specific modeling assumptions, and
- (2) the selection of these flow cases are expected to result in conservatively high doses which may not be indicative of a more likely or expected set of modeling assumptions (e.g., the deterministic flow settings of the Evaluation Case: F1).

For stochastic analyses, each of the 12 flow cases is given an equal weighting (1/12). In addition, each of these flow cases was used to generate Tc-99 release time breakthrough curves for the following values for the technetium solubility limits in saltstone: 1.0E-08 mol/L (the nominal value), 1.0E-09 mol/L (one-tenth of the nominal value) and 1.0E-07 mol/L (ten times the nominal value). All of the simulated cases assume that the SDU concrete is initially oxidized.

3.3.3 IHI Scenario

This section describes the updates to the GoldSim model that were made to improve the IHI exposure level analysis. For the IHI analysis, a set of seven wells was chosen to represent the possible location of a well, used by an inadvertent human intruder (see Figure 3.3-3). For each time step in a simulation, the maximum dose produced by any of the seven wells is used to generate a single curve, which represents the time history of the IHI exposure level. Saturated zone radionuclide transport from the SDUs to each of the seven wells is evaluated using the same methodology used to derive the MOP concentrations at the 100-meter boundary (see SRR-CWDA-2011-00178, Rev. 0, Section 3.2.3.2). For each SDU, a set of concentrations at each of the seven wells is derived using SDU release breakthrough curves as boundary conditions applied to GoldSim pipe elements. The outputs of the one-dimensional pipe-element solutions (analytical solutions) for concentrations at the well are then multiplied by Green's Function based GoldSim plume-function factors, which superimpose the effects of horizontal and vertical transverse dispersion. Prior to the dose calculations, the final concentrations at each well are assembled by superposition of the contributions to the well from each of the SDU releases. Note that for computational efficiency, SDU releases that are not expected to reach a well (see the streamlines in Figure 3.3-3 are set to zero concentrations and not evaluated.

Figure 3.3-3: IHI Well Locations



3.3.4 Floor Discretization

Prior versions of the SDF GoldSim Model lumped three of the layers between the saltstone and unsaturated zone into a single unit, the floor. Version 4.101, explicitly models the three layers (the floor, upper mud mat, and lower mud mat) as individual layers, subject to their own flow rates and chemical transition times. Note that the HDPE layer sandwiched between the upper and lower mud mats is not explicitly model, but is implicitly considered in the PORFLOW generated flow rates used in the GoldSim model. The floor/upper mud mat/lower mud mat system in Version 4.101 of the model is now represented by four parallel sets of 20 mixing cells linked in series. The top ten cells of each set represents the floor in each set, the next five, the upper mud mat and the bottom five, the lower mud mat. The four sets of mixing cells represent the floor system beneath the inner saltstone cylinder, the outer saltstone cylinder, the columns, and the wall (see SRR-CWDA-2011-00178, Rev. 0, Section 3.2.1). Note that the thin cylinder, approximating the influence of concrete columns, separates the inner and outer saltstone cylinders in the FDCs.

4.0 STRUCTURE OF THE SDF GOLDSIM MODEL

Section 4.1 presents a brief overview of updates to the basic structure of the SDF GoldSim Model implemented in Version 4.101. Section 4.2 describes the structural changes associated with the implementation of two new capabilities in in Version 4.101 of the model: (1) the reading in of data from SDF PORFLOW Model output files, and (2) the grouping of FDCs to increase the computational efficiency of the model.

4.1 Model Organization

The upper level of the SDF GoldSim Model is partitioned into two main segments, 1) abstraction of the SDF PORFLOW model, and 2) the dose calculation module. The solute transport module is comprised of a set five GoldSim containers storing the input data, one container containing the model calculation logic, and two containers containing transport model output. The container in which the radionuclide transport calculations occur is comprised of four main containers. Three containers contain the GoldSim elements controlling radionuclide-transport calculations (one each for SDU 1 and SDU 4, and one for the FDCs). The contents of the fourth container are used to calculate the transverse dispersion factors for the saturated zone transport module, which are superimposed on the one-dimensional transport model results generated in the SDU 1, SDU 4, and FDC containers to approximate three-dimensional results. The FDC container is comprised of nested looping containers, which serve the same purpose as nested do-loops and are used to loop through the radionuclide transport calculations for the 64 FDCs or a subset of them. Within the innermost of the looping containers is a GoldSim SubModel element, which serves as a complete “inner model” that is imbedded within the “main model.” For each FDC, the SubModel element is run using its own time stepping scheme. Once the SubModel has been run for each FDC or subset of FDCs, the “main model” will run through its set of time steps, calculating Vault1 and SDU 4 results along with the dose values at each time step.

Like all GoldSim models, the SDF GoldSim Model is organized hierarchically, with the top level of the model shown in Figure 4.1-1. Model containers, represented as yellow boxes, hold major model components. Brief descriptions of the upper-level containers and their contents are introduced here:

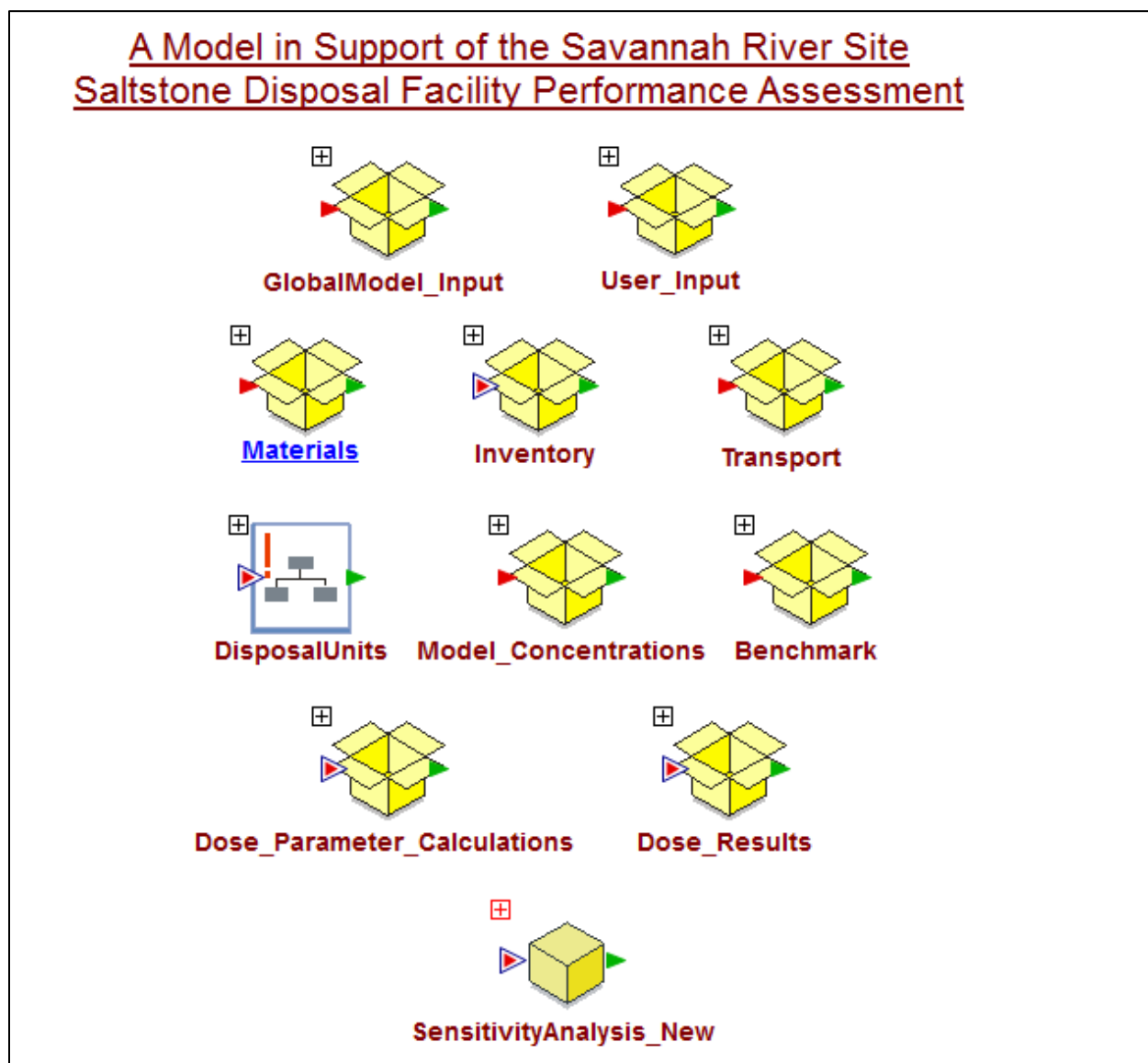
- *UserInput* contains global modeling parameters that control the setup and execution of the model. These parameters include switches that enable specific transport phenomena to be included or excluded, control the specific sources of contamination, and indicate whether or not a transport simulation is to be performed and used as the basis for dose or whether SDF PORFLOW Model results are used as the basis for dose.
- *GlobalModel_Input* container holds various modeling constants that are used throughout the model.
- *Transport* contains the data elements necessary define the geometry of the system being analyzed. In addition to specific data, the container is also comprised of stochastic elements that are used to describe the uncertainty in the geometrical aspects of the system where applicable.
- *Materials* contains the list of radionuclides simulated in the model and their basic properties (atomic weight, half-lives, etc.) and all parameters defining the porous media

that are used in the model (such as porosities and bulk densities). Other parameters defining the transport process in a porous media includes the linear soil/water partition coefficients (K_{ds}) for the various media. The basic definition of the fluid (water) element (including diffusion coefficients) is found in this container, but cloned fluid elements are found in various other containers where the diffusion coefficients are redefined for specific zones such as saltstone, walls, and floor materials. In addition, it should be noted that the FDC submodel contains its own basic fluid element and zone specific clones.

- The *Inventory* container is comprised of inventory data, including nominal values and stochastic elements that define uncertainty in the estimated values. In addition *Inventory* contains an alternative inventory option, in which tank-based inventories are used and the tank inventories are transferred to the FDCs. The transfer distribution pattern is based on random sampling of the FDC filling order.
- The *Transport* container is comprised of parameters that define the saturated-zone flow fields and geometry for both MOP and IHI calculations.
- The *DisposalUnit* Container includes three transport calculation containers, one for each SDU type, Vault1, SDU 4, and FDCs (Figure 4.1-2). The FDC container contains a looping environment that cycles through the 64 FDCs or a subset of the 64 FDCs (see Table 3.2-1) using a single GoldSim submodel (GTG-2010e). The submodel activates the FDC container for a single FDC, all FDCs, or a subset of representative FDCs. Radionuclide releases from each source and subsequent migration to the 100-meter boundary or IHI well are simulated to derive the concentrations used in dose calculations. *FDC_output* contains the time series elements used to capture results generated in the transport submodel and copied into the time series elements one source FDC at a time. The *PlumeCalc_Sectors* container contains the GoldSim Plume Function calculations (GTG-2010e), that generate a dilution/attenuation factor for transverse dispersion used to determine the contribution from each SDU to the concentration at each MOP sector (at the sector midpoint) or IHI observation well (see Figure 3.3-3). The dilution/attenuation factors reflect the influence of transverse horizontal and vertical dispersion on the concentrations generated by the 1-D saturated zone transport pipe-element calculations performed in *DisposalUnits*. *Tc99Input* contains the external elements used to read in Tc-99 mass flux breakthrough curves for SDU 1 and SDU 4 (similar elements for the FDCs are found in the FDC submodel). The *VaultData* container contains the SDU geometry data for each of the three vault types. The *PoreFlushes* container is comprised of data elements containing pore flush calculation data. Note that the pore-flush data is not presently being used in the model since the transition times are read from the SDF PORFLOW Model generated files.
- The *Model_Concentrations* container is comprised of the set of elements used to assemble the final concentrations used in the dose calculations.
- *Benchmark* is comprised of a set of time-series elements containing the PORFLOW concentration outputs used for PORFLOW/GoldSim concentrations comparisons. Time history results comparing result elements for comparing GoldSim and PORFLOW Sector Concentrations are included.

- *Dose_Parameter_Calculations* is comprised of elements used to calculate doses based on concentrations assembled in *Model_Concentrations*.
- *Dose_Results* contains the results from the dose calculations.
- *SensitivityAnalysis_New* contains the elements necessary to collect information for the sensitivity analysis, including final values of model endpoints (e.g., water concentrations or dose to a human receptor) and the values of each input stochastic used for each realization in a probabilistic analysis.

Figure 4.1-1: SDF GoldSim Model Organization



4.1.1 Radionuclide Transport Modeling

The *DisposalUnits* container is comprised of seven active containers (Figure 4.1-2). Containers *Vault_1*, *Vault_4*, and *FDCs* contain the GoldSim elements used to calculate

vadose zone releases of radionuclides and the 1-D advective-dispersive transport of radionuclides through the saturated zone.

Vault_1 and *Vault_4* contain the radionuclide-transport calculation logic for SDU 1 and SDU 4, respectively. The *FDCs* container is comprised of the equivalent logic for the 64 FDCs. *FDCs* contains a series of nested looping containers that are analogous to do-loops, allowing the model to evaluate the 64 FDCs or a subset of them. The outermost of the nested containers *FDCs*, contains the looping container *OuterLoop* (Figure 4.1-3) which is designed to loop through the 64 source types (or a subset of them), calling the transport submodel each time. The two data elements in the container define the number of FDCs (*NFDCa*) and when desired a specified FDC to simulate (*RunThisFDC*). A specified FDC is run by setting *FDC_Choice* (which controls *RunThisFDC*) in *User_Input* to the desired FDC Number (see Table 3.2-1). If *FDC_Choice* is set to zero, the submodel will loop 64 times. If a specific source is defined (e.g., 33 for FDC V12C, as listed in Table 3.2-1), only the requested source will be evaluated and results in the submodel can be saved. *FDCs* deactivates when the time stepping begins for the dose calculations or when PORFLOW data is used for the dose calculations.

Figure 4.1-2: Contents of Container *DisposalUnits*

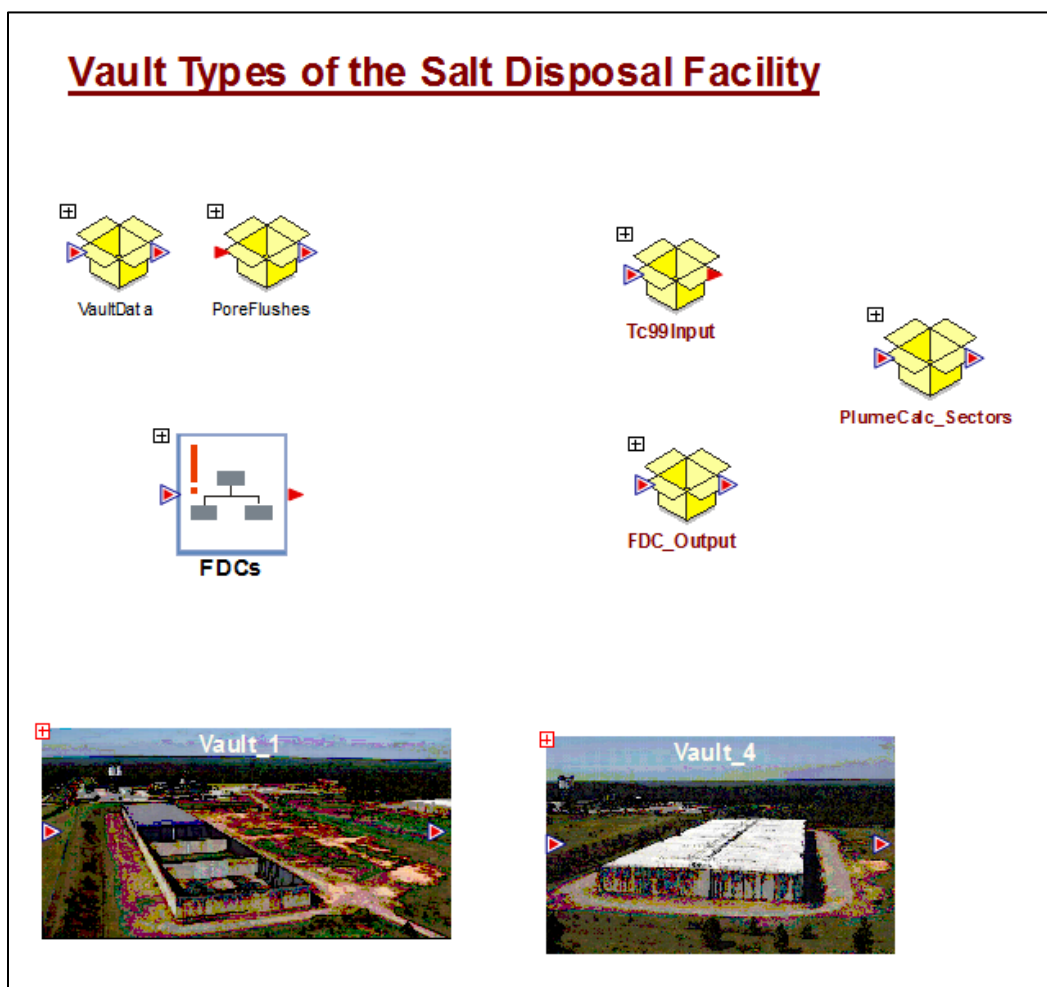
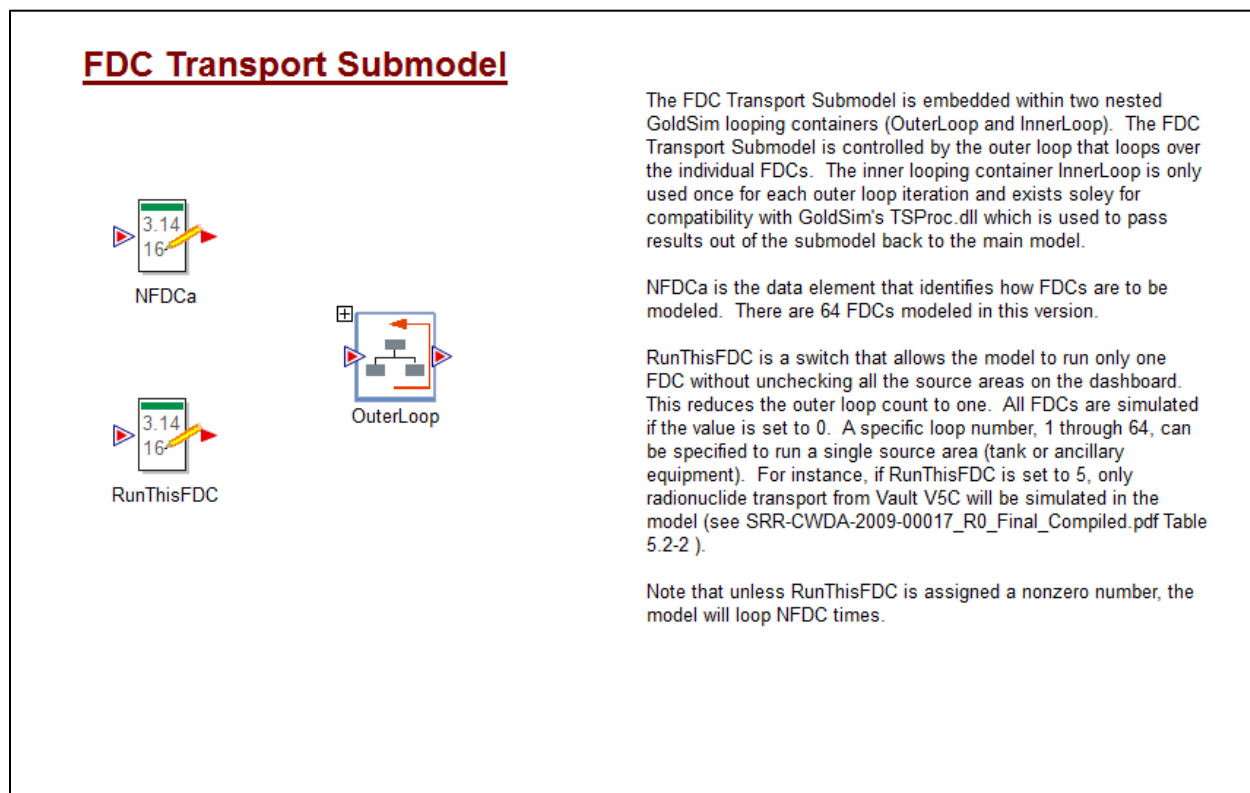


Figure 4.1-3: Contents of Container *FDCs*



Nested inside the looping container *OuterLoop*, is an inner looping container, *InnerLoop* (Figure 4.1-4). *InnerLoop* is used only once for each outer loop iteration (as indicated by the data element *NInnerLoop* and exists solely for compatibility with GoldSim's C++ software *TSProc.dll*, which is used to pass results out of the transport submodel back to the main model. *OuterLoop* also contains two selector elements which are used to control which source is being run and when the analysis is completed (Figure 4.1-4).

The transport submodel for evaluating the FDCs, *FDC_TransportSubmodel* is located within the innermost of the nested looping containers (Figure 4.1-5), and it is within this GoldSim submodel element that the mass transport calculations are performed. In addition to *FDC_TransportSubmodel*, *InnerLoop* contains a selector switch to indicate when the inner loop is finished.

TS_ProcFDCs (Figure 4.1-6), contains an external element (GTG-2010d), that controls the use of *TSProc1.dll*, which is a DLL used to copy time series, from the submodel into the main model. Note that *TSProc1.dll* is a renamed copy of *TSProc.dll*.

Figure 4.1-4: Contents of Container *OuterLoop*

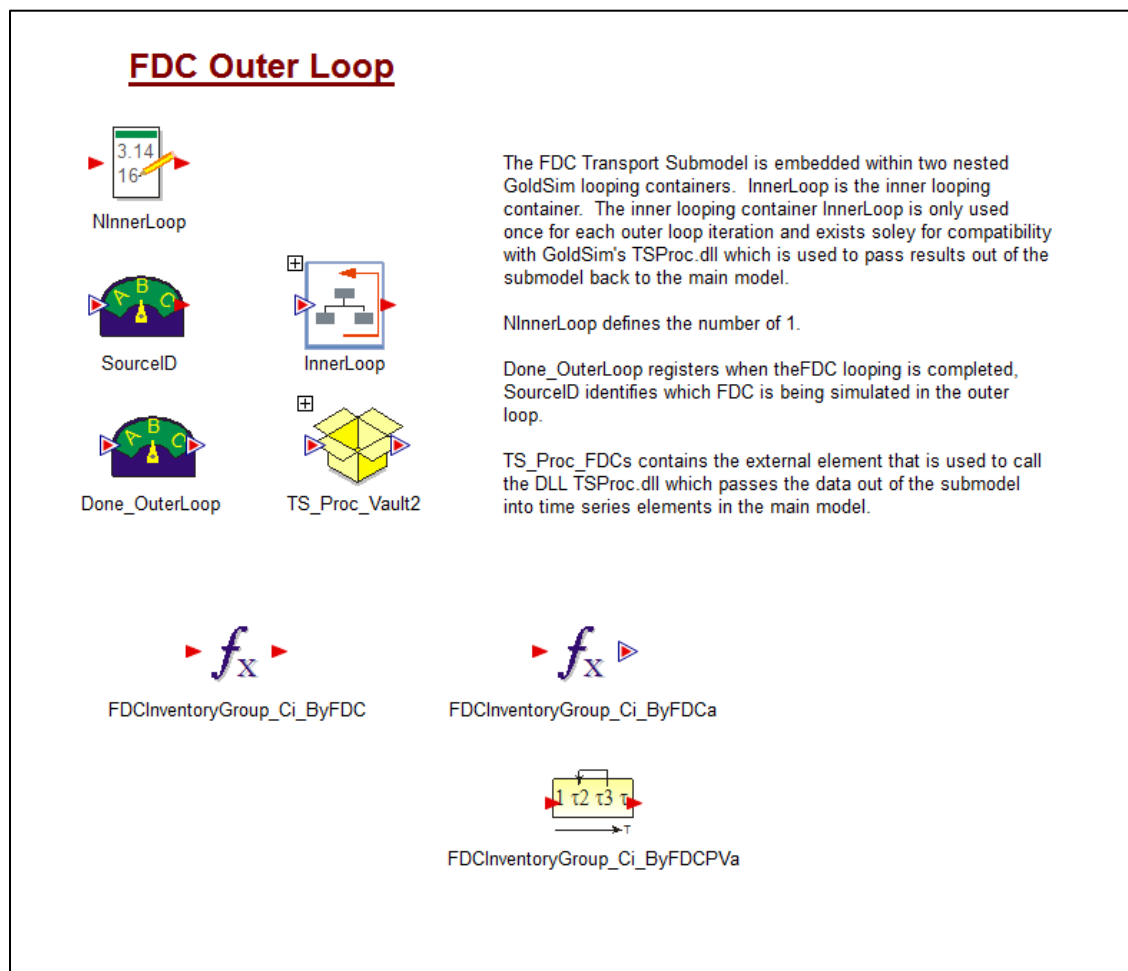


Figure 4.1-5: Contents of Container *InnerLoop*

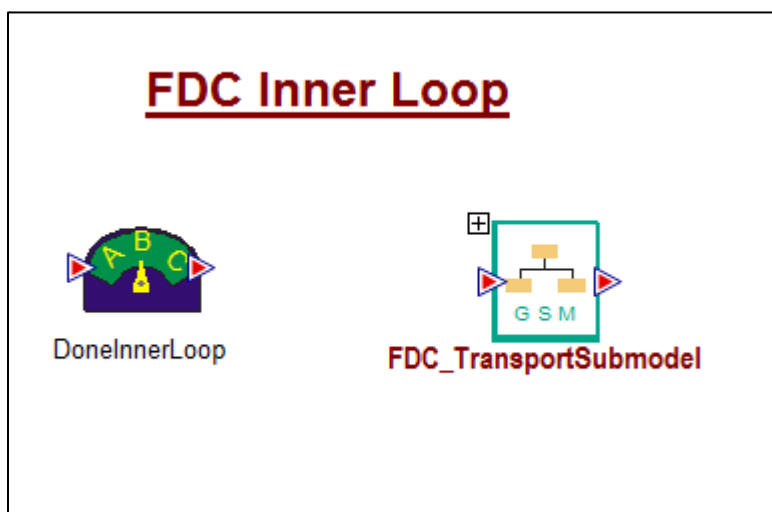
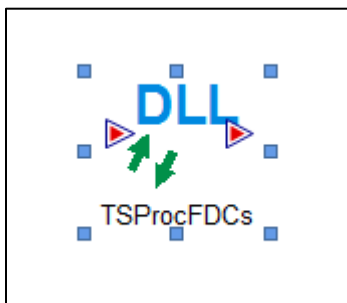


Figure 4.1-6: External Element Controlling *TSProc1.dll*



FDC_TransportSubmodel, is comprised of (see Figure 4.1-7) a disposal unit modeling component (*FDCs*). *FDCs* is a conditional container which is only activated when results for a specified FDC are desired. Several other upper level containers are also present in *FDC_TransportSubmodel* (Figure 4.1-7). These containers include *FDC_Transport_Results*, *Materials*, and *InputData*.

Due to limitations of conditional containers, time series elements cannot be used within the *FDCs* container (Figure 4.1-2). Therefore, the time series elements used to transfer data from the submodel to the main model, via *TSProc.dll*, are assembled in the container *FDC_Transport_Results* (see Figure 4.1-8).

Species elements and reference fluid elements must be defined separately in the main model and submodel. The species element and the base reference-fluid element for the submodel are located in the *Materials* container (Figure 4.1-7). Note that cloned versions of the fluid element found in *Materials* are located in containers where material-specific diffusion coefficients are assigned.

The other upper level container within *FDC_TransportSubmodel* is *InputData* (Figure 4.1-7) which serves as a transfer site for data passed from the main model to the submodel. The data from the main model is passed directly to the submodel through the submodel-interface in *FDC_TransportSubmodel* shown in Figure 4.1-9. Selector and expression elements located within *InputData* serve an organizational purpose as they capture the data from the interface and reset the variable name to the name from the main model for consistency.

It should be noted that data is also outputted from the submodel through the interface. The output data is then returned to the main model using the software *TSProc.dll* in conjunction with an external properties element (GTG-2010d).

Within the submodels *FDCs* container (as well as the *Vault_1* and *Vault_4* containers), are located the cell networks and pipe elements used evaluate the transport of radionuclides through the SDUs and saturated zone. Figure 4.1-10 depicts the organizational scheme within the container *Vault_4* and Figure 4.1-11 the organizational scheme within the container *FDCs*.

Figure 4.1-7: Contents of *FDC_TransportSubmodel*

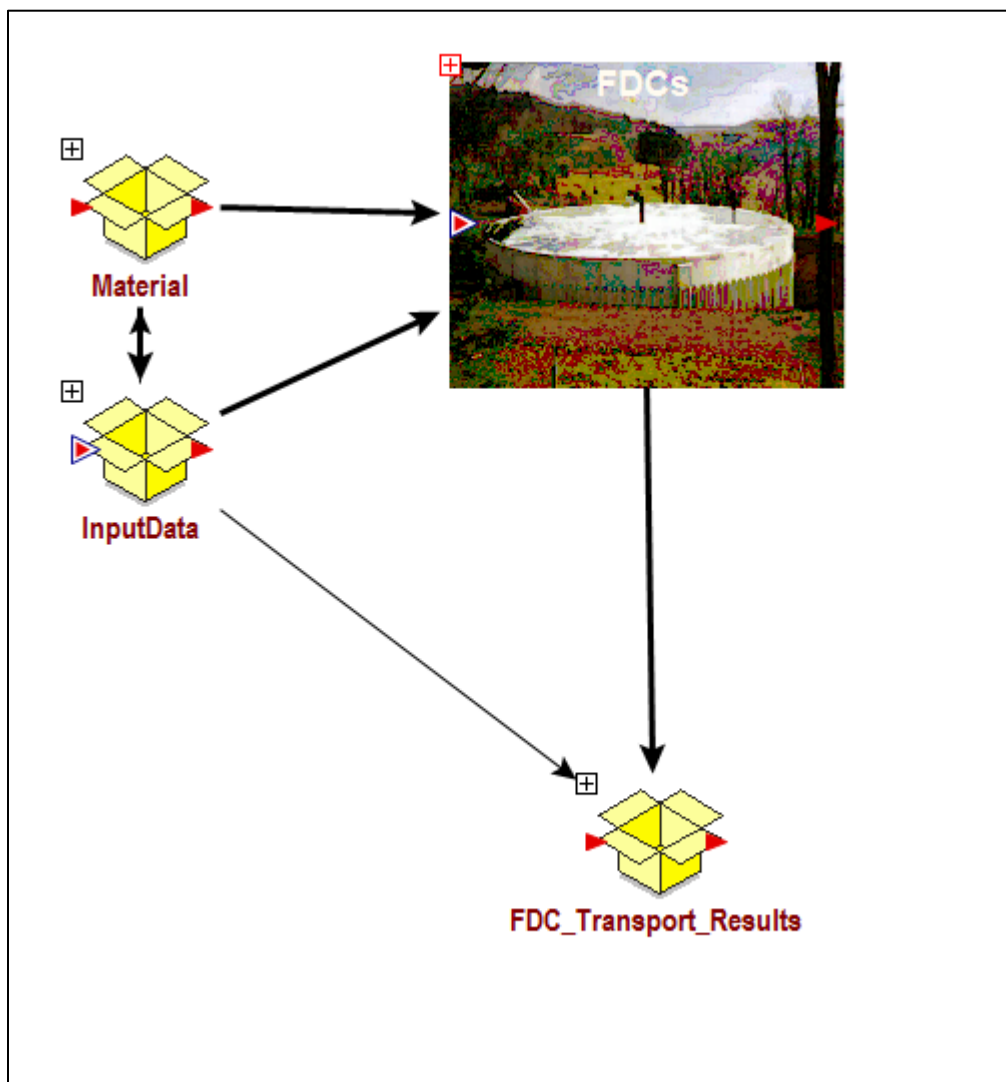


Figure 4.1-8: Typical GoldSim Time Series Element Used in *FDC_Transport_Results*

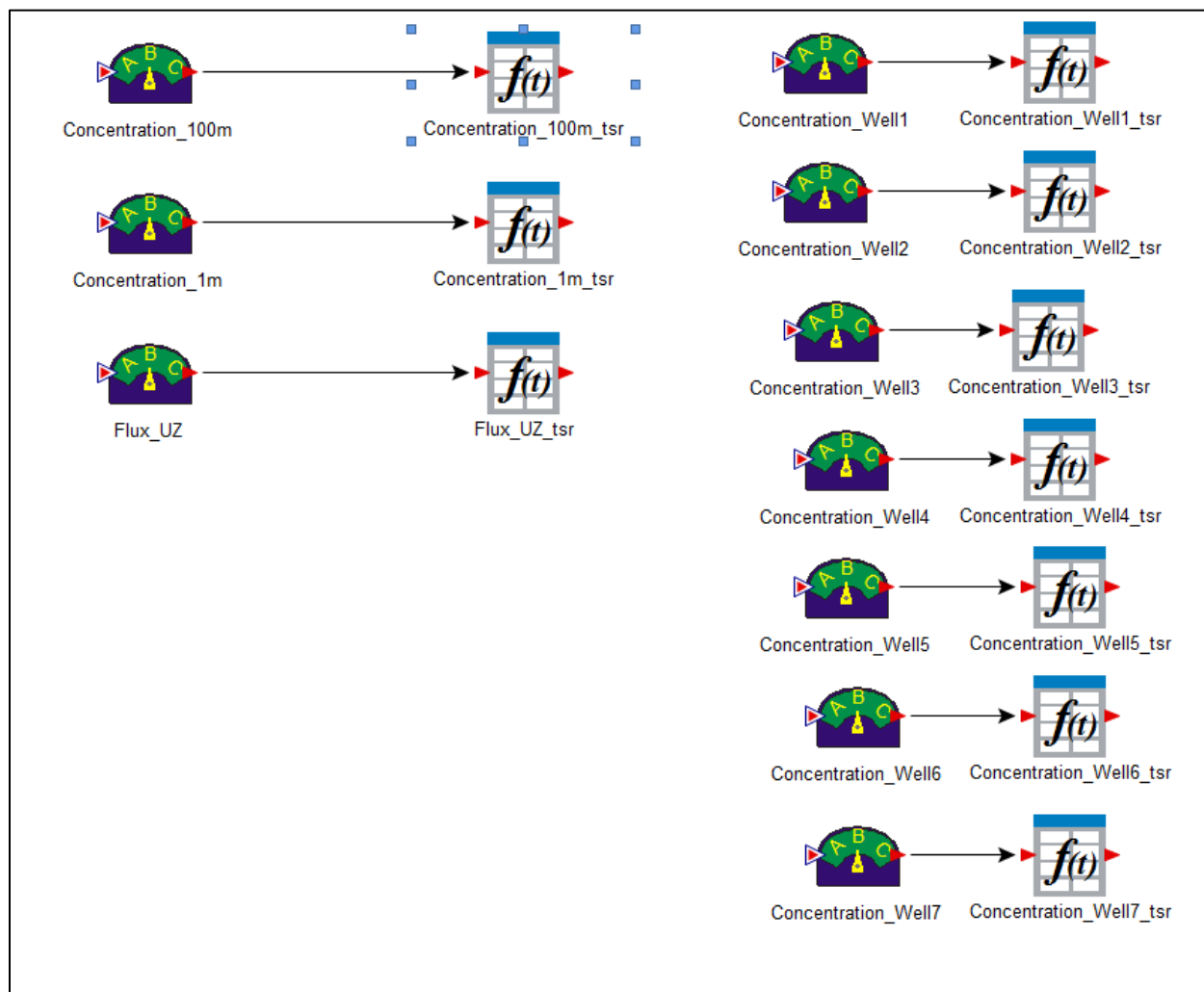


Figure 4.1-9: *FDC_TransportSubmodel* Submodel-Interface

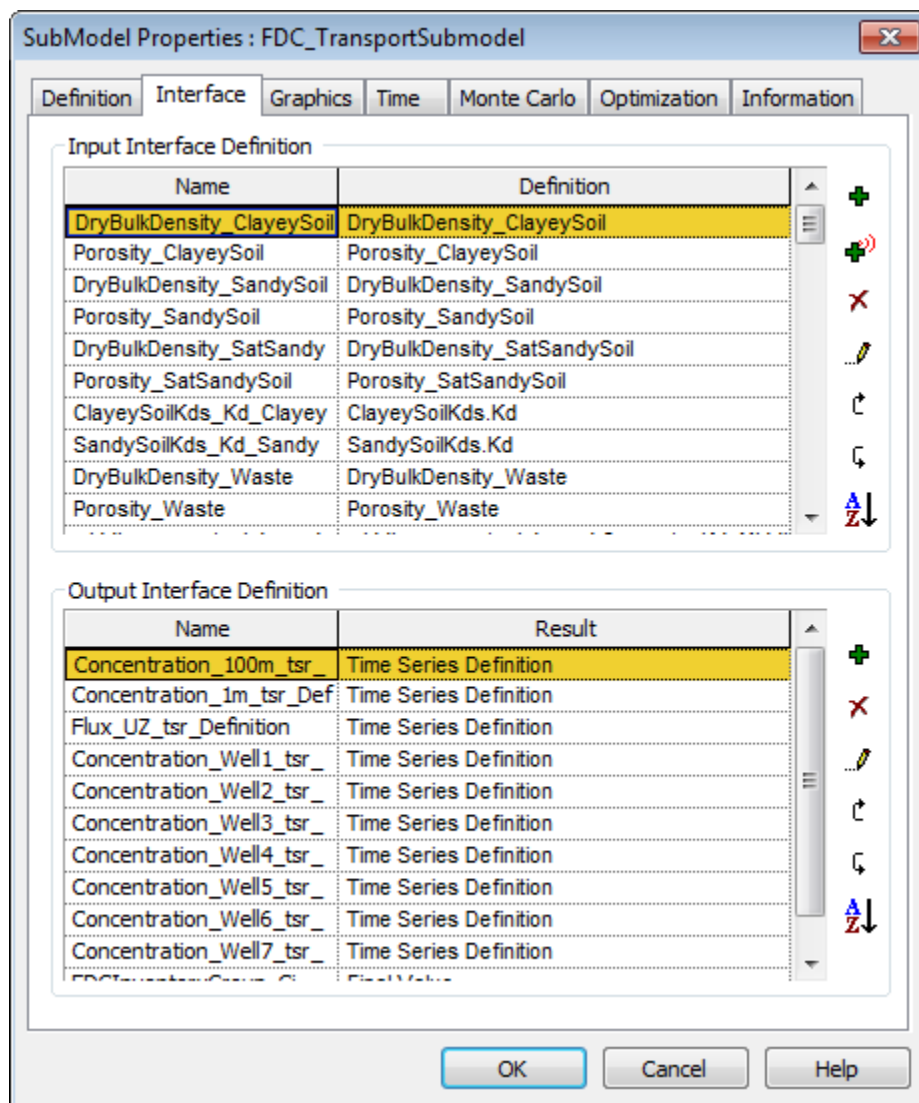


Figure 4.1-10: Contents of the *Vault_4* Container

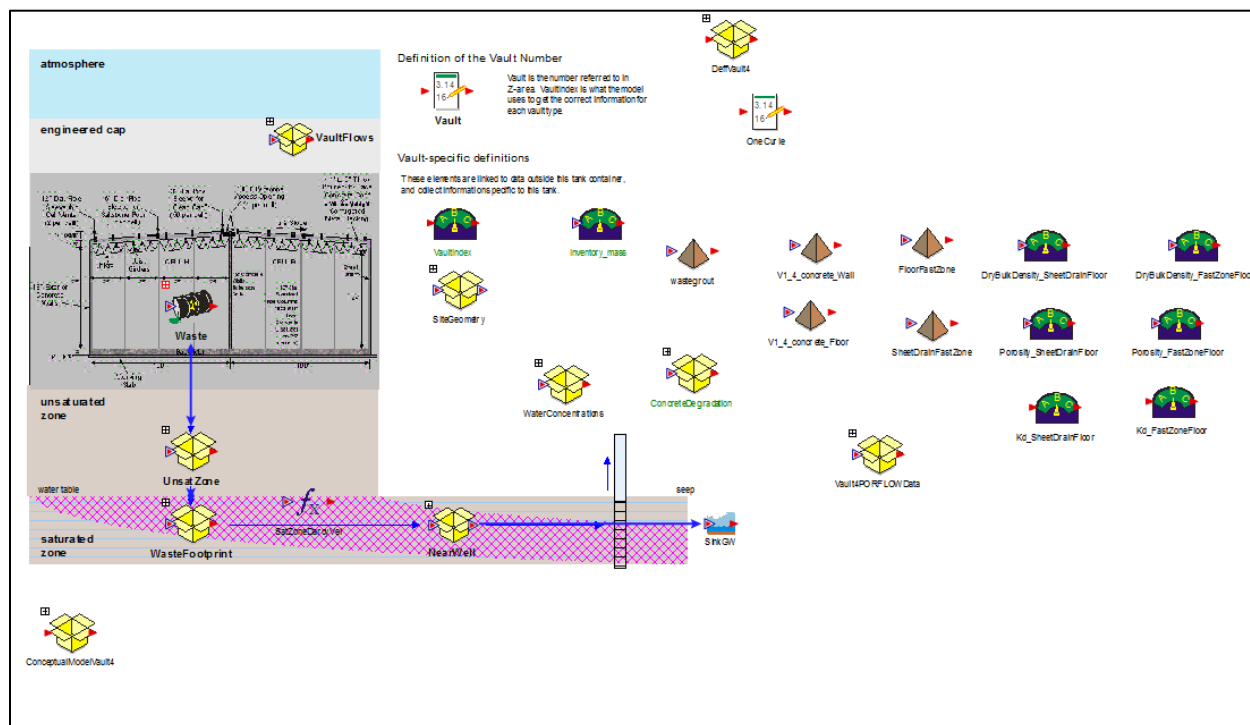
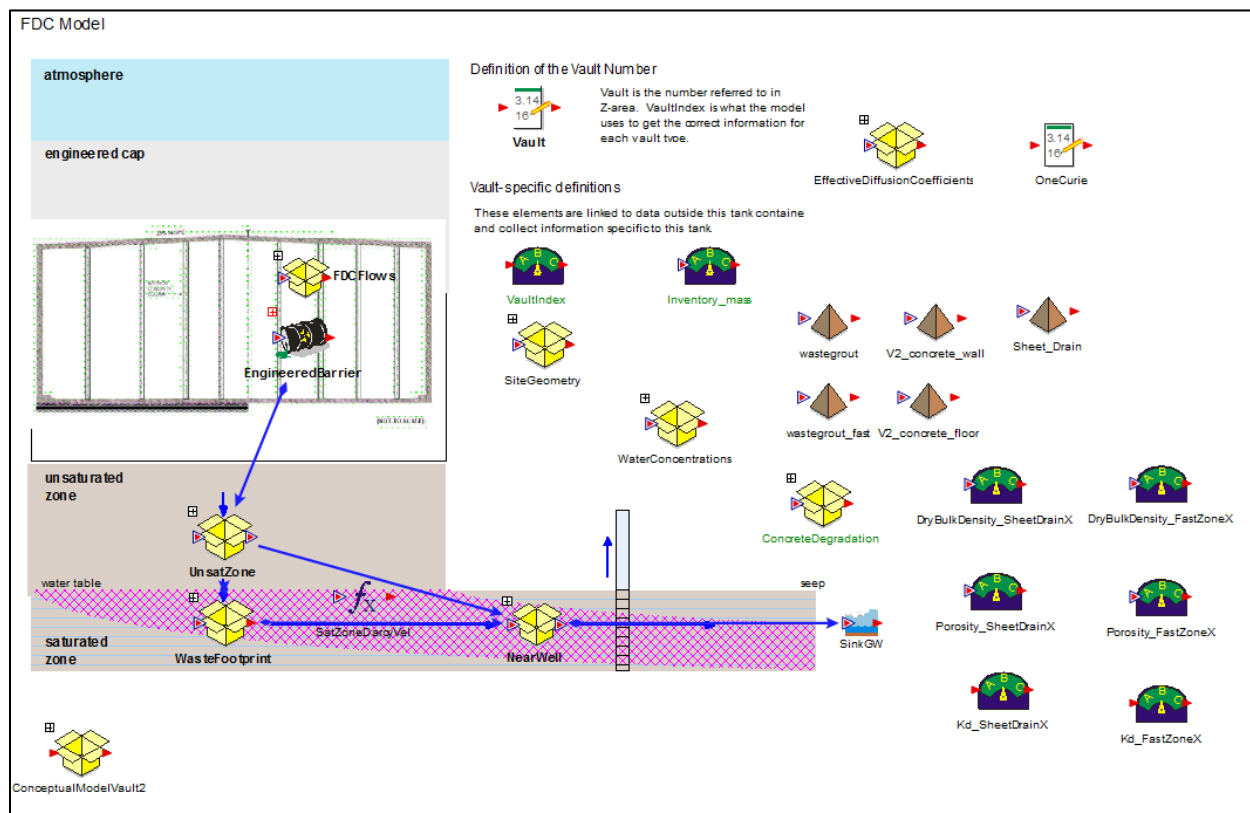


Figure 4.1-11: Contents of the *FDCs* Container



The SDF GoldSim Model containers *Vault_1*, *Vault_2*, *FDCs* are comprised of mixing-cell networks and pipe-elements (analytical solutions) that evaluate radionuclide migration from the saltstone (and for SDU 1 and SDU 4, the walls), through the remainder of the engineered barrier, through the backfill and unsaturated zone. The radionuclide releases from the unsaturated zone are applied as boundary conditions to pipe-elements representing the saturated zone where concentrations are evaluated at the 100-meter boundary and IHI Wells.

Radionuclide concentrations at the mid-points of sectors along the 100-meter boundary (Figure 2.0-1) form the basis of the GoldSim Model MOP dose calculations. The SDU components of the SDF GoldSim Model also contain pipe-elements that simulate the transport of radionuclides from SDUs to IHI wells adjacent to specified SDUs (see Figure 3.3-3). It is at these wells that concentrations used in the IHI dose calculations are calculated. The SDU components of the containers *Vault_1*, *Vault_2*, *FDCs* are organized in a hierarchy, with the top level of the SDU transport components for SDU 4 shown in Figure 4.1-10 and the *FDCs* shown in Figure 4.1-11. Model containers, represented as yellow boxes, are used to organize the calculation logic. Using the *FDC* submodel as an example, a brief description of the upper-level containers and their contents is introduced here:

- The source element *EngineeredBarrier* contains the mixing-cell network that represents: (1) the engineered barrier comprised of the saltstone, sheet-drains, columns, floor components, joints, walls, and backfill and (2) the UZ. Within the engineered barrier and UZ, radionuclide transport is controlled by advection, molecular diffusion, linear sorption, and radionuclide decay. Using the *FDC* model as an example, the engineered barrier above the floor is comprised of a mixing-cell network that is discretized into 20 layers defined by containers (Figure 4.1-12). Each layer (i. e. *CellRow_20*) is represented by a set of containers, comprised of mixing cells, representing the material zones (saltstone, sheet-drains, columns, walls, HDPE liners, and backfill) of the engineered barrier (Figure 4.1-13). From the saltstone cells, mass can diffuse or advect between the saltstone cells and the rest of the cell network. Several simplifying assumptions are made in conjunction with the abstraction model used in the SDF GoldSim Model. With exception of the wall-to-floor joint cells in the *FDCs*, only vertical advection through the engineered barrier (and UZ) is considered in the model abstraction upon which the three SDU models are based. The flow regime is defined by spatially averaged vertical components of Darcy velocity which are read into the model for each material zone including, the inner and outer saltstone zones, the sheet-drains, the columns, the walls, the floor (and for the *FDCs*, floor, upper mud mat, and lower mud mat), HDPE liners (for the *FDCs* only), and backfill. Because of the importance of diffusion into the walls and from the walls into the backfill in the SDUs during early times, the abstracted model also considers the influence of molecular diffusion on horizontal radionuclide migration within the model.
- For each layer in the *FDC* model, there is a *Grout* container comprised of two containers of mixing cells linked in series (Figure 4.1-14), one containing the cells representing the inner zone of saltstone (Figure 4.1-15) and the other representing the outer zone of saltstone (Figure 4.1-16). The inner and outer zone mixing cells are separated by a set of cells located in the *FastZone* container representing the columns (or a potential fast zone) in the *FDCs* (Figure 4.1-17) and SDU 4. The fast zone in SDU 1 is located in the

Grout container. The other containers found in each layer container are the *SheetDrain* (Figure 4.1-18), *Wall* (Figure 4.1-19), *HDPE* (Figure 4.1-20), and *Fill* (Figure 4.1-21) containers. Within each layer, the mixing-cells in each container and adjacent containers are connected to each other by diffusive links. In addition, each cell within a layer is connected to the equivalent cells above and below them with an advective link. The cells in the bottom layer *CellRow_20*, are attached to cells representing the zones below them found in the containers *VaultFloor1*, *VaultFloor2*, *FastZone*, and *Joint*.

- The *VaultFloor1* and *VaultFloor2* containers (see Figure 4.1-12) are each comprised of one chain of 20 mixing cells that represent the floor beneath the inner saltstone zone (Figure 4.1-22) and outer inner saltstone zone, respectively. The containers *VFUMM* and *VFLMM* within *VaultFloor1* and *VaultFloor2*, each contain 5 cells linked in series that represent the upper and lower mud mats, respectively. Similar to the *VaultFloor1* and *VaultFloor2* containers, the *FastZone* container (see Figure 4.1-12) is comprised of one chain of 20 mixing cells that represent the floor, upper mud mat and lower mud mat beneath the column. The *Joint* container (see Figure 4.1-12) is comprised of a chain of six mixing cells that represent the wall-to-floor joint beneath the wall. The joint cells in turn provide a fast zone beneath the wall that flows into the backfill. The joint cells also flow into the top cell in the string of 20 cells linked in series found in the *WallFloor* container. The cells in the *WallFloor* container are arranged in the same manner as the rest of the floor cells. The strings of cells found in the *VaultFloor1*, *VaultFloor2*, *FastZone*, and *WallFloor* containers flow into the set of mixing cells located in the *UnsatZone* container.
- The *UnsatZone* container (Figure 4.1-11) is comprised of one chain of 20 mixing cells linked in series that represent the unsaturated zone beneath the FDC (Figure 4.1-25). Note that 10 of the cells (Cells 9 – 19) are located in the container *UZADD*. The bottom cells found in *VaultFloor1*, *VaultFloor2*, *FastZone*, *WallFloor*, and *Fill* containers flow into the top cell in the set of mixing cells located in the *UnsatZone* container. Outflow from the 20th cell (*UZCell_Out*) in the *UnsatZone* container, defines the radionuclide release to the saturated zone. The benchmarking container contains time-history result elements that compare the simulated radionuclide releases for a subset of species with the SDF PORFLOW Model results.
- The *WasteFootprint* container (Figure 4.1-11) is comprised of one chain of 10 mixing cells that represents the saturated zone beneath the unsaturated zone (Figure 4.1-26). The waste footprint cells are used to determine the adjacent SDU's contribution to well concentration at the wells used for the IHI dose calculations.
- The *NearWell* container (Figure 4.1-11) is comprised of a pipe-element representing 1-D transport to the 100-meter boundary, plus an additional seven pipe elements describing radionuclide transport from upgradient SDUs through the saturated zone to the seven IHI wells (Figure 4.1-27). Contributions from these pipes are used in conjunction with concentrations from the footprint cells to determine the concentrations at the IHI observation wells.

- The *SiteGeometry* container is comprised of GoldSim elements used to set the geometric dimensions for the FDC and associated natural barriers (unsaturated zone thickness and saturated zone streamtrace distance to the 100-meter boundary).
- The *ConcreteDegradation* container is comprised of GoldSim selector elements which are used to control the K_d values based on E_h and pH transition times read in to the model. The SetColumnKdMatrix container is a looping container that contains the logic to update the K_d s for the segmented columns in the FDCs.

Figure 4.1-12: Contents of the *VaultCells* Container for FDCs

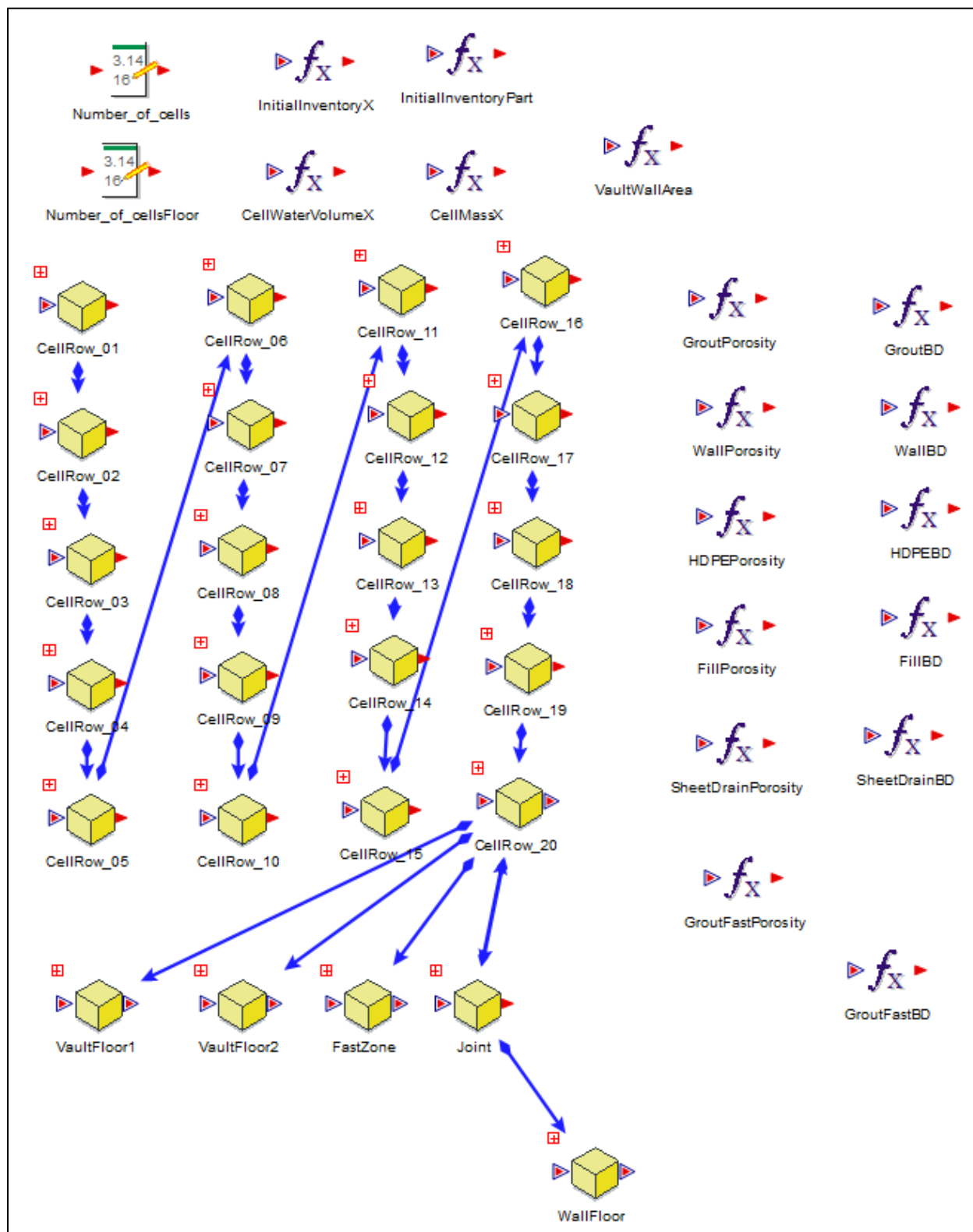


Figure 4.1-13: Contents of the *VaultCells* Container for FDCs

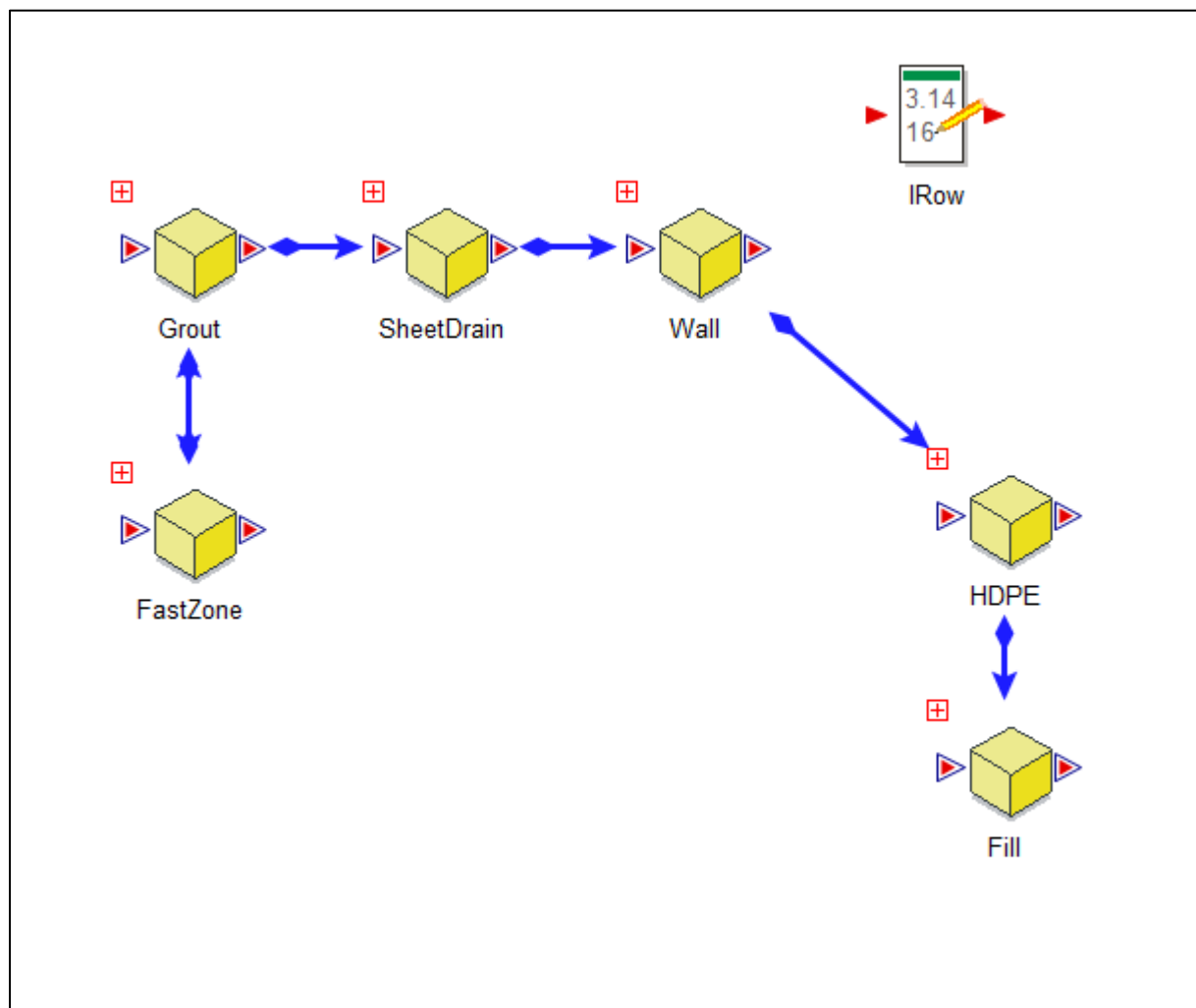


Figure 4.1-14: Contents of the *Grout* Container for FDCs

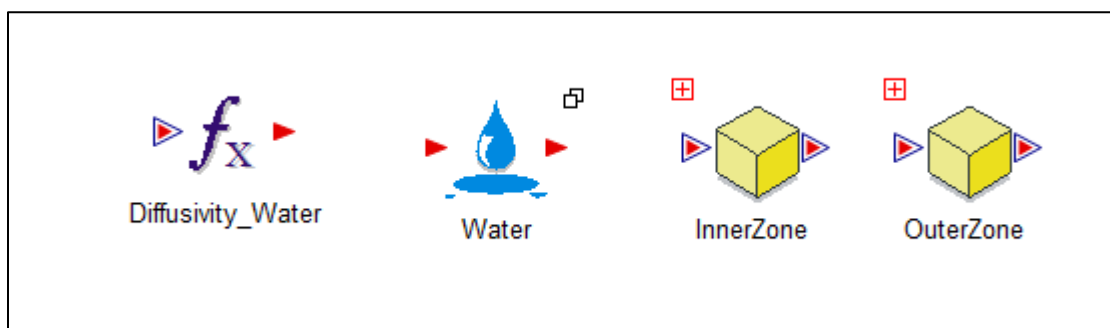


Figure 4.1-15: Contents of the *InnerZone* Container for FDCs

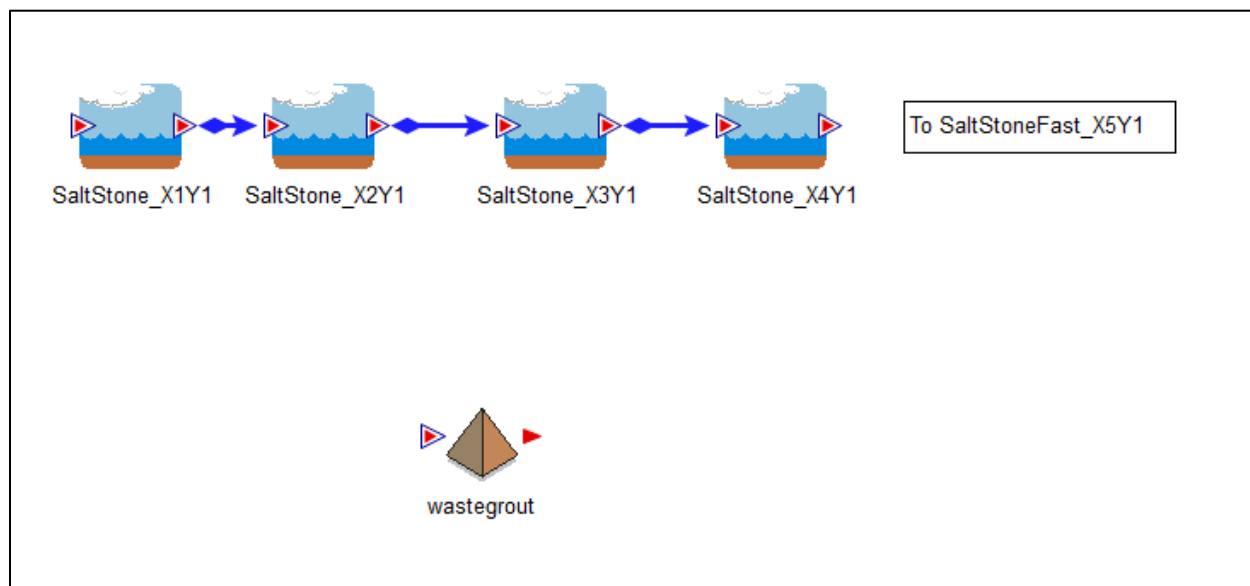


Figure 4.1-16: Contents of the *OuterZone* Container for FDCs

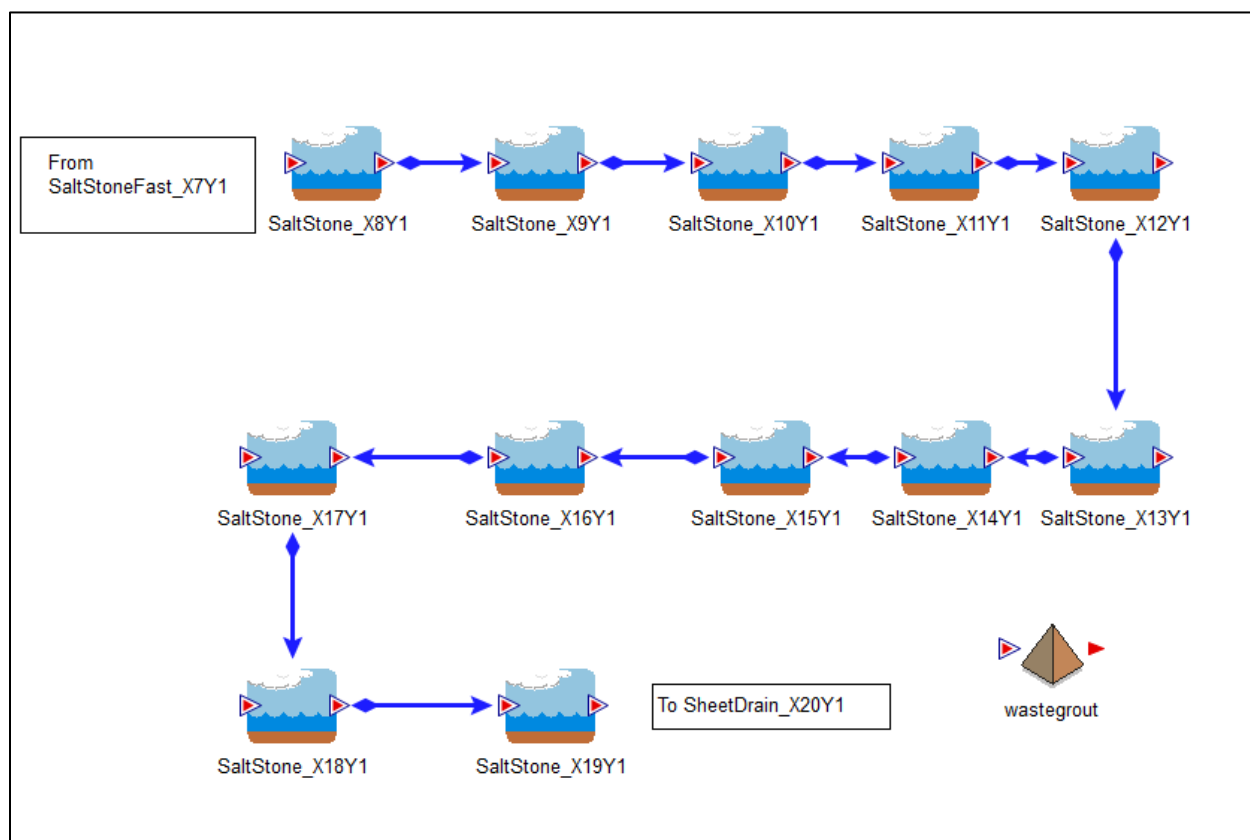


Figure 4.1-17: Contents of the *FastZone* Container for FDCs

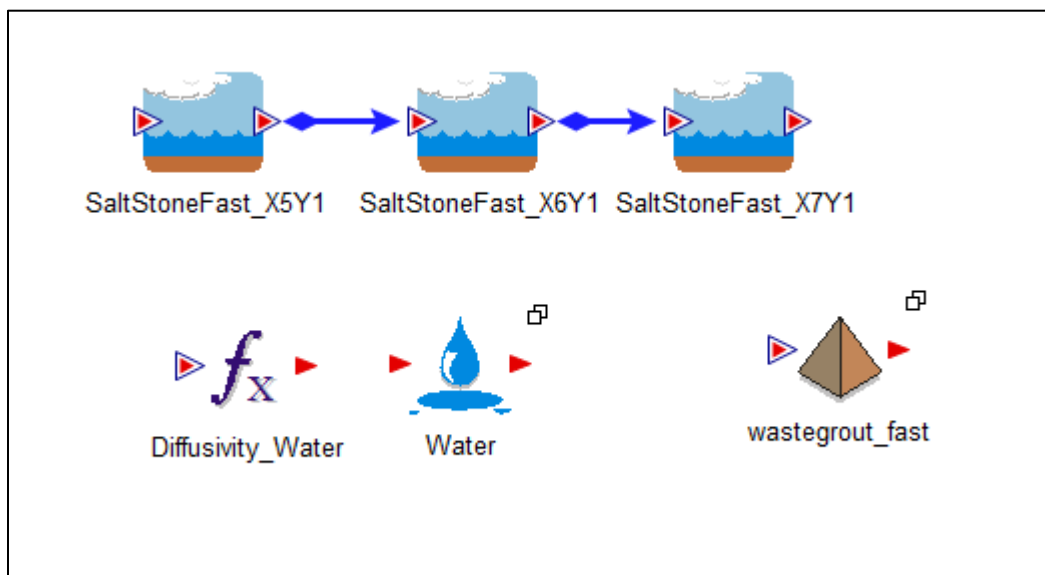


Figure 4.1-18: Contents of the *SheetDrain* Container for FDCs

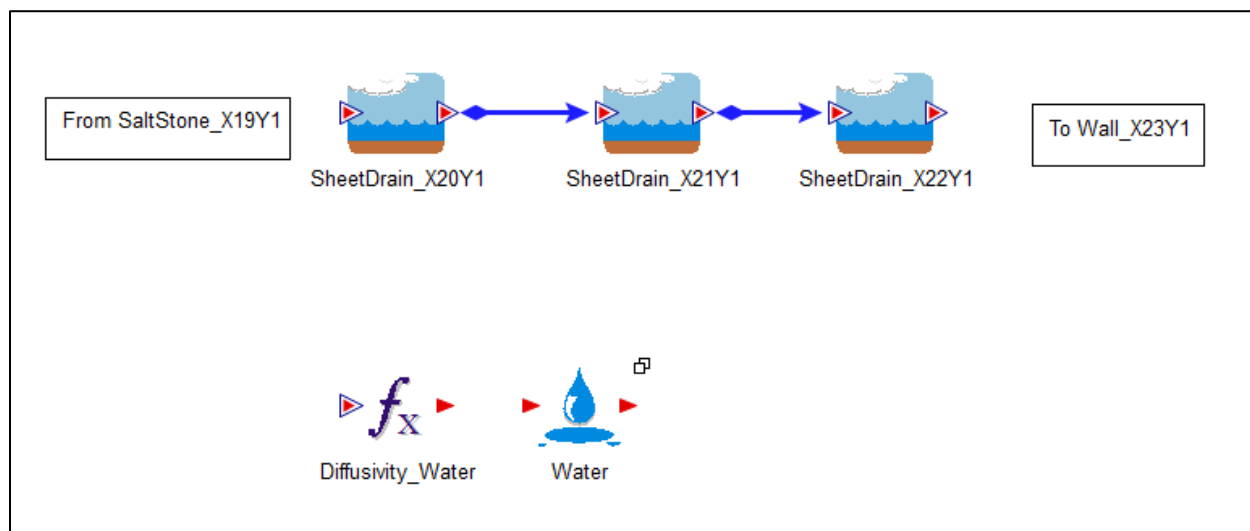


Figure 4.1-19: Contents of the *Wall* Container for FDCs

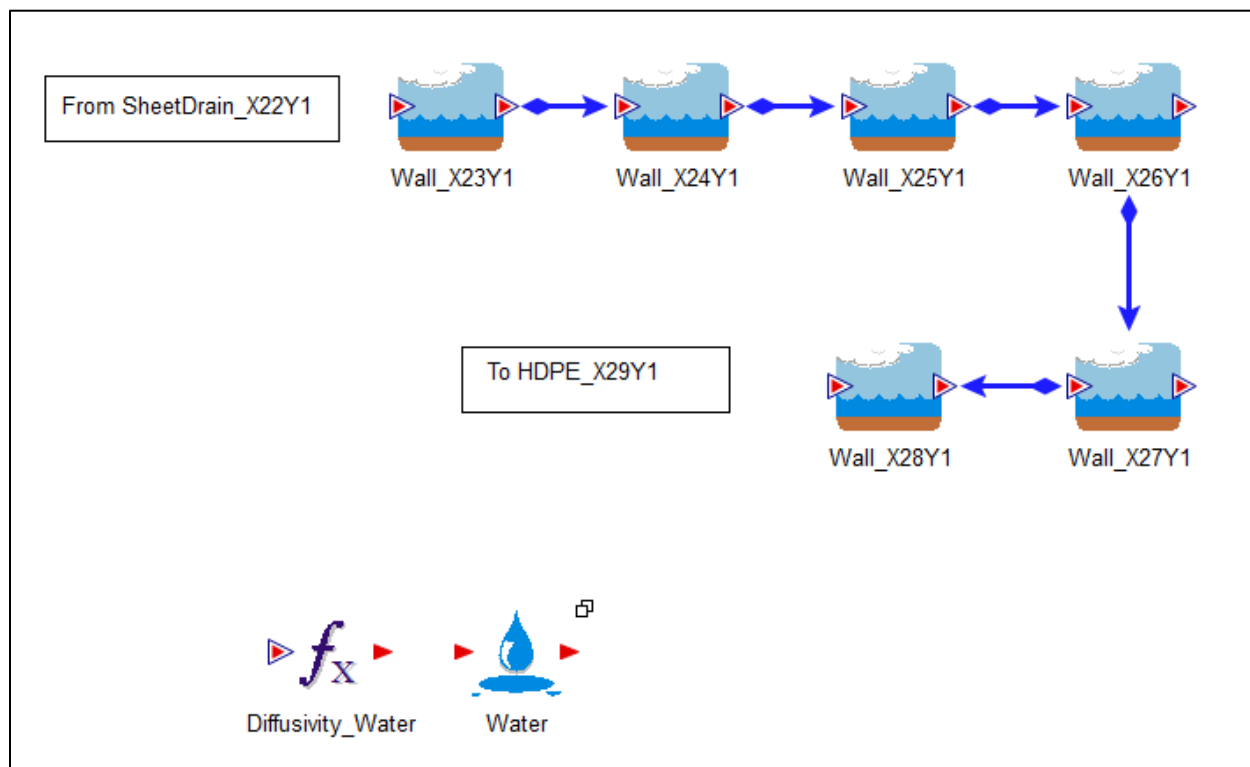


Figure 4.1-20: Contents of the *HDPE* Container for FDCs

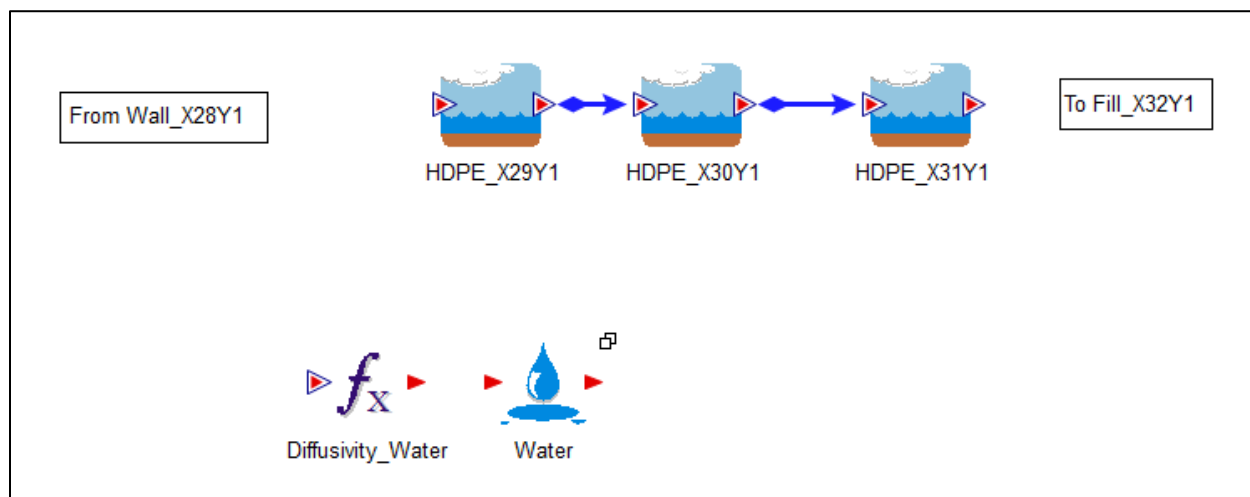


Figure 4.1-21: Contents of the *Fill* Container for FDCs

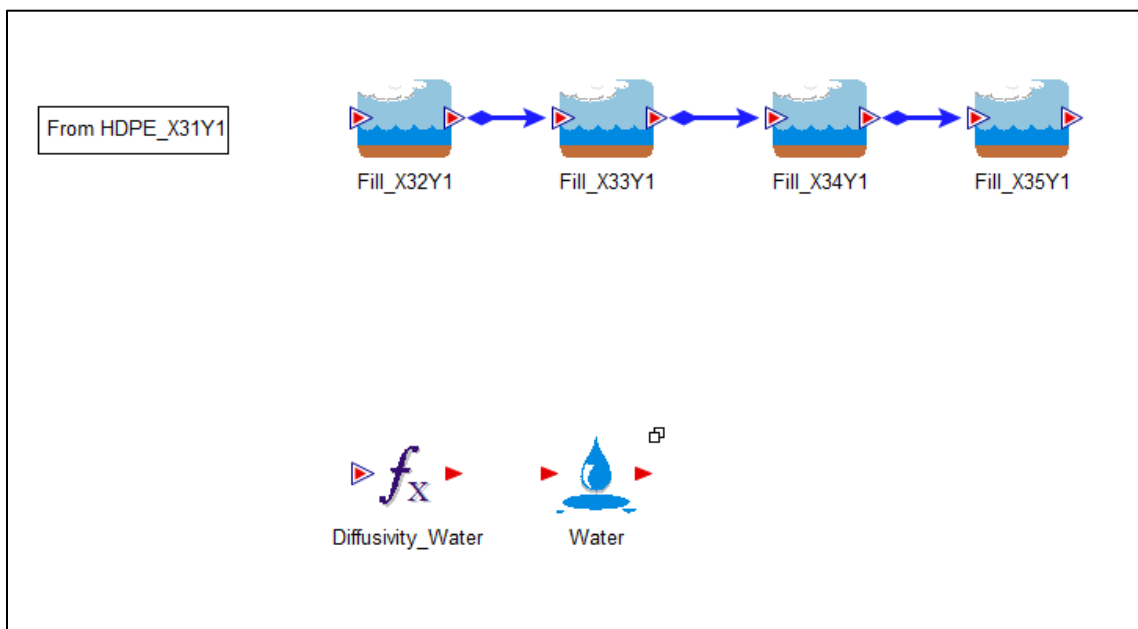


Figure 4.1-22: Contents of the *VaultFloor1* Container for FDCs

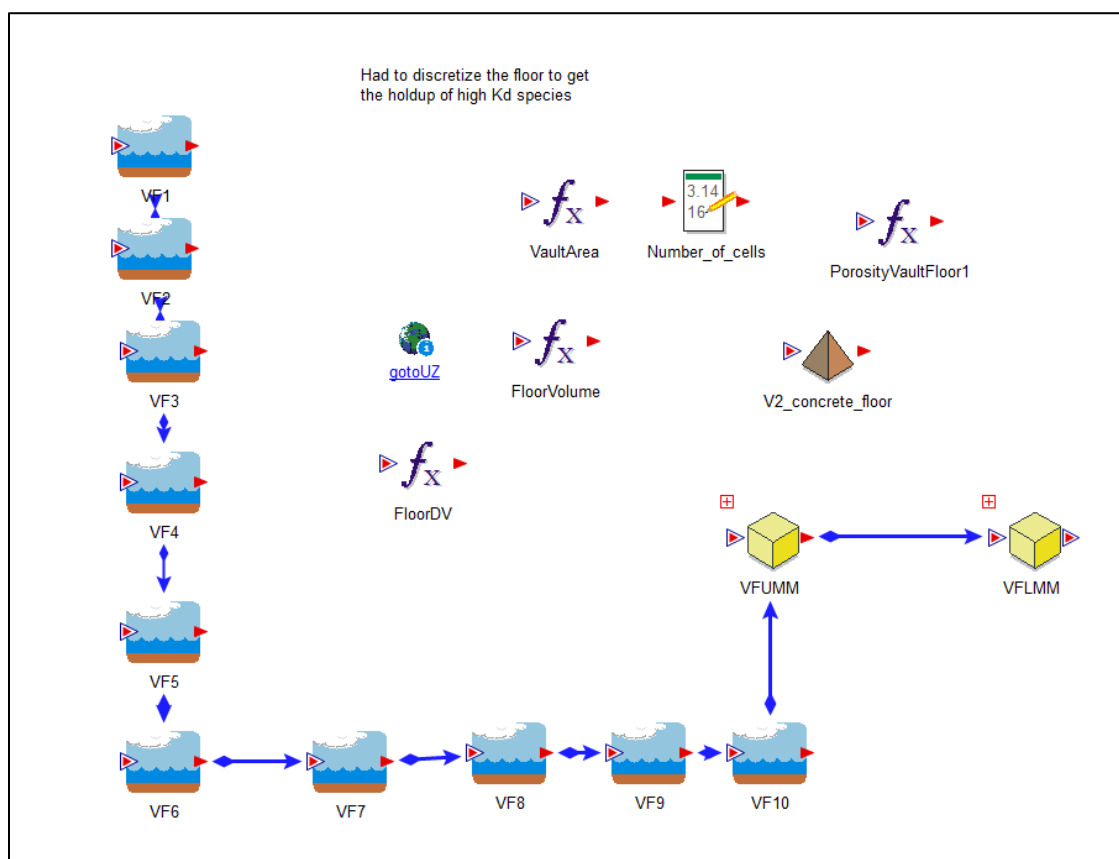


Figure 4.1-23: Contents of the *FastZone* Container for FDCs

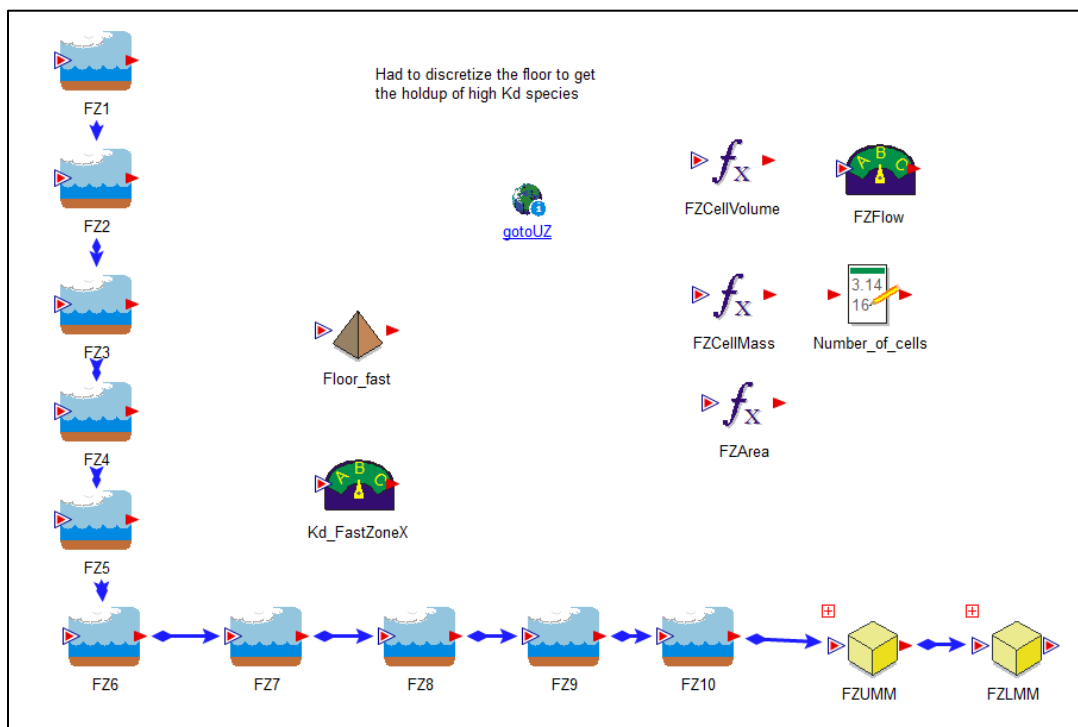


Figure 4.1-24: Contents of the *Joint* Container for FDCs

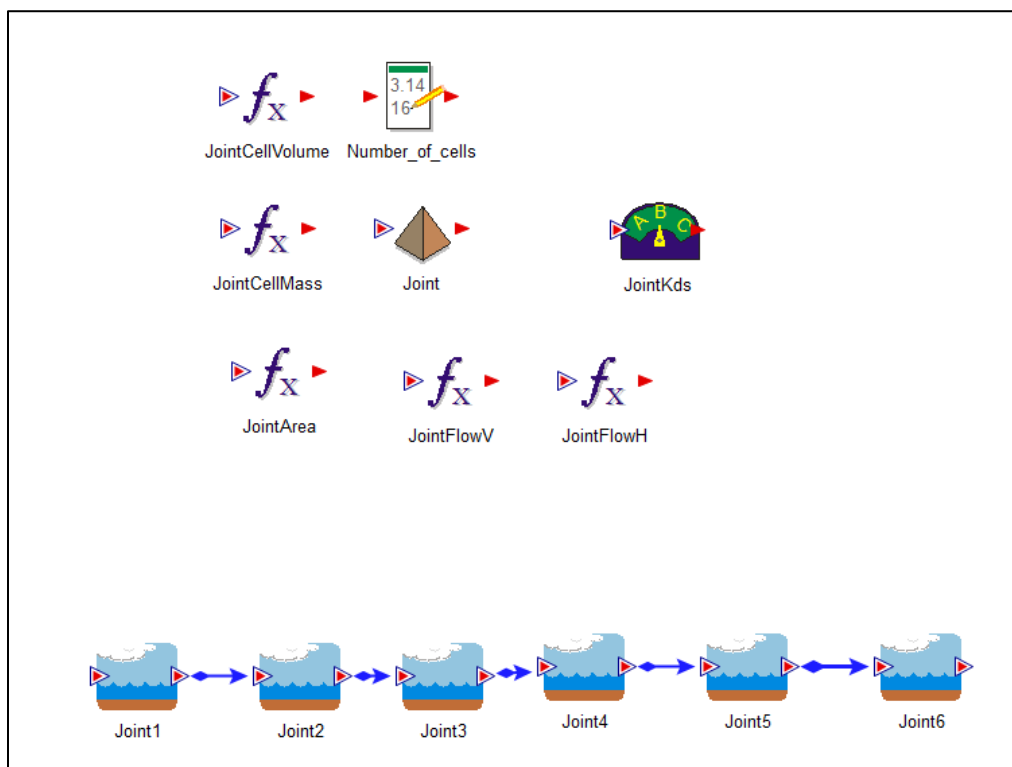


Figure 4.1-25: Contents of the *UnsatZone* Container for FDCs

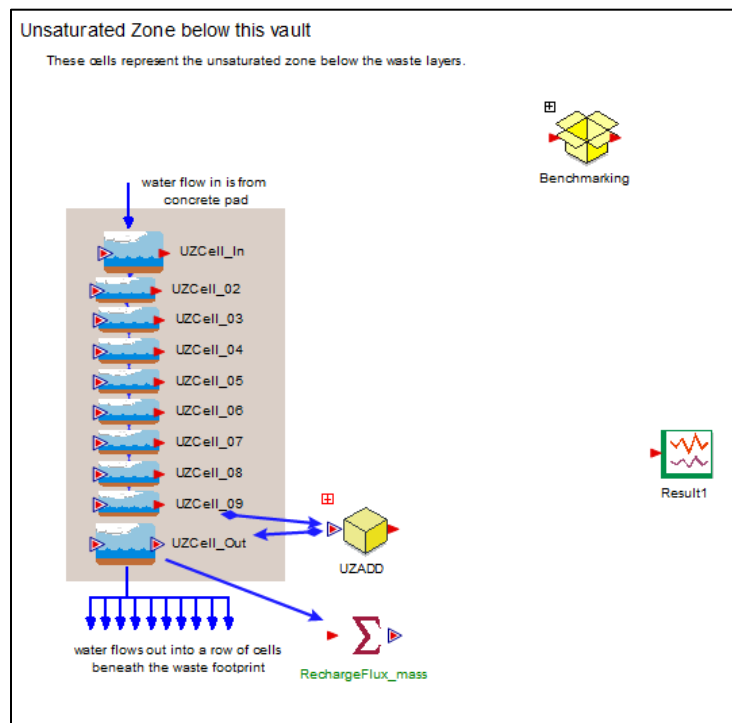


Figure 4.1-26: Contents of the *WasteFootprint* Container for FDCs

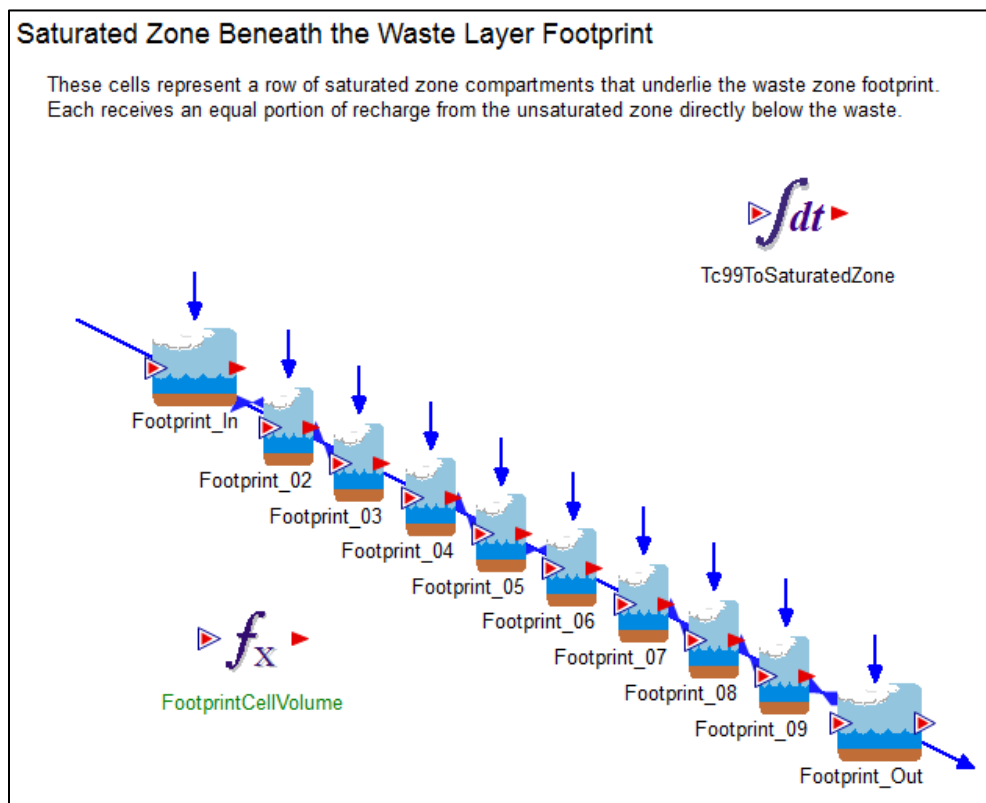
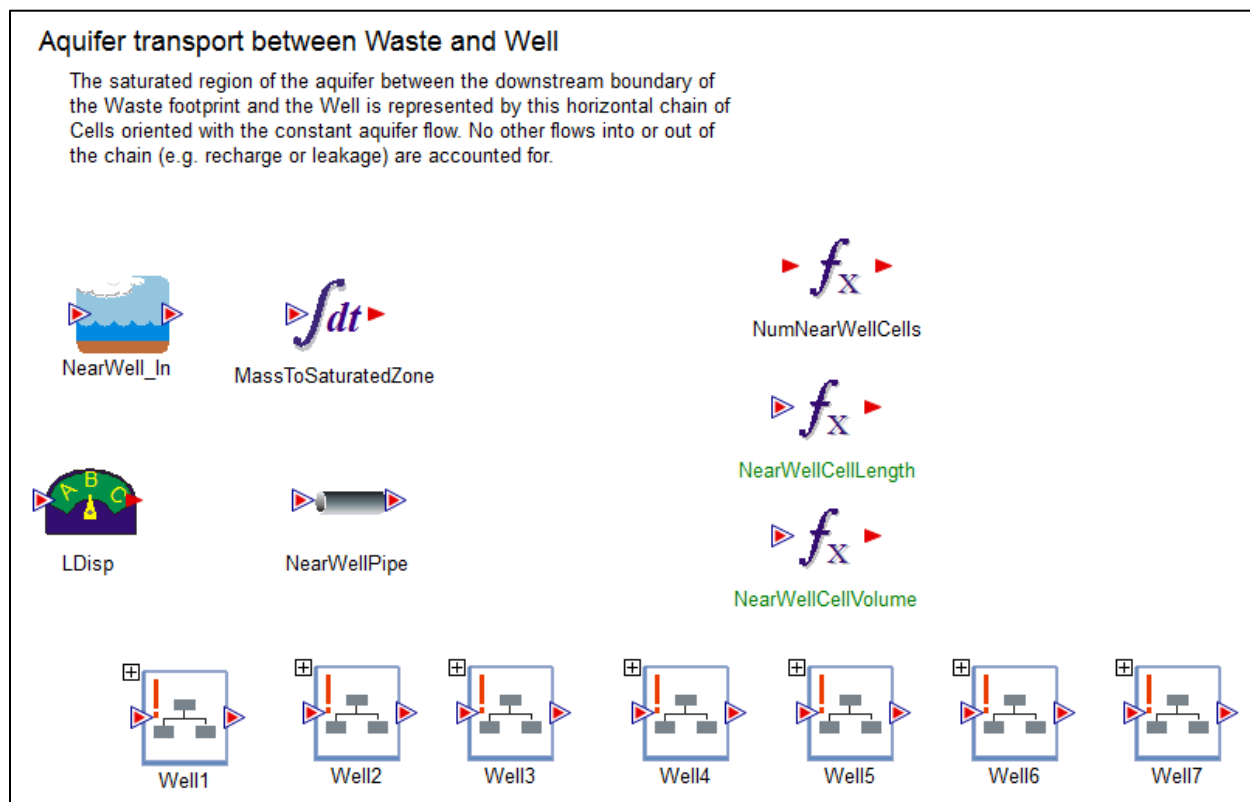


Figure 4.1-27: Contents of the *NearWell* Container for FDCs



4.2 New Model Capabilities

In Version 4.101 of the SDF GoldSim Model, SDF PORFLOW Model output files used as input data for the GoldSim stochastic model are imported into the SDF GoldSim Model using GoldSim External elements in conjunction with the FORTRAN based module, *ReadPORFLOWData.dll*. *ReadPORFLOWData.dll* is a dynamic link library used by the GoldSim model to read in the sampled flow-field data, time histories of diffusion coefficients, and radionuclide-release breakthrough curves generated by PORFLOW-based PA models. In addition, the computational efficiency of the SDF GoldSim Model was enhanced by allowing the model user to group the FDCs by location so that a single FDC could be used to represent a set of several FDCs (see Section 3.2). Section 4.2.1 describes the structure and implementation of the PORFLOW file reading module and Section 4.2.2 describes the structure and implementation of the FDC grouping module.

4.2.1 Importing PORFLOW Files

In the SDF GoldSim Model, the process of reading PORFLOW generated data from external files, is performed using GoldSim external (DLL) elements (Figure 4.2-1). The GoldSim external (DLL) elements provide an interface between the GoldSim model and the DLL (*ReadPORFLOWData.dll*) which contains a subroutine that reads the external files. From GoldSim, the DLL is called using GoldSim's external function which passes the instructions through its input interface to the dynamically allocated variable *input()* in

ReadPORFLOWData.dll. The DLL then reads the data files and assigns the requested data to the 1-dimensional variable array *output()*. The structure of the vector-variable, is controlled by the output interface of the external function element. The required structure of the external function interface and the general structure of the DLL are described in Appendix C of GTG-2010c. The data passed through the external element's interface to control the DLL (*ReadPORFLOWData.dll*) are described in Table 4.2-1.

Table 4.2-1: Instruction Data Passed to *ReadPORFLOWData.dll*

Number	Variable Name	Variable Meaning
1	FileExt	File extension number if desired (normally set to zero)
2	FileIndex	File number of file to be used
3	LocNumber	The location of the desired table in a file of ordered two-dimensional tables each table representing a PORFLOW flow simulation.
4	szTable	The number of dependent-variable columns in the referenced table
5	Indep	Column containing the independent Variable (time)
6	Depend	Column containing the first dependent Variable
7	Iname	0 = Data for all realizations are in a single file; 1 = Data for each realization are in a different file
8	IDU	Unit indicator for file (i.e. SDU Type (1, 2 for FDCs, 4)) Omit if Iname = 0
9	IRLZ	The realization number
10 thru the number of dependent variables to be returned	Variable Names	The position of dependent-variable column in the referenced table for each one-dimensional table or scalar variable to be Note that that scalar data is indicated by using the negative of the column number (-5 for column 5)
Final Line	Blank	A zero indicating that no more data is requested

The control data passed from the GoldSim model to the DLL tells the DLL which control data file to read, and the control file, along with data passed into the DLL, tells the DLL which file to read and where it is located. A typical control input file is depicted in Figure 4.2-2.

The control input file used by *ReadPORFLOWData.dll*, is called *ReadPFData.in*. If the parameter *FileExt* (see Table 4.2-1) is not set to 0 but to 4, the DLL looks for a control file named *ReadPFData4.in*. The variable *FileIndex* indicates which one of the five file names in *ReadPFData4.in*, will be read. The two variables *IDU* and *IRLZ* in Table 4.2-1, control the location of the data file to be read within a structured set of folders. The variable *IDU*

denotes the disposal unit and *IRLZ* the realization. The last two lines in the file depicted in Figure 4.2-2 indicate the positions within the file names that *IDU* and *IRLZ* are found for each of the 5 filenames. Note that *IDU* (4 for SDU 4) is in the 20th column and *IRLZ* starts in the 25th column. The DLL will pad the realization number with zeros as needed. The other lines required by the control file include:

- the first line which indicates how many file names are included,
- the first line after the file names line which tells how many header lines are found at the top of files with multiple tables listed in series,
- the second line after the file names line which tells how many header lines are found before each table,
- the third line after the file names line which tells how rows are in each table (in multi-table files this must be an exact number that is the same for each table, if not any number that is the same or larger than the number of rows will suffice).

The typical structure used to implement *ReadPORFLOWData.dll* in the SDF GoldSim Model can be seen by examining Figure 4.2-1. The control data feeds to the DLL (items 1 – 9 in Table 4.2-1) are located in the container *DLLData*, (see Figures 4.2-1 and 4.2-3). The column locations of the flow data to be imported into the GoldSim model are listed in the data element *FloPar_vec* shown in Figure 4.2-1. The time series imported into the GoldSim model are captured by the time series elements located in the two containers *DarcyVelocity_TS* and *Saturation_Ts* found in the container *TimeSeries* (see Figures 4.2-1 and 4.2-4). The time series elements, located in *DarcyVelocity_TS* and used to capture Darcy velocity data are shown in Figure 4.2-5. The expression elements located in *ScalarData* and used to capture Darcy velocity data are shown in Figure 4.2-6. The other container depicted in Figure 4.2-1, *FlowData*, contains selector elements used to feed data to the transport calculation and data elements used to assemble the flow data for segmented columns into vector form (see Figure 4.2-7).

Figure 4.2-1: GoldSim External Element Used for Reading in Flow Data

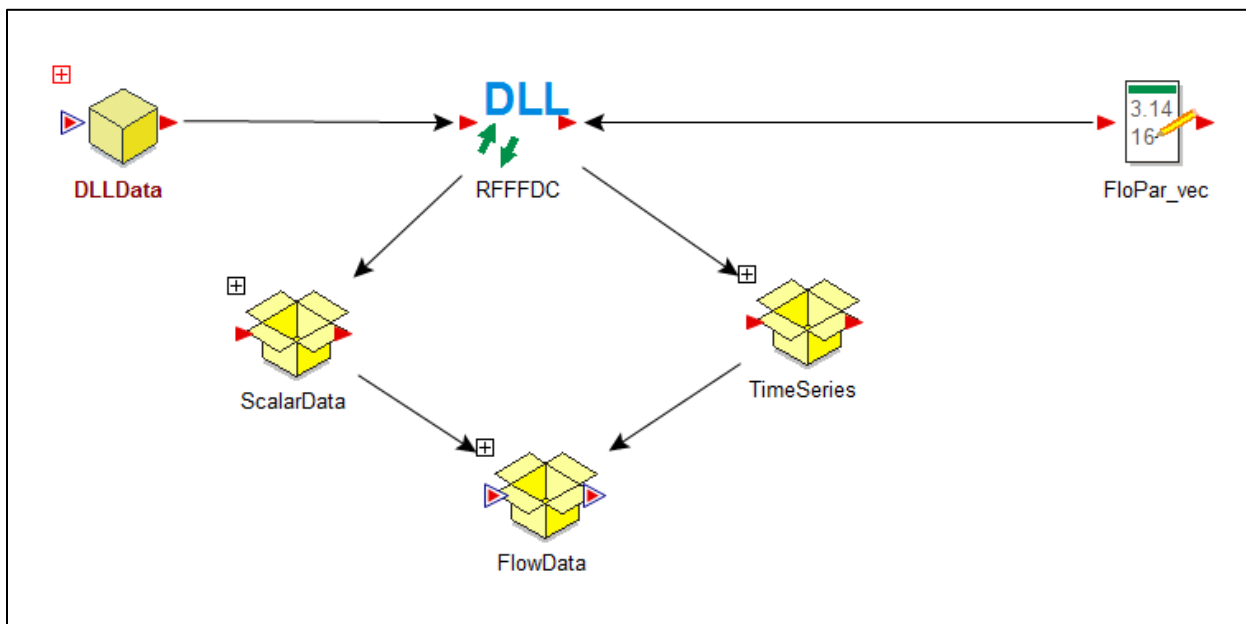


Figure 4.2-2: *ReadPORFLOWData.dll* Control File *ReadPFData4.in*

```

5                ! number of data files to be read
C:\SaltstoneData1\V4\RLZ001\Flow\GoldSim.tab
C:\SaltstoneData1\V4\RLZ001\Transport\De_Tc-99.tab
C:\SaltstoneData1\V4\RLZ001\Transport\Sol1\C_DOMAIN.flx
C:\SaltstoneData1\V4\RLZ001\Transport\Sol2\C_DOMAIN.flx
C:\SaltstoneData1\V4\RLZ001\Transport\Sol3\C_DOMAIN.flx
0 0 3 3 3      ! number of lines in the top-of-file header
1 1 0 0 0      ! number of rows in the header for each data table
200 200 20001 20001 20001    ! number of rows in each data table
20 20 20 20 20
25 25 25 25 25

```

Figure 4.2-3: Contents of the GoldSim Container *DLLData*

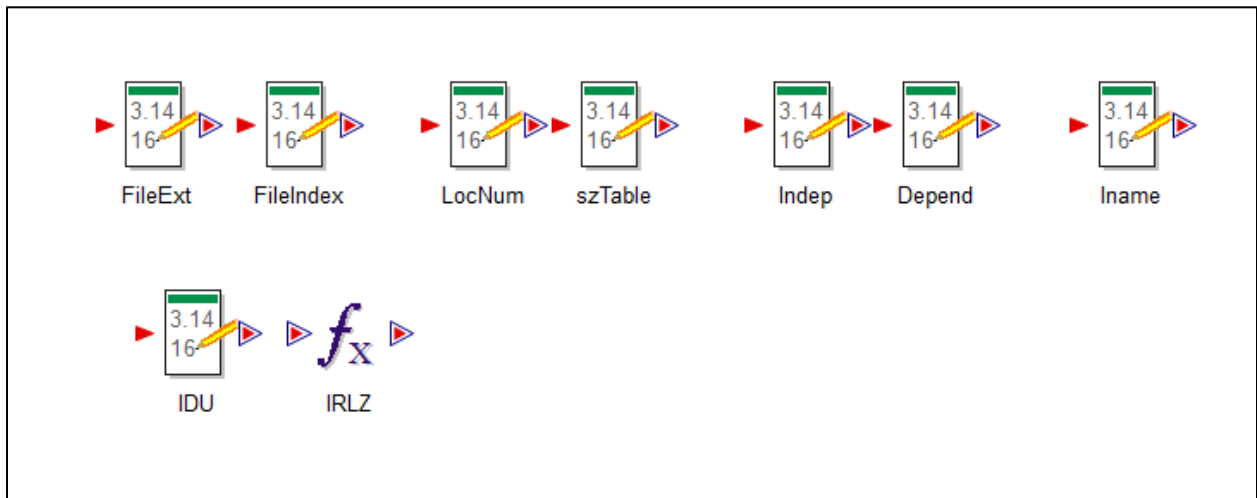


Figure 4.2-4: GoldSim External Element Used for Reading in Flow Data

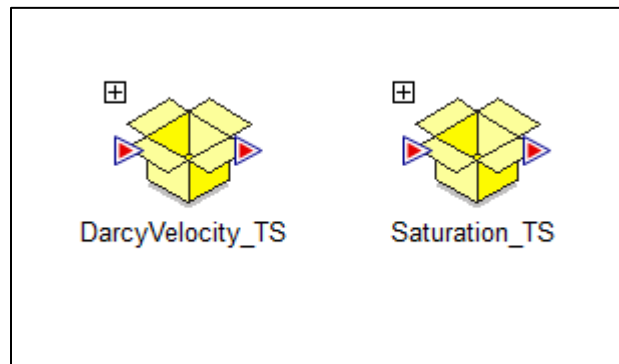


Figure 4.2-5: GoldSim Time-Series Elements Used for capturing Darcy Velocities

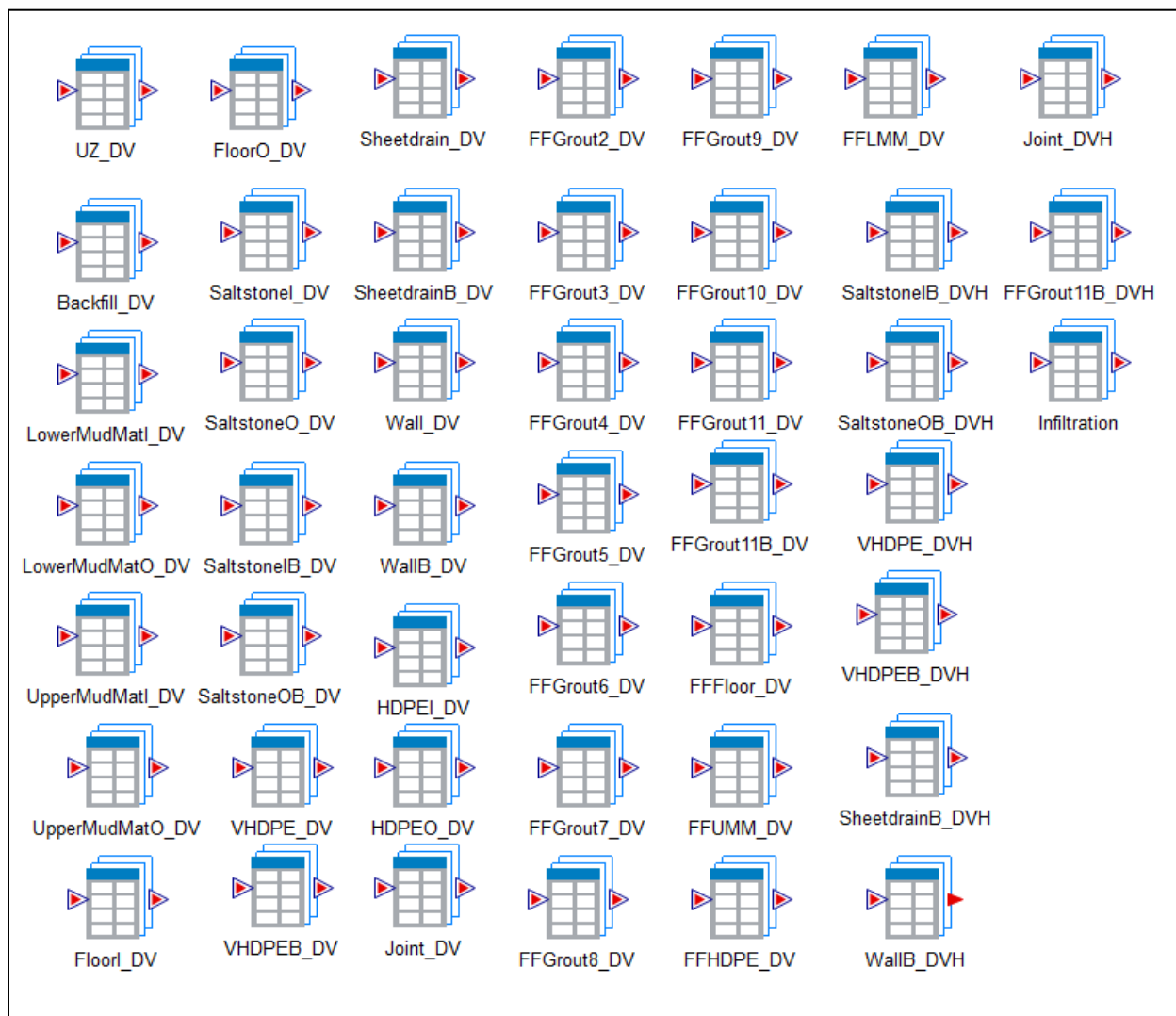
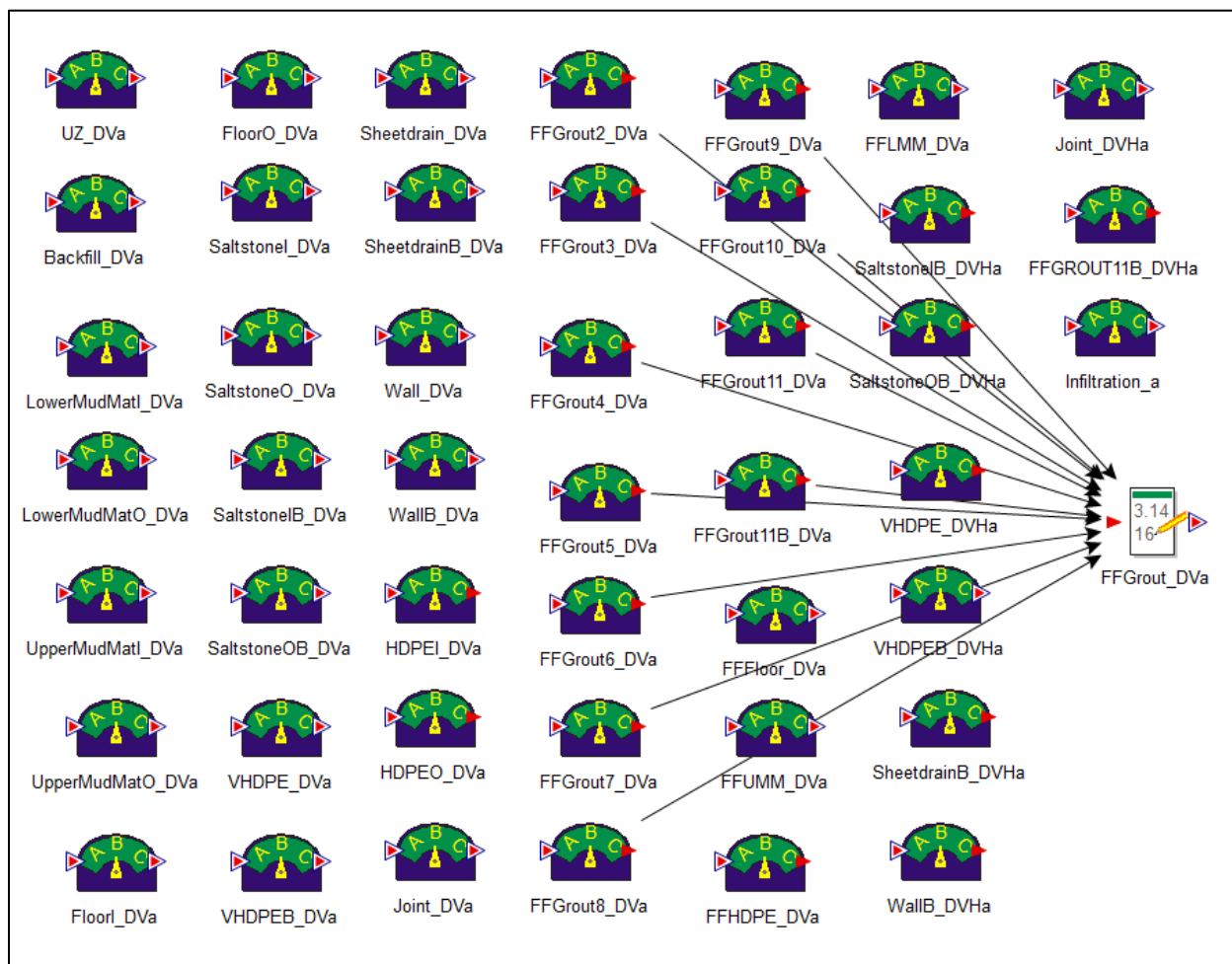


Figure 4.2-6: GoldSim Expression Elements Used to Capture Transition Times



Figure 4.2-7: GoldSim Scalar and Vector Data Feeds



4.2.2 Evaluating FDCs by Group

As noted in Section 3.2, in order to reduce the time needed to perform stochastic simulations with the SDF GoldSim Model, the model was updated to allow for assembling FDCs into groups, which can be evaluated by solving the transport equations for only a single representative FDC within each group. In other words, for each group, radionuclide releases from a representative FDC and saturated zone transport from that FDC to the 100-meter boundary, would be evaluated. The resultant 100-meter boundary concentration from the representative FDC is then used in conjunction with the FDC specific plume functions to generate concentrations for each SDU. When using the grouping option, the model automatically determines an average saturated zone path-length for each group and an average inventory. The grouping process is similarly applied to the IHI analysis.

The implementation of the FDC grouping logic is found in the SDF GoldSim Model container \InputData\VaultData\Inventory found in the GoldSim submodel, *FDC_TransportSubmodel* (Figure 4.2-8). The implementation utilizes a GoldSim looping container *SetGroupInventory* (Figure 4.2-8), which cycles through the 64 SDUs, assembling the group-averaged data for each of the representative SDUs. The group-averaged data for the MOP and IHI analyses includes the SDU inventories, the Darcy velocities along the streamtraces, the path lengths to the 100-meter boundary, and the path lengths to the seven IHI wells (where applicable). Note that the IHI well concentration contributions are calculated for only SDU/well combinations where the release from the SDU is likely to reach the well (see the streamtraces in Figure 3.3-3). The group-averaged parameters are calculated and assembled within the looping container (Figure 4.2-9). The radionuclide transport calculations are then performed for only the representative SDUs.

The use of the FDC grouping logic is controlled by user input options found in the *User_Input* container shown in Figure 4.1-1. The control parameters for FDC grouping are shown in Figure 4.2-10. The logical data input element *FDCGroupingSwitch* is set to “TRUE” to use the grouping option. There are two choices of grouping patterns available, found in the data elements *FDCGroup1* and *FDCGroup2*. In general, the data in *FDCGroup1* should not be changed and the user should update *FDCGroup2* to reset the groups. A model user can also examine the influence of a subset of SDUs by redefining *FDCGroup2* as the row number for active SDUs and zeros for inactive SDUs. The data element *GroupIndex* dictates whether *FDCGroup1* (*GroupIndex*=1) or *FDCGroup2* (*GroupIndex*=2) is used. The suggested grouping pattern is presented in Table 3.2-1. Note that the FDC names listed in Table 3.2-1 are consistent with the names used in the Saltstone Disposal Facility PA (SRR-CWDA-2009-00017) and the SDF GoldSim Model Version 4.101 (as well as all previous versions). The PA FDC map is presented here in Figure 4.2-11. For future reference the present naming convention which includes only six named SDUs is presented in Figure 4.2-11.

Figure 4.2-8: FDC Grouping Structure Module

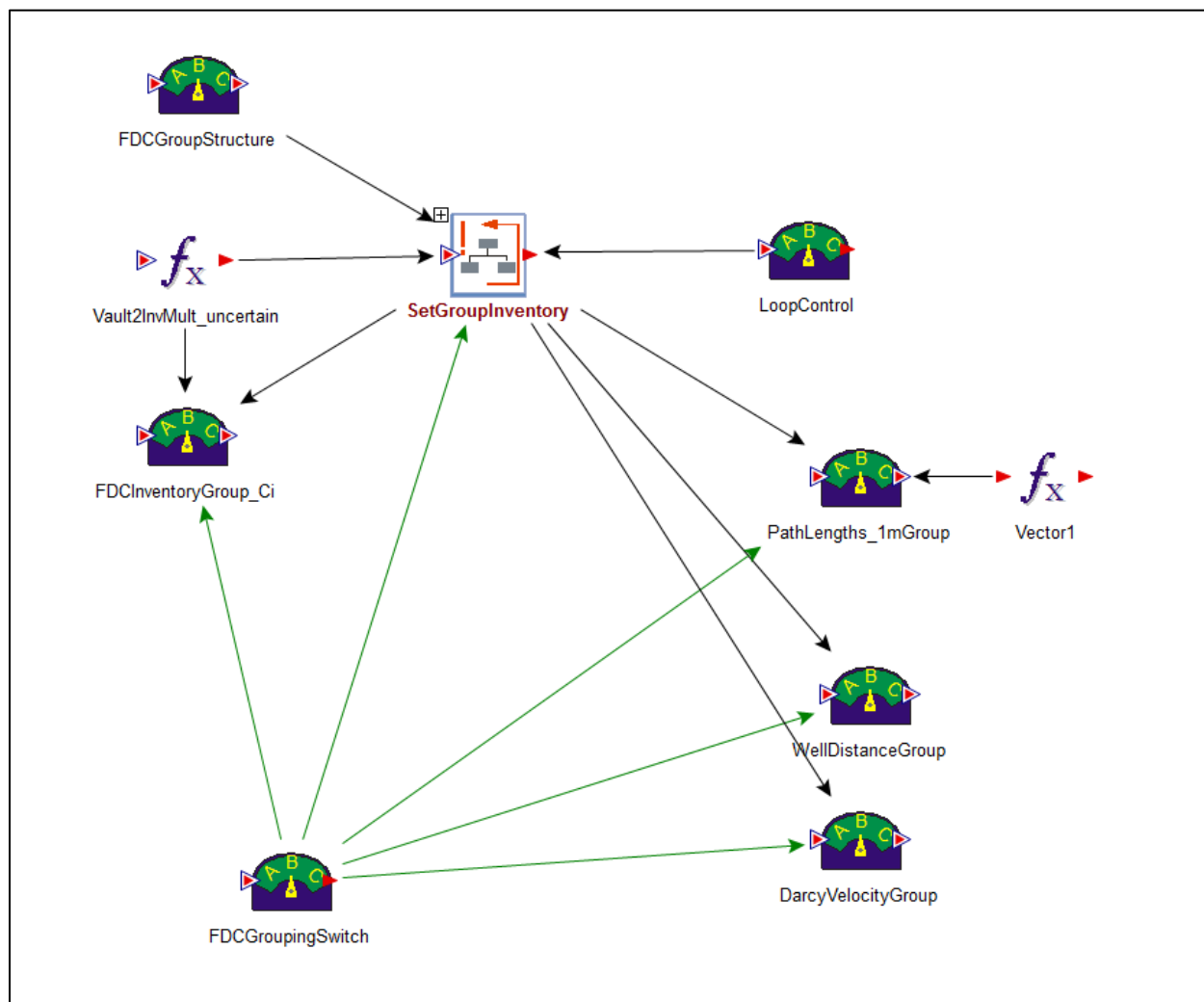


Figure 4.2-9: Contents of Looping Container SetGroupsInventory

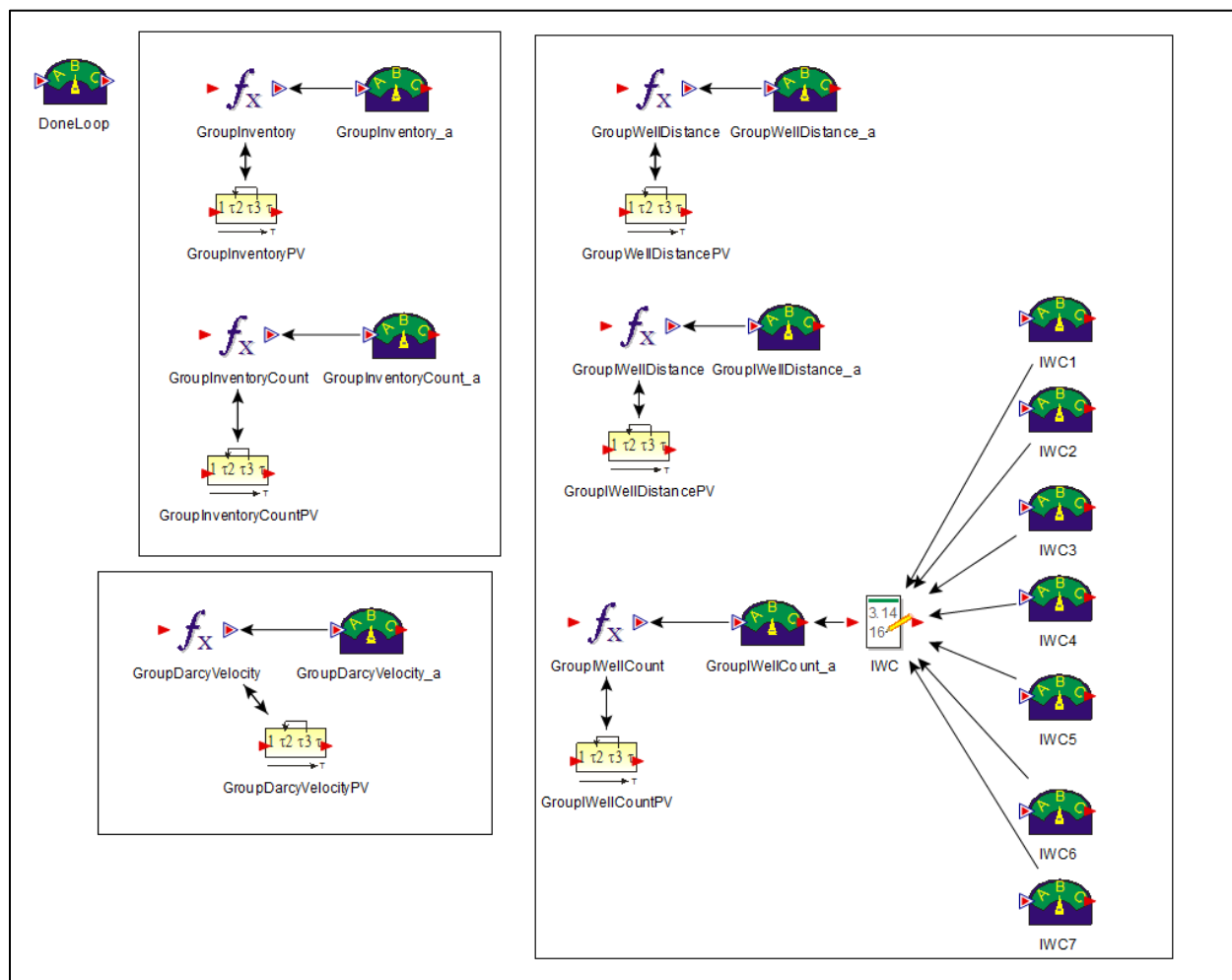


Figure 4.2-10: User Input Controls for FDC Grouping

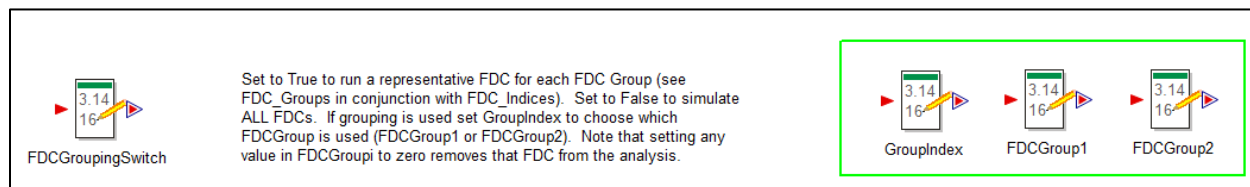


Figure 4.2-11: SDF Anticipated FDC Layout (from SRR-CWDA-2009-00017, Rev. 0)

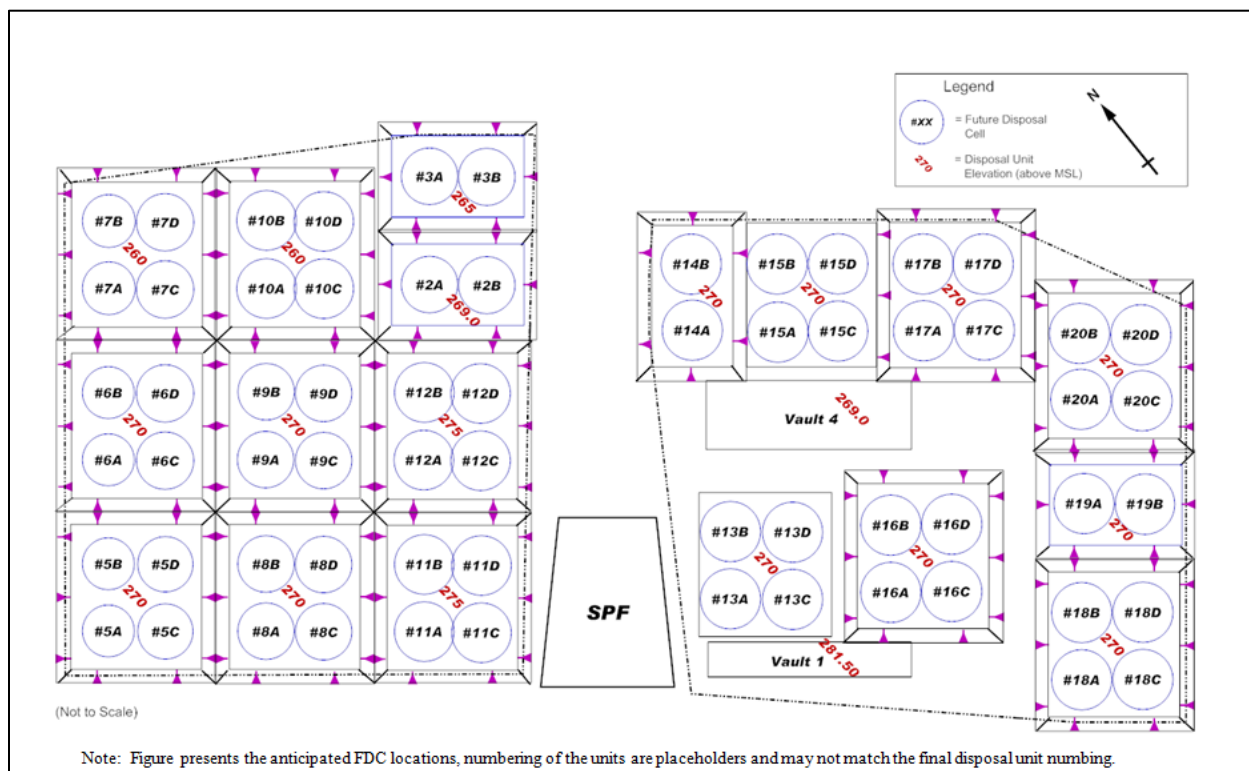
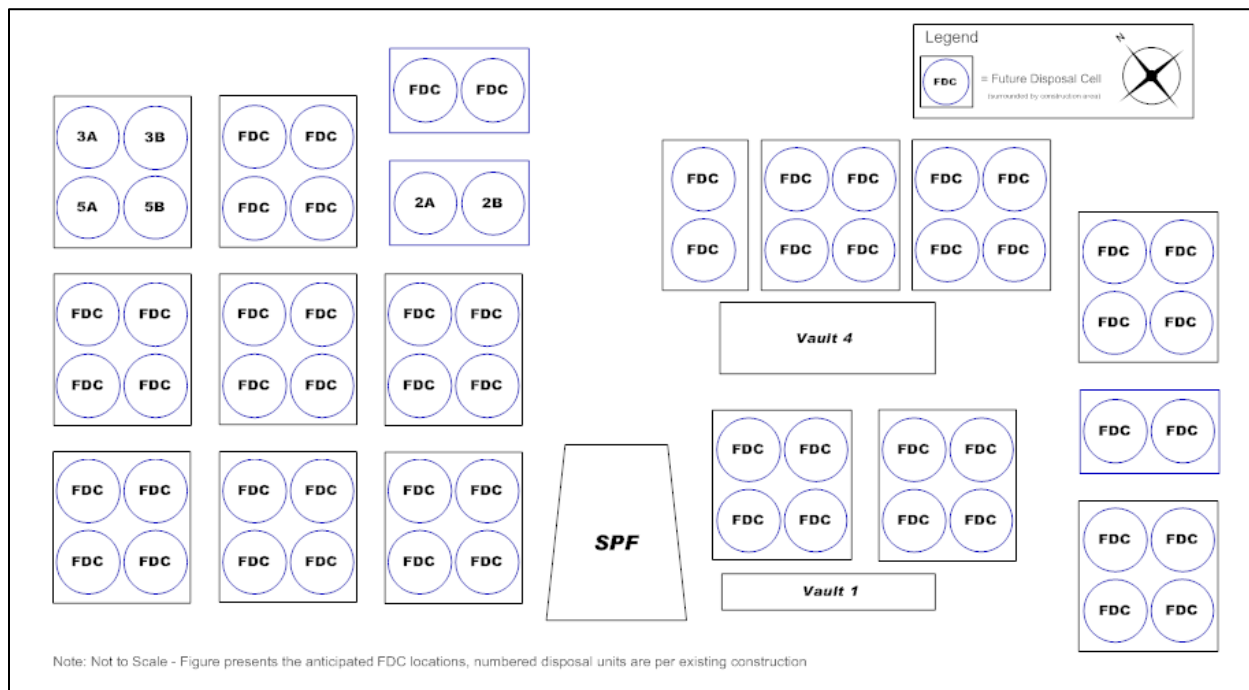


Figure 4.2-12: SDF Anticipated FDC Layout (present)



5.0 MODEL BENCHMARKING

The SDF GoldSim Model is a probabilistic model designed to perform parameter uncertainty and parameter sensitivity analyses used to help evaluate the potential for radionuclide migration from the SDUs to the accessible environment. The probabilistic model used for this Special Analysis and future Special Analyses was constructed using the GoldSim systems analysis software and represents an enhancement to previous versions. A description of the probabilistic model and the enhancements provided for the upcoming Special Analysis, is presented in Section 3. The probabilistic model uses an abstraction of the SDF PORFLOW Model to perform radionuclide transport simulations. Dose calculations for the SDF GoldSim Model are performed using the same dose calculator that were used to determine the PORFLOW dose results.

Use of the abstraction model reduces the analysis time needed for multi-realization processes, such as Monte Carlo sampling or Latin Hypercube Sampling (LHS). In order for the probabilistic model abstraction to be used in lieu of the SDF PORFLOW Model, its validity must first be tested by comparing the abstraction model results with SDF PORFLOW Model results for a representative case. A reasonable degree of agreement between the two models is necessary to give confidence that the trends produced in the probabilistic analysis reflect the trends that would occur if the SDF PORFLOW Model is run repeatedly in a probabilistic mode.

Because of the simplifications associated with the abstraction use in the GoldSim model (i.e., reduction in dimensionality, coarser spatial and temporal discretization, etc.), a perfect match between GoldSim and PORFLOW results is not expected, but basic features of breakthrough curves reflecting processes such as material degradation and changes in chemical environments should be similar.

The following sections describe the approach used to benchmark the SDF GoldSim Model to the SDF PORFLOW Model and the results of that benchmarking.

5.1 Benchmarking Results

The benchmarking analysis was comprised of four phases. The first phase focused on how well the abstraction model (i.e., the SDF GoldSim Model) can approximate the PORFLOW-generated radionuclide releases from the SDUs. In the first phase, breakthrough curves of radionuclide releases to the saturated zone from the two models were compared. The second phase focused on how well the abstraction model approximates the radionuclide transport behavior in the saturated zone. PORFLOW-to-GoldSim model comparisons of radionuclide concentrations within specified sectors along the 100-meter boundary (Figure 2.0-1) form the basis of how well the abstraction model approximates in the dilution/attenuation processes in the saturated zone. Breakthrough curves representing the radionuclide concentrations over time for each of the several sectors form the basis of this comparison.

The third and fourth phases focused on how well the GoldSim-generated and PORFLOW-generated exposure-level time histories for the MOP and IHI scenarios, matched. Comparisons of the maximum total dose for the MOP scenario as well as the dose contributions from the major contributing radionuclides are the basis for the third phase of the benchmarking. Note that the maximum total dose to the MOP is the highest dose reported at each time step regardless of sector. Comparisons of the maximum total dose time histories and IHI well specific dose time

histories form the basis fourth phase of the analysis. Note that the maximum total dose to the IHI is the highest dose reported at each time step regardless of well.

The SA Evaluation Case, which is used in the benchmarking process, represents an alternate scenario for the time-based degradation of the SDU components, including the grout, HDPE liners, wall, floor and basemats, simulated to help answer specific questions asked by the NRC.

The species evaluated during benchmarking represent the most important dose contributors noted in the SDF PORFLOW Model simulations; I-129, Cs-135, Tc-99, and Ra-226. An additional species of less importance to dose results, Np-237, is also included to evaluate the ability of the model to handle extremely sorbent species. Because the “shrinking core” release model for Tc-99, utilized in PORFLOW, is not part of the abstracted model, the SDF GoldSim Model samples Tc-99 mass fluxes, from a set of pre-generated breakthrough curves. The set of curves were generated by the SDF PORFLOW Model and are used as boundary conditions for the saturated zone model in the SDF GoldSim Model (Section 3.3.2).

5.1.1 Mass Releases to the Saturated Zone

For all SDU types, I-129, Ra-226, and Np-237, mass flux breakthrough curves at the water table from the GoldSim and PORFLOW models, are compared during the benchmarking process. Cs-135 results are not presented for SDU 1 because the inventory of Cs-135 in SDU 1 is considered to be negligible. Also note that Tc-99 comparisons are not presented in this section because the releases are directly sampled from PORFLOW model outputs. Tc-99 concentration and dose level time-history comparisons are presented in later sections as indicators of how well the GoldSim saturated zone transport and dose models represent the PORFLOW saturated zone transport and dose models. The breakthrough curves presented here represent the total mass fluxes released at the bottom of the unsaturated zone.

5.1.1.1 SDU 1

A comparison of the SDF PORFLOW Model and SDF GoldSim Model mass releases of I-129 presented in Figure 5.1-1 indicate that the GoldSim model can produce a good approximation of the spike-type releases of I-129 from SDU 1 generated by the PORFLOW model. The GoldSim model produces a peak release that is slightly (3.7 %) higher than the PORFLOW results (see Table 5.1-1). The GoldSim model Ra-226 release presented in Figure 5.1-2, also closely resembles the PORFLOW model releases when breakthrough starts to occur at 20,000 years. The GoldSim Model peak at 20,000 years is 4.0 % higher than the PORFLOW model peak. A comparison of Np-237 releases at the water table from the two models presented in Figure 5.1-3 shows a similar release pattern.

Relative to results for the other two species, a greater difference in the breakthrough curves is seen with the peaks differing by 40 % and the PORFLOW-generated breakthrough curve lower than the Goldsim curve. The difference between the curves is reflective of the differences in the dimensionality of the flow field conceptualizations (vertically downward in the GoldSim model and fully two-dimensional in the PORFLOW model as described in Section 3.4.2). The models also differ in the degree of refinement (the PORFLOW model is more finely discretized), the GoldSim model uses zone-averaged flow rates based on the PORFLOW results, and floor joints are modeled as a single series of mixing cells in the GoldSim model. These differences are accentuated by radionuclide retardation associated

with the extremely high K_d 's of neptunium (5,000 mL/g to 10,000 mL/g) in cementitious materials. Figure 5.1-4 depicts the two breakthrough curves in semi-log form showing that the general trends of the two models are similar with the PORFLOW release breakthrough curve showing a more dispersed form.

Table 5.1-1: SDF GoldSim and PORFLOW Model Peak Unsaturated Zone Release Comparisons for SDU 1

Radionuclide	PORFLOW Peak Release (g/yr)	PORFLOW Time of Peak Release (yr)	GoldSim Peak Release (g/yr)	GoldSim Time of Peak Release (yr)	Percent Difference
I-129	4.5E-04	5,580	4.7E-04	5,580	3.7 %
Cs-135	N/A	N/A	N/A	N/A	N/A
Ra-226	4.2E-06	20,000	4.4E-06	20,000	4.0 %
Np-237	2.4E-06	20,000	3.2E-06	20,000	40.0 %

Figure 5.1-1: SDU 1 I-129 Release to the Saturated Zone

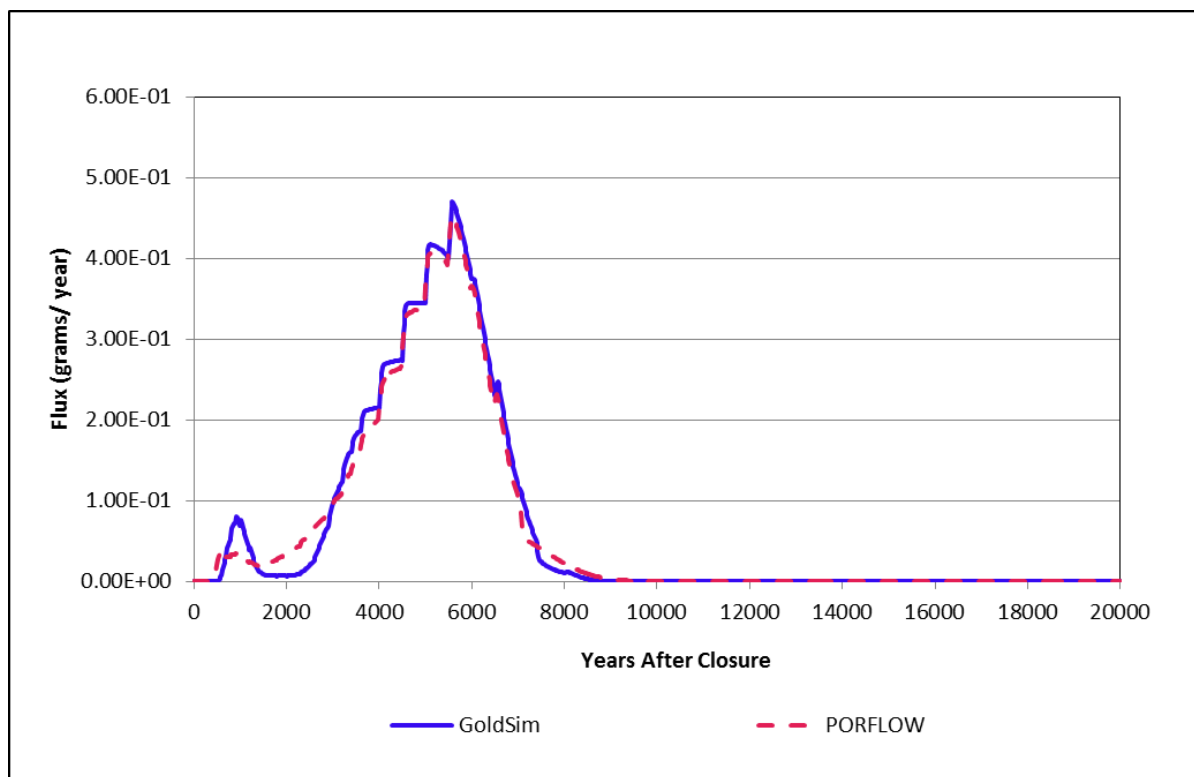


Figure 5.1-2: SDU 1 Ra-226 Release to the Saturated Zone

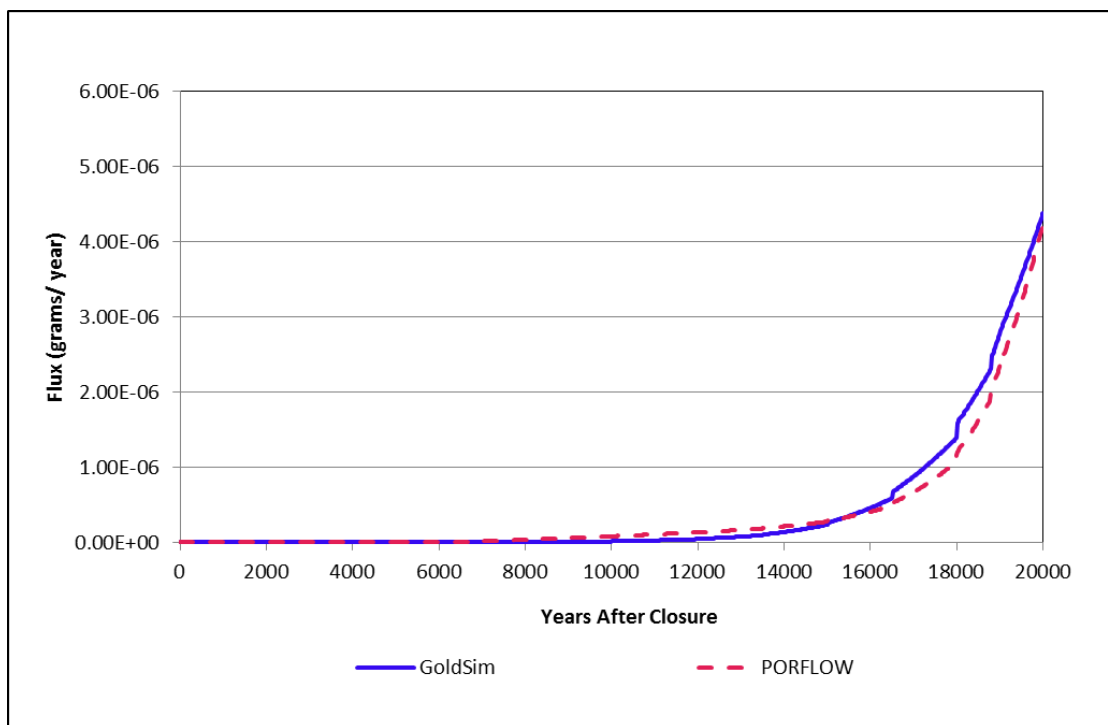


Figure 5.1-3: SDU 1 Np-237 Release to the Saturated Zone

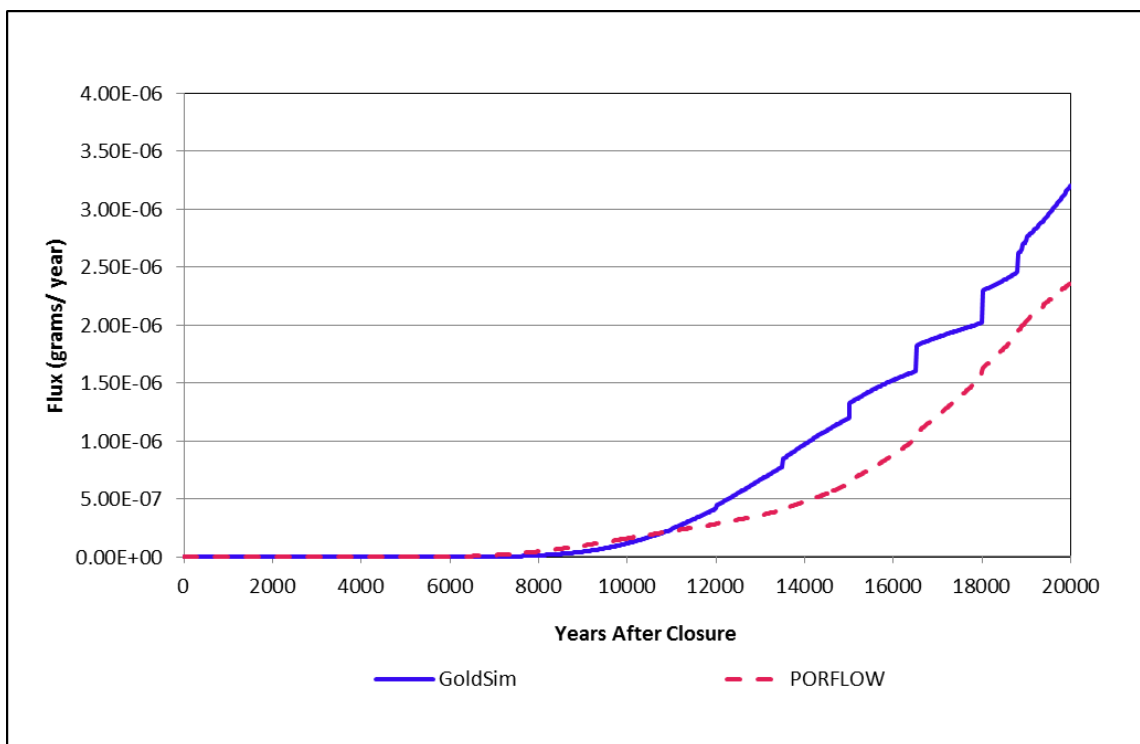
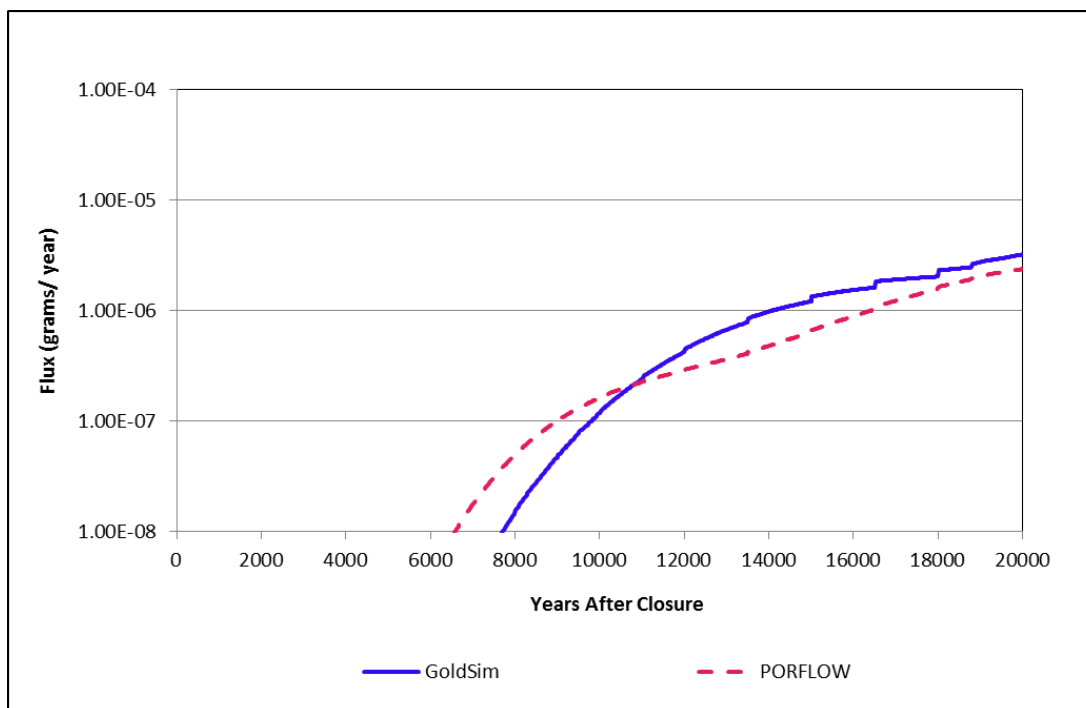


Figure 5.1-4: Semi-Log Plot of SDU 1 Np-237 Release to the Saturated Zone



5.1.1.2 SDU 4

Similar to results for SDU 1, the SDU 4 SDF PORFLOW Model and SDF GoldSim Model I-129 mass releases presented in Figure 5.1-5 indicate that the GoldSim model can produce a good approximation of the I-129 releases from SDU 4 generated by the PORFLOW model. The GoldSim model produces a peak release that is slightly (-9.6 %) lower than the PORFLOW results (see Table 5.1-2).

The GoldSim model Cs-135 release presented in Figure 5.1-6, also closely resembles the PORFLOW model releases with peak releases occurring at 5,120 years. The GoldSim Model peak at 5,120 years is 6.2 % higher than the PORFLOW model peak.

The GoldSim model Ra-226 release presented in Figure 5.1-7 also resembles the PORFLOW model releases with the GoldSim Model peak at 20,000 years being 18.2 % lower than the PORFLOW model peak at the same time. The Ra-226 curves do not match quite as well as in the SDU 1 comparison, but when viewed in a semi-log plot the similarity of the trends of the curves is readily seen (Figure 5.1-8).

A comparison of Np-237 releases at the water table from the two models presented in Figure 5.1-9 differ, but when looked at on a semi-log scale (Figure 5.1-10) the breakthrough curves have the same basic trend, with the PORFLOW curve being more dispersed. The difference in Np-237 peaks for the two models is only 8.2 % (Table 5.1-2), but the time of the peak values differs by 7,800 years. The difference between the curves can be partially attributed to differences in the dimensionality of the flow-field conceptualizations (vertically downward in the GoldSim model and fully two-dimensional in the PORFLOW model as described in Section 3.4.2). Other differences found in the abstraction model include zone-averaged flow rates, coarser discretization of the model, and floor joints simulated individually in the

PORFLOW model, combined into a single column of cells in the GoldSim model (Section 3.4.2). These differences are accentuated by a radionuclide retardation associated with the extremely high K_d s of neptunium (5,000 mL/g to 10,000 mL/g) in cementitious materials. In addition to controlling the main release of Np-237, the high cementitious K_d s of neptunium play an important role on the localized effects in the model, accentuating the differences between the two models. Because of the high K_d s, the dominant source of release for the first 20,000 years in SDU 4 is in the area of the walls. In the wall area, horizontal flow from the backfill into the wall and floor occurs, a process not considered in the abstraction model. This limitation in the model is not considered important because it only influences a small percentage of the Np-237 in SDU 4. Figure 5.1-10 depicts the two breakthrough curves in semi-log form showing that the general trends of the two models are similar with the PORFLOW release exhibiting a greater degree of dispersion.

Table 5.1-2: SDF GoldSim and PORFLOW Model Peak Unsaturated Zone Release Comparisons for SDU 4

Radionuclide	PORFLOW Peak Release (g/yr)	PORFLOW Time of Peak Release (yr)	GoldSim Peak Release (g/yr)	GoldSim Time of Peak Release (yr)	Percent Difference
I-129	1.7E+00	3,480	1.5E+00	3,620	-9.6 %
Cs-135	3.7E+00	5,120	4.0E+00	5,120	6.2 %
Ra-226	3.8E-05	20,000	3.1E-05	20,000	-18.2 %
Np-237	3.6E-04	20,000	3.3E-04	12,200	-8.3 %

Figure 5.1-5: SDU 4 I-129 Release to the Saturated Zone

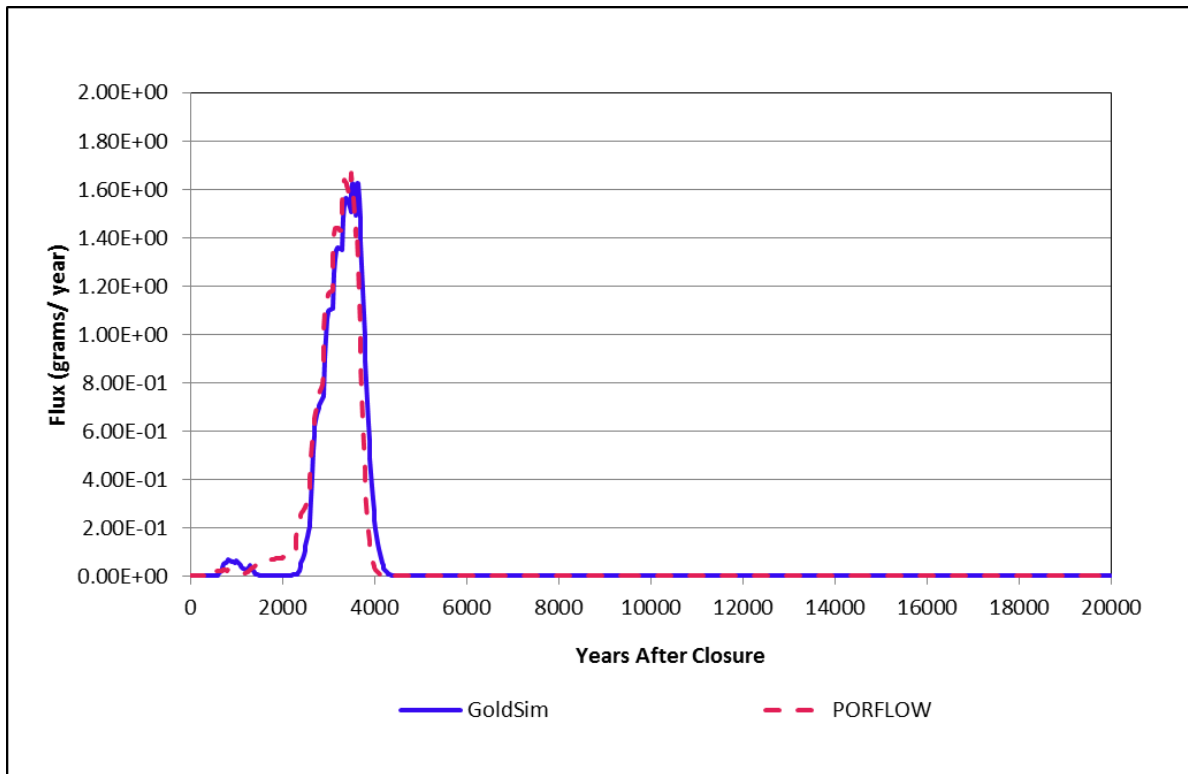


Figure 5.1-6: SDU 4 Cs-135 Release to the Saturated Zone

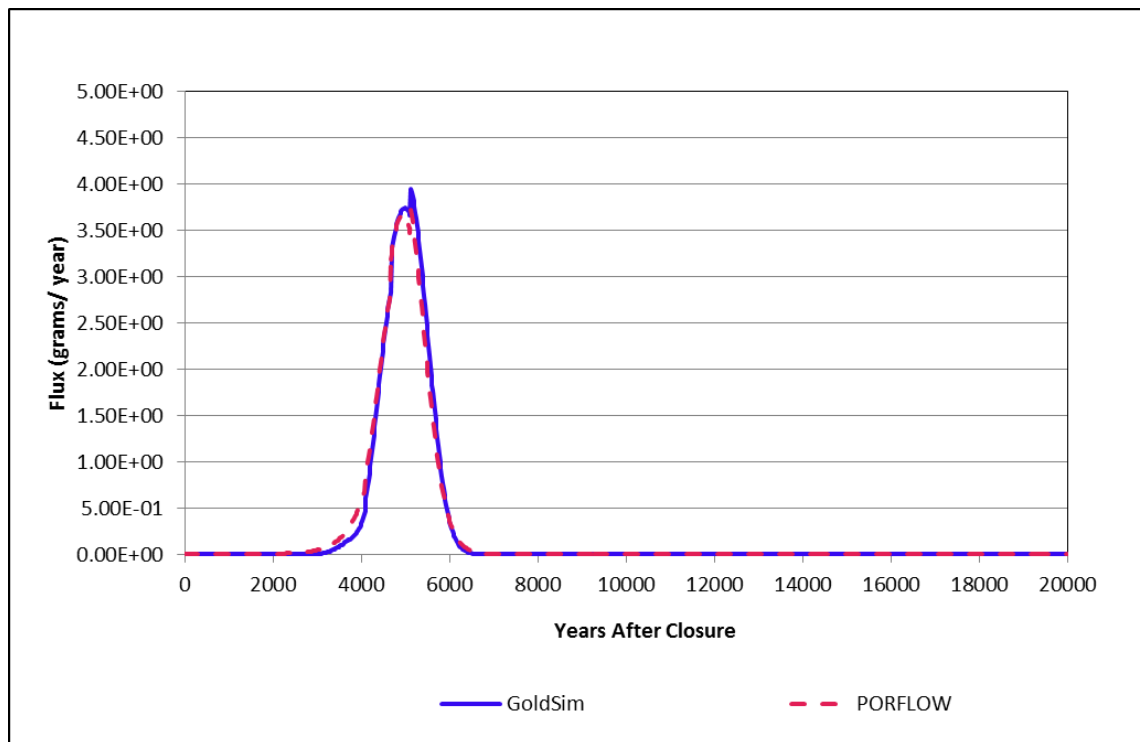


Figure 5.1-7: SDU 4 Ra-226 Release to the Saturated Zone

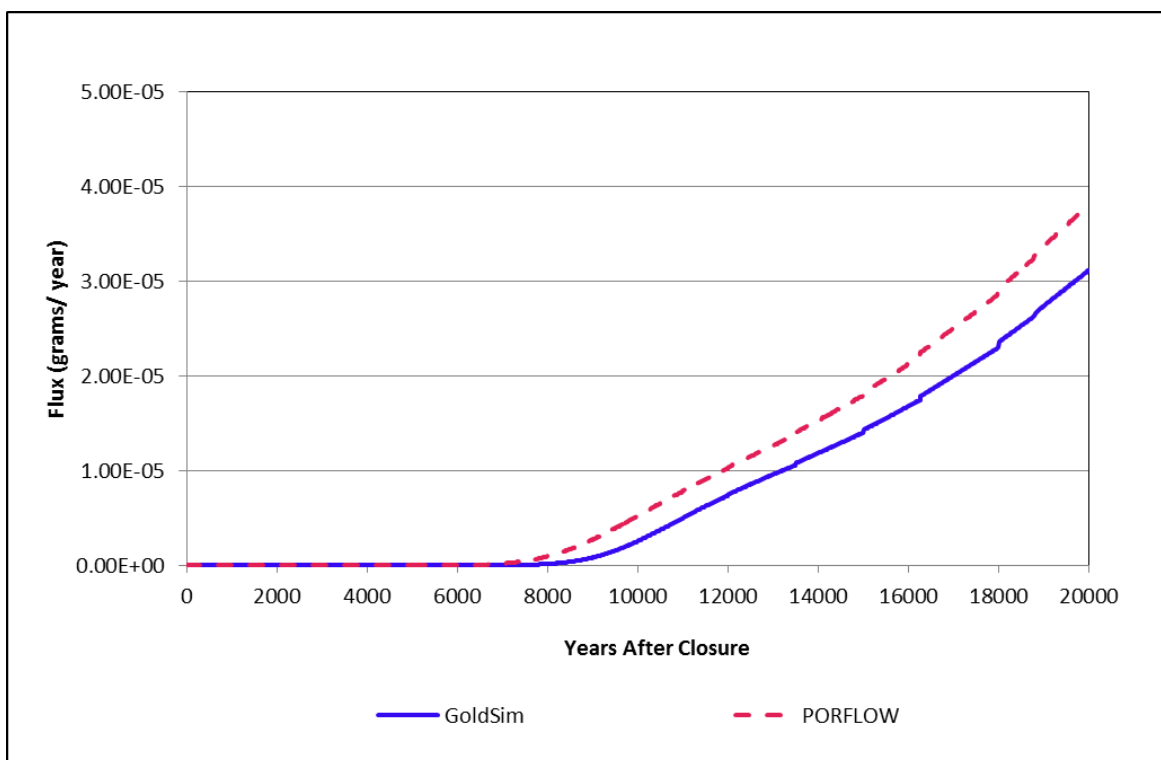


Figure 5.1-8: Semi-Log Plot of SDU 4 Ra-226 Release to the Saturated Zone

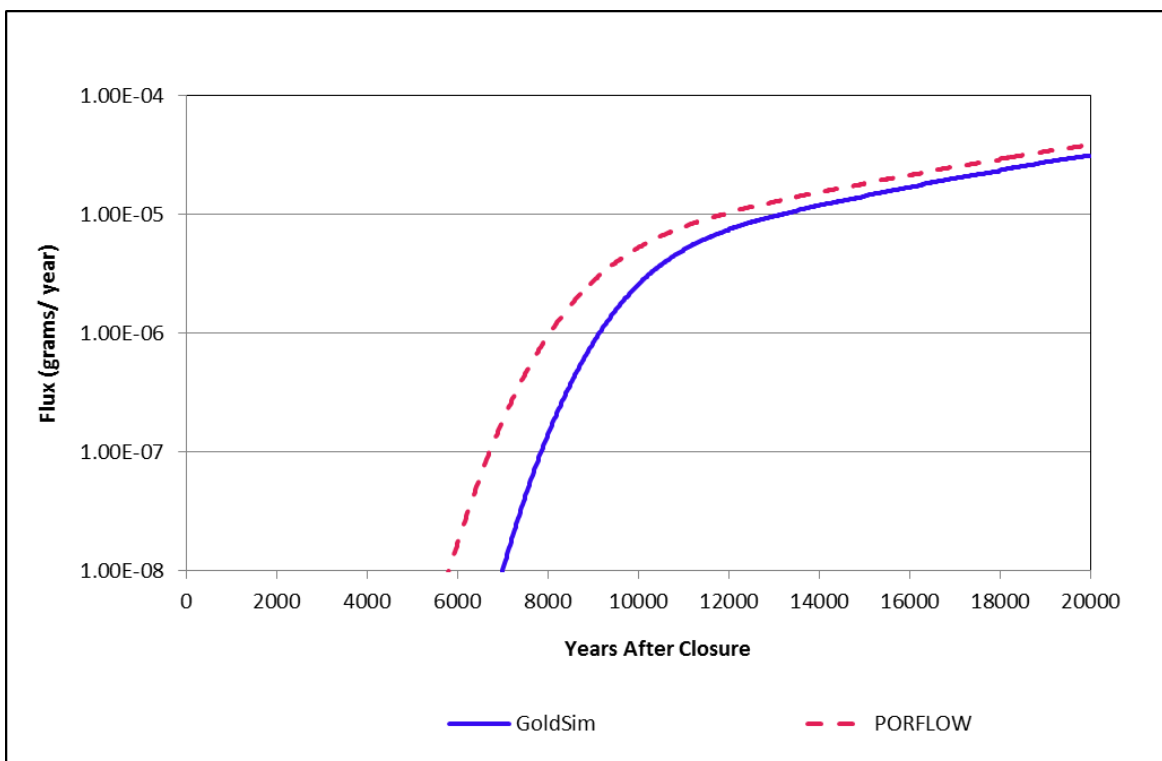


Figure 5.1-9: SDU 4 Np-237 Release to the Saturated Zone

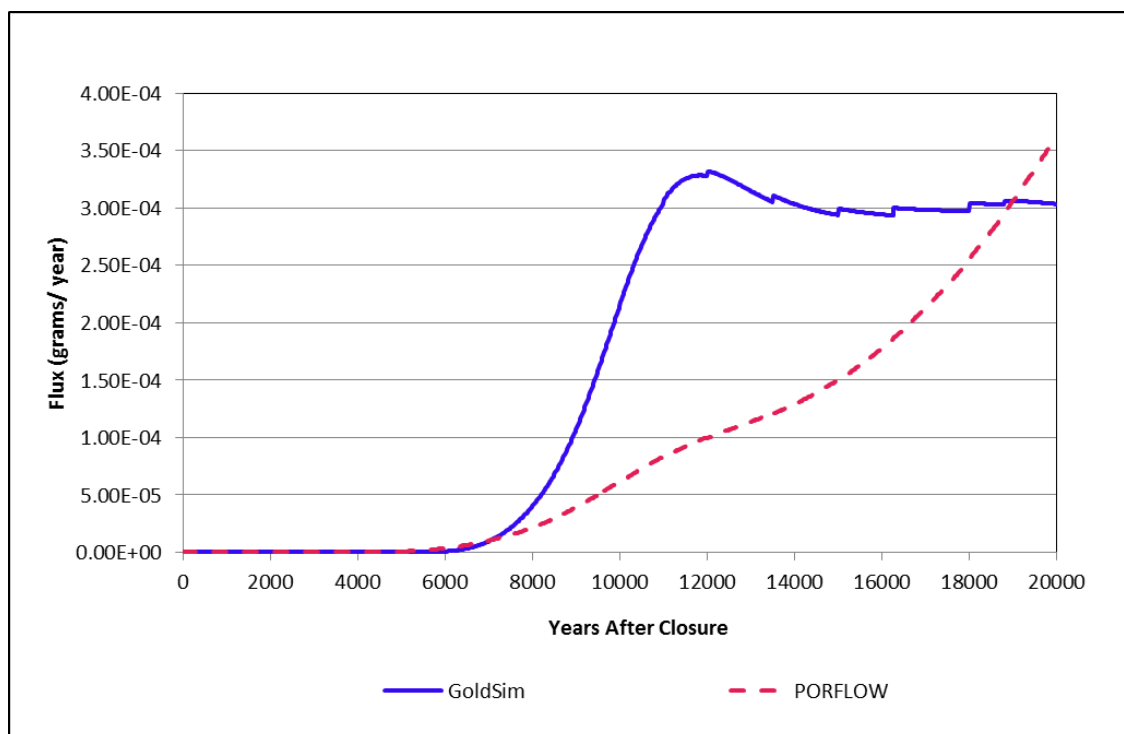
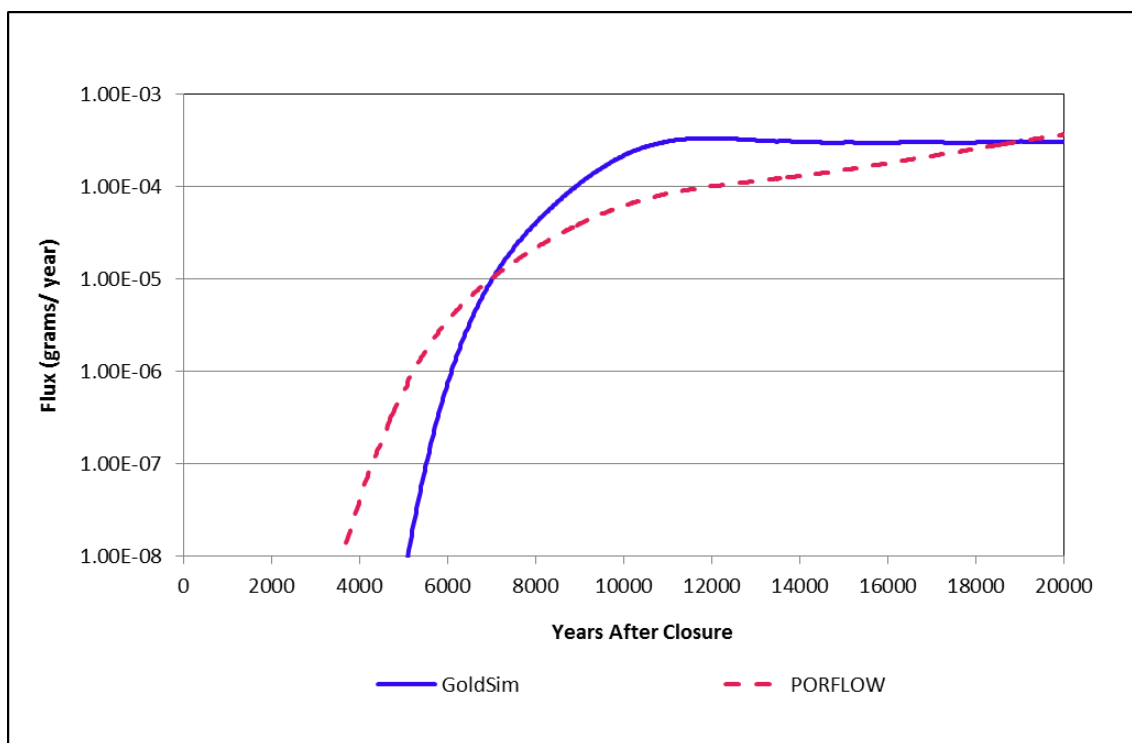


Figure 5.1-10: Semi-Log Plot of SDU 4 Np-237 Release to the Saturated Zone



5.1.1.3 FDCs

In the future SDUs (represented here as FDC), SDF PORFLOW Model and SDF GoldSim Model I-129 mass releases presented in Figure 5.1-11 indicate that the GoldSim model can produce a good approximation of the I-129 releases and trends generated by the PORFLOW model. The GoldSim model produces a peak release that is 12.6 % higher than the PORFLOW results (see Table 5.1-3).

The GoldSim model Cs-135 release presented in Figure 5.1-12, closely replicates the PORFLOW model release in shape but the GoldSim breakthrough curve does arrive sooner (the peak is at 12,020 years as opposed to 13,520 years) and is slightly more dispersed with a peak value that is 18.3 % lower than the PORFLOW peak. The difference in breakthrough times can be associated with the higher unsaturated-zone K_d in cesium in conjunction with the more rigorous handling of the flow-field in the PORFLOW model where horizontal flow in the unsaturated zone causes much of the release to the saturated zone to occur directly below the column. In the PORFLOW model, the vertical velocity in the unsaturated zone increases from below the column outward, a pattern not reflected in the spatially averaged flow rate used in the GoldSim model. Note that this difference in breakthrough timing does not occur in the SDU 4 results (see Figure 5.1-6) where the unsaturated zone flow is more dominantly vertical and the vertical component of flow does not vary as much from the SDU centerline outward. The trends in the release curves are still adequately similar and the earlier release in the GoldSim model is conservative.

The GoldSim model Ra-226 release presented in Figure 5.1-13 also resembles the PORFLOW model releases with the GoldSim Model peak at 20,000 years being 18.2 % higher than the PORFLOW model peak at the same time. A comparison of Np-237 releases at the water table, generated by the two models presented in Figure 5.1-14 shows quite similar releases with the difference in peak values being only 4.1 % (Table 5.1-2).

Table 5.1-3: SDF GoldSim and PORFLOW Model Peak Unsaturated Zone Release Comparisons for FDCs

Radionuclide	PORFLOW Peak Release (g/yr)	PORFLOW Time of Peak Release (yr)	GoldSim Peak Release (g/yr)	GoldSim Time of Peak Release (yr)	Percent Difference
I-129	1.1E+00	7,660	1.3E+00	7,580	12.6 %
Cs-135	2.6E-05	13,520	2.1E+00	12,020	-18.3 %
Ra-226	5.4E-08	20,000	7.5E-08	20,000	18.2 %
Np-237	2.9E-09	20,000	3.0E-09	20,000	4.1 %

Figure 5.1-11: FDC I-129 Release to the Saturated Zone

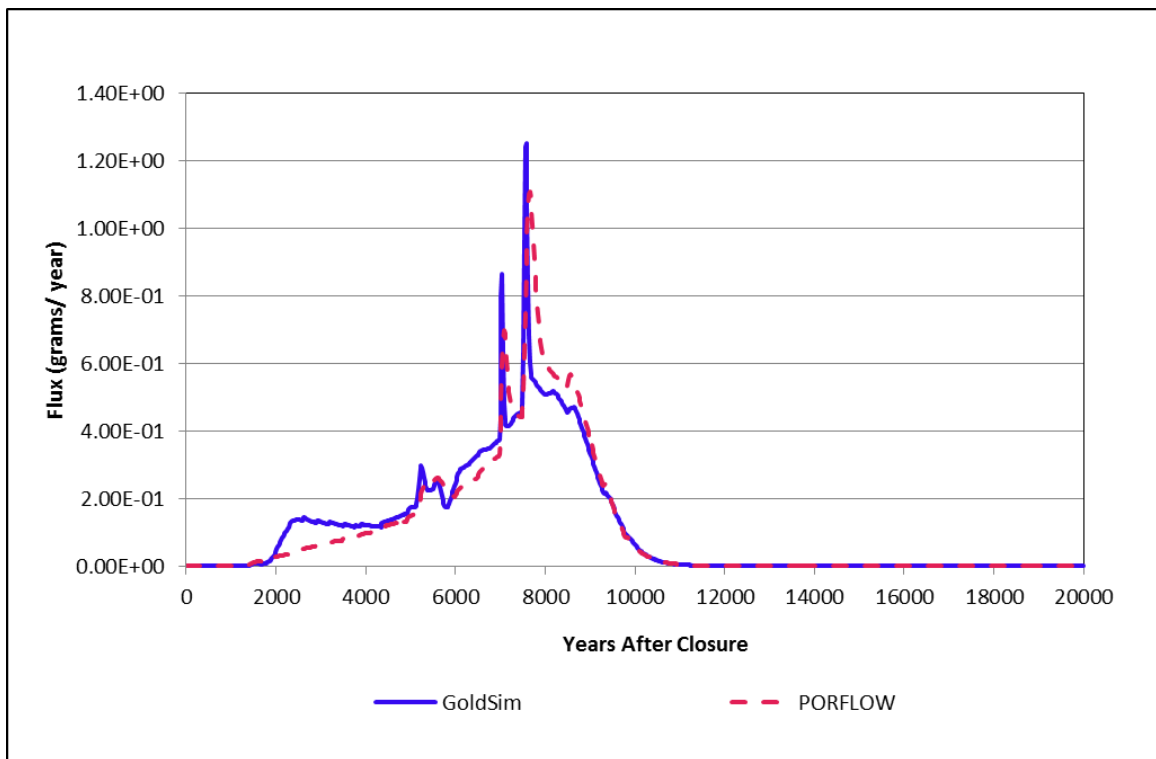


Figure 5.1-12: FDC Cs-135 Release to the Saturated Zone

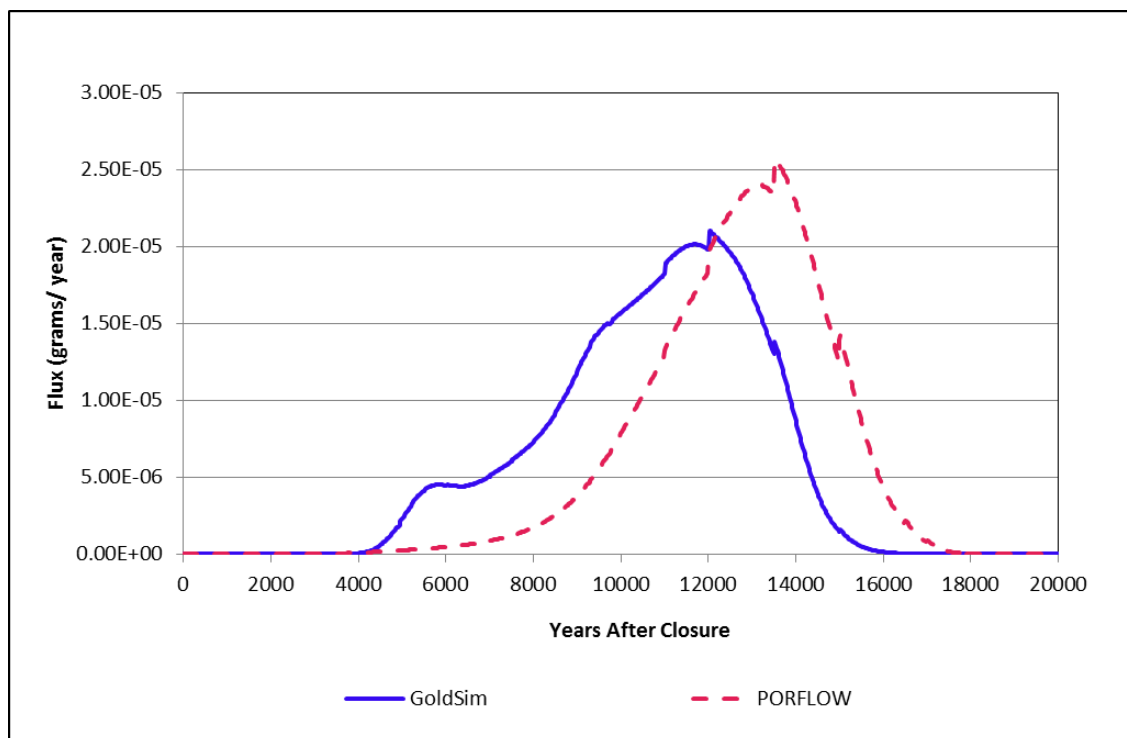


Figure 5.1-13: FDC Ra-226 Release to the Saturated Zone

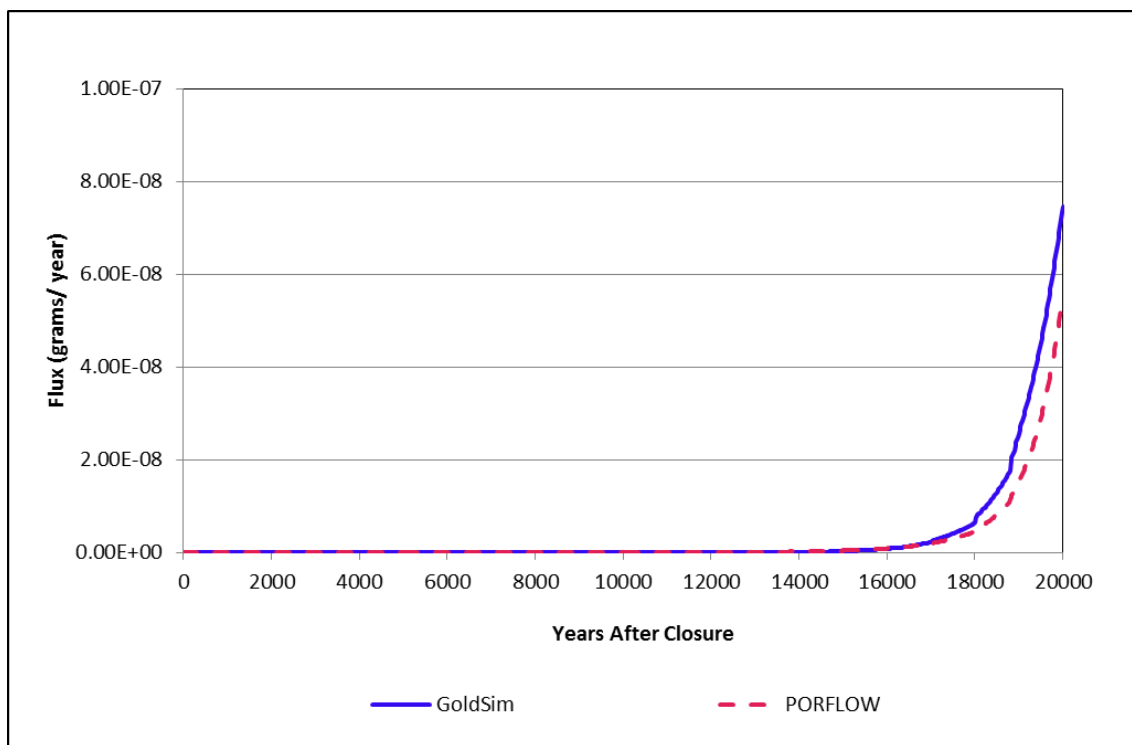
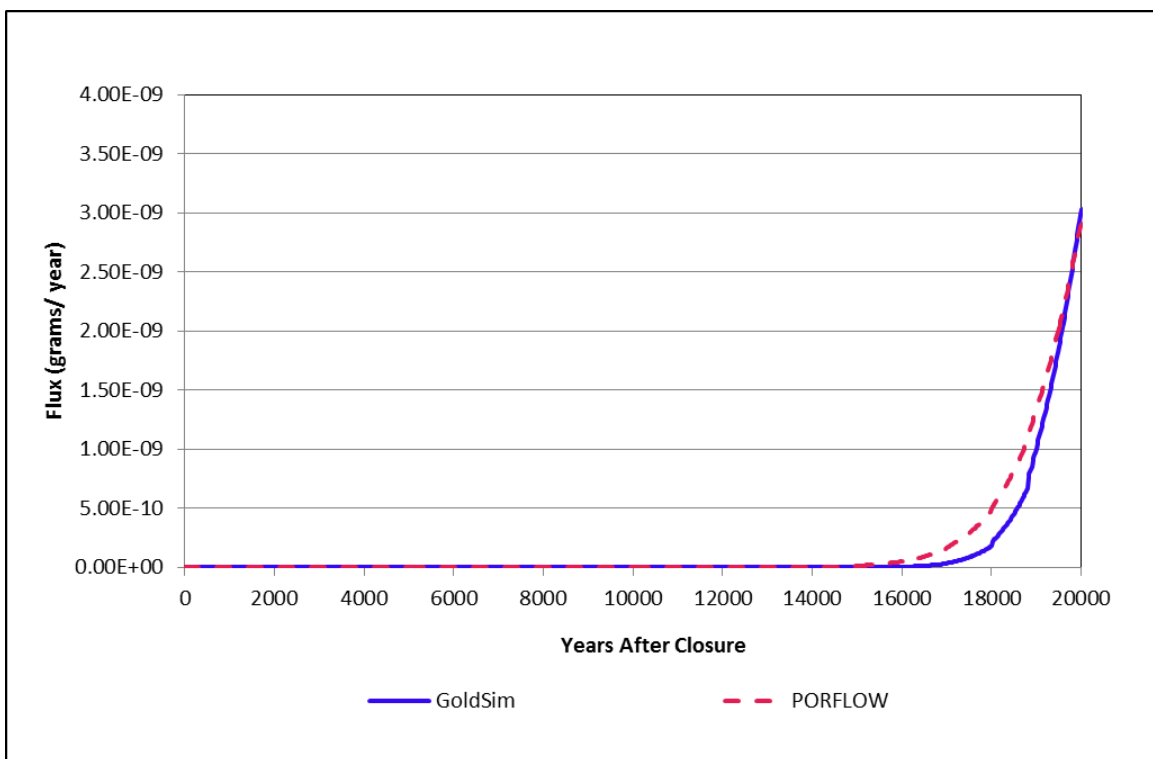


Figure 5.1-14: FDC Np-237 Release to the Saturated Zone



5.1.2 Radionuclide Concentrations at the 100-Meter Boundary

The second phase of the benchmarking process focuses on examining how well the abstracted model approximates the radionuclide transport behavior in the saturated zone. Radionuclide concentrations (in picocuries per liter), in four sectors (B, G, H, and I), were examined for this task (see Figure 2.0-1). Sector B was selected for this analysis because it contains the highest PORFLOW and GoldSim model concentrations of the southern SDU sectors. Sector G was chosen because it contains the peak GoldSim model concentration for the northern SDU locations and Sector I was chosen because it contains the peak PORFLOW model concentration for the northern SDU locations. Sector H was selected due to its proximity to Sector I, and the similarity between PORFLOW Sector H and I results. Concentration comparisons between PORFLOW and GoldSim model results showed less consistency in Sector I, which is located above a groundwater divide, than for Sector H. For this exercise, breakthrough curves of PORFLOW and GoldSim model results for the five species (I-129, Cs-135, Ra-226, Tc-99, and Np-237) were examined.

5.1.2.1 Sector B

An examination of PORFLOW- and GoldSim-generated radionuclide concentrations presented in Figure 5.1-15 indicates that the SDF GoldSim Model can provide a computationally efficient approximation of 100-meter boundary radionuclide concentrations in Sector B. There is a good consistency in the trends observed in the two sets of model results throughout the 20,000-year simulation. The basic dilution/attenuation processes in

the saturated zone are captured by the abstraction. Note that there are also differences but they will have little impact on the utility of the abstraction model to evaluate peak doses.

As noted above, Tc-99 in the saturated zone, as modeled in GoldSim, uses sampled mass-release time histories from a set of PORFLOW simulations as a boundary condition. Comparing the PORFLOW-generated and GoldSim-generated Tc-99 concentration breakthrough curves for Sector B it can be seen that the saturated zone as modeled in GoldSim closely approximates the saturated zone as modeled in PORFLOW.

A comparison of the Cs-135 breakthrough curves in Figure 5.1-15 shows that the peak of the PORFLOW concentration breakthrough curve is accurately reproduced, but at lower concentrations the breakthrough curve appears to be broader. This difference in breakthrough curves is consistent with the SDU 4 mass flux release curve when shown in semi-log presented in Figure 5.1-16. Therefore, the modeled results from the saturated zone abstraction are consistent with the PORFLOW model results. It should be noted that after 6,500 years, the GoldSim concentrations decrease at a faster rate than the PORFLOW concentrations. This difference in the curves is associated with the occurrence of the “green clay” layer (i.e., the Gordon Confining Unit), which is modeled explicitly in the PORFLOW model, but not in the GoldSim model. The “green clay” layer provides a storage zone for more sorptive elements such as cesium, from which the radionuclides like Cs-135 are more slowly released. Since the breakthrough curves differ at well below peak levels, the simplification in the GoldSim model is not important in dose calculations.

A comparison of the I-129 breakthrough curves in Figure 5.1-15 also shows that the PORFLOW concentration breakthrough curve is accurately represented. As with Cs-135, the influence of the “green clay” layer at lower concentrations can be seen. Note that the difference, between the I-129 and Cs-135 PORFLOW model breakthrough curve slopes (at low concentrations) is reflective of the lower I-129 K_d value. Comparing the PORFLOW- and GoldSim-generated Ra-226 and Np-237 breakthrough curves presented Figure 5.1-15 with the mass flux release curves presented in Figures 5.1-8 and 5.1-10, respectively, it can also be seen that the saturated zone as modeled in GoldSim performs well.

Figure 5.1-15: Maximum Radionuclide Concentrations at 100-Meter Boundary for Sector B

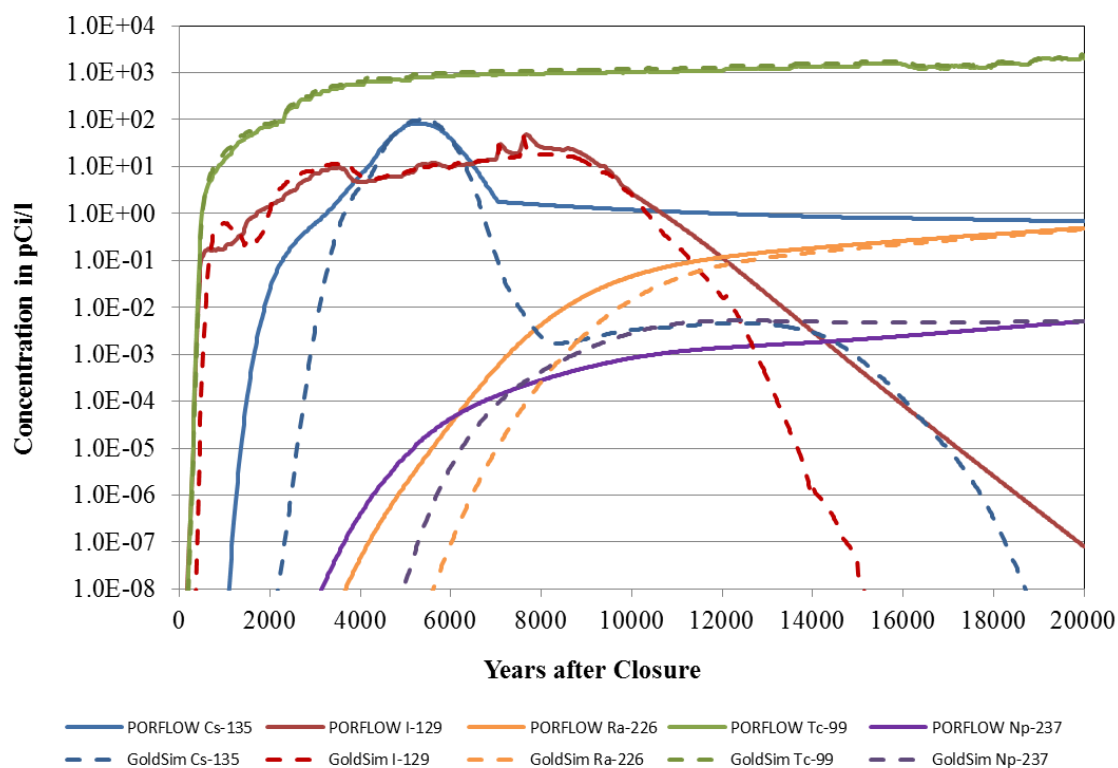
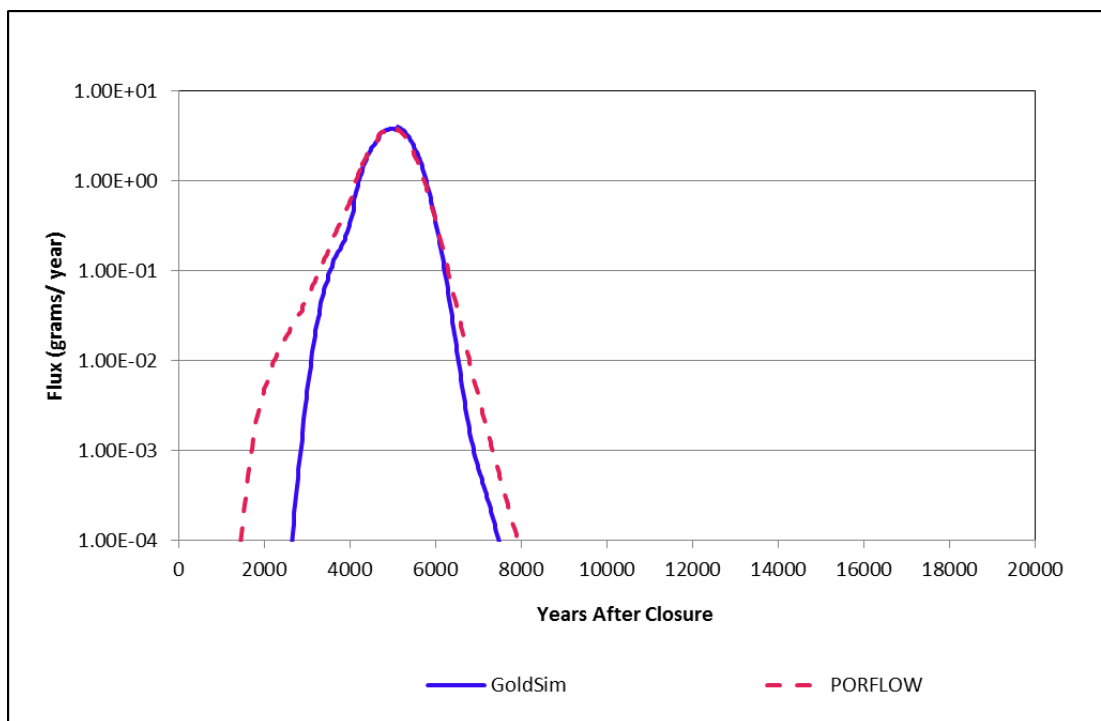


Figure 5.1-16: Semi-Log Plot of the SDU 4 Cs-135 Release to the Saturated Zone



5.1.2.2 Sector G

An examination of PORFLOW- and GoldSim-generated radionuclide concentrations presented in Figure 5.1-17 indicates that the SDF GoldSim Model can also provide a computationally efficient approximation of 100-meter boundary radionuclide concentrations in northern sectors such as Sector G. There is a consistency in the trends observed in the two sets of model results throughout the 20,000-year simulation. The basic dilution/attenuation processes in the saturated zone are captured by the abstraction, but again there are also differences that will have little impact on the utility of the abstraction model to evaluate peak doses.

As discussed in more detail in Section 5.1.1.4.1, comparing the PORFLOW-generated and GoldSim-generated Tc-99 concentration breakthrough curves for Sector G, shows that the saturated zone as modeled in GoldSim closely approximates the results of the more rigorous PORFLOW saturated zone transport simulations. A comparison of the Cs-135 breakthrough curves in Figure 5.1-17 shows differences that reflect the temporal differences in the peaks of the PORFLOW and GoldSim model mass flux release curves discussed in in Section 5.1.1.3. Again, the tail of the PORFLOW Cs-135 breakthrough curve shows the influence of the “green clay” layer at lower concentrations.

A comparison of the I-129 breakthrough curves presented in Figure 5.1-17 also shows that the PORFLOW concentration breakthrough curve is accurately represented by the GoldSim model results. As with the Cs-135 breakthrough curve, the influence of the “green clay” layer at lower concentrations can be seen. Note that at very low concentrations the GoldSim-generated I-129 breakthrough curve behaves strangely. This seems to reflect a breakdown of the analytic solution used in the GoldSim pipe model, which may be associated with the

numerical inversion of the LaPlace domain solution in the model. This is only occurs at very low concentrations and does not affect the results.

Comparing the PORFLOW- and GoldSim-generated Ra-226 breakthrough curves presented Figure 5.1-17 with Figure 5.1-18 below which is a semi-log plot of the SDU 2 Ra-226 release curve, it can be seen that the saturated zone as modeled in GoldSim closely approximates the results generated by the saturated zone as modeled in PORFLOW. Note that the mass-flux release curves differ mainly at very low concentrations.

Comparing the PORFLOW- and GoldSim-generated Np-237 breakthrough curves presented Figure 5.1-17 a major difference is seen between the two models. The PORFLOW-generated Np-237 breakthrough occurs well before the GoldSim model breakthrough. This difference is associated with another simplification used in the GoldSim abstraction. The GoldSim abstraction does not explicitly model the Gordon Aquifer in the radionuclide transport analysis. The early-time segment of the Np-237 breakthrough curve seen in the PORFLOW results presented in Figure 5.1-17 reflects transport through the Gordon Aquifer of a portion of the SDU 4 Np-237 mass release presented in Figure 5.1-10. The omission is acceptable because PORFLOW simulations indicate that the concentrations in the Gordon Aquifer tend to be much lower than in the UTR-UZ and UTR-LZ and would therefore not be important in peak dose analyses.

Figure 5.1-17: Maximum Radionuclide Concentrations at 100-Meter Boundary for Sector G

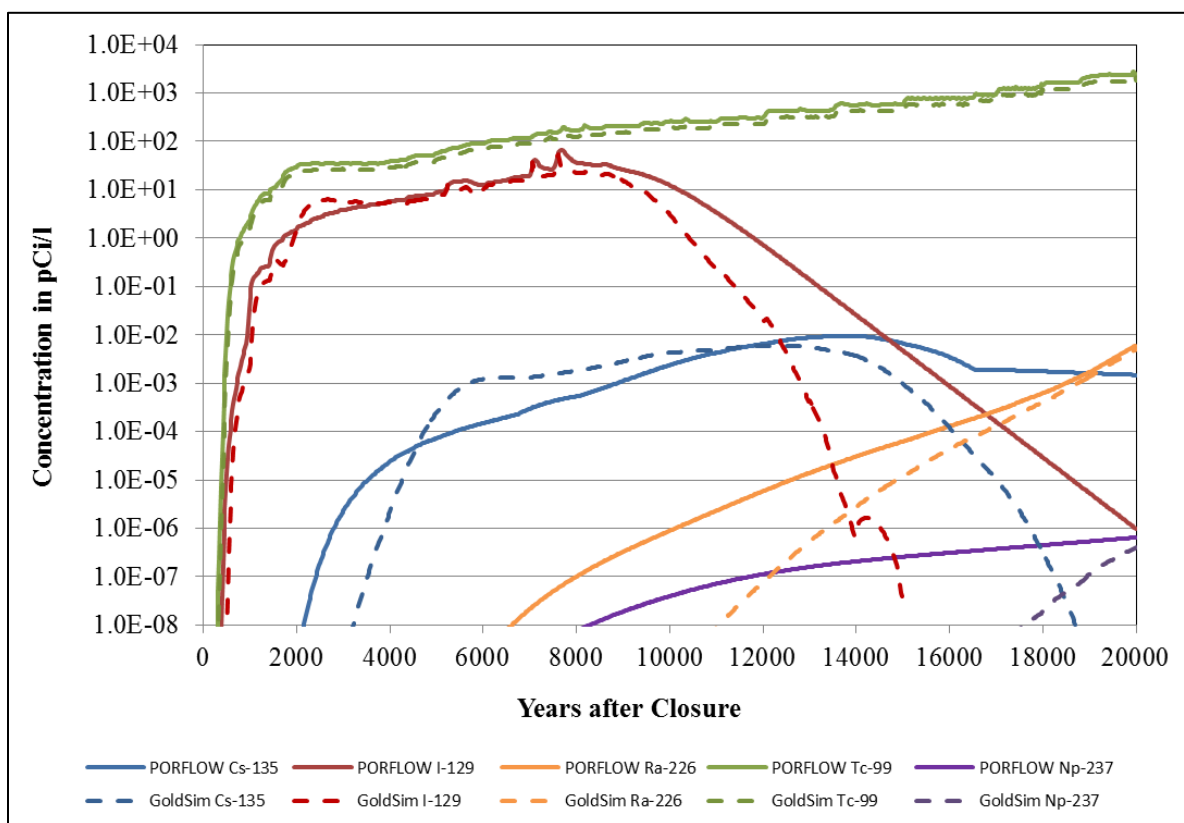
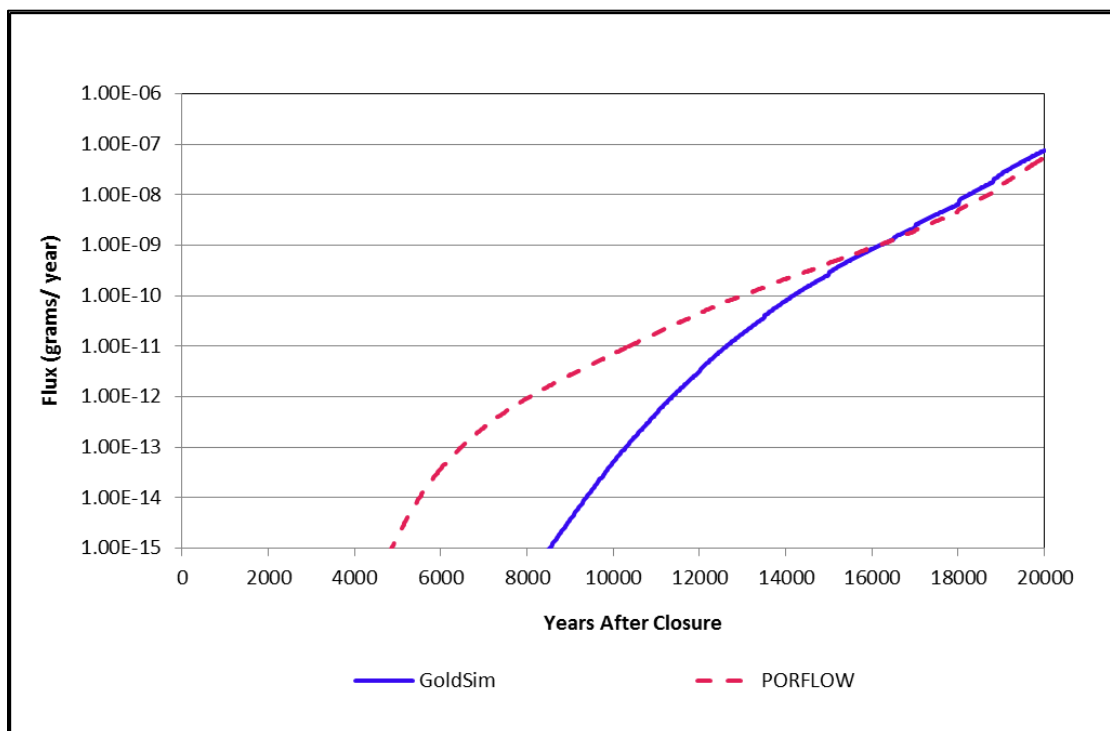


Figure 5.1-18: Semi-Log Plot of an SDU 2 Ra-226 Release to the Saturated Zone



5.1.2.3 Sector H

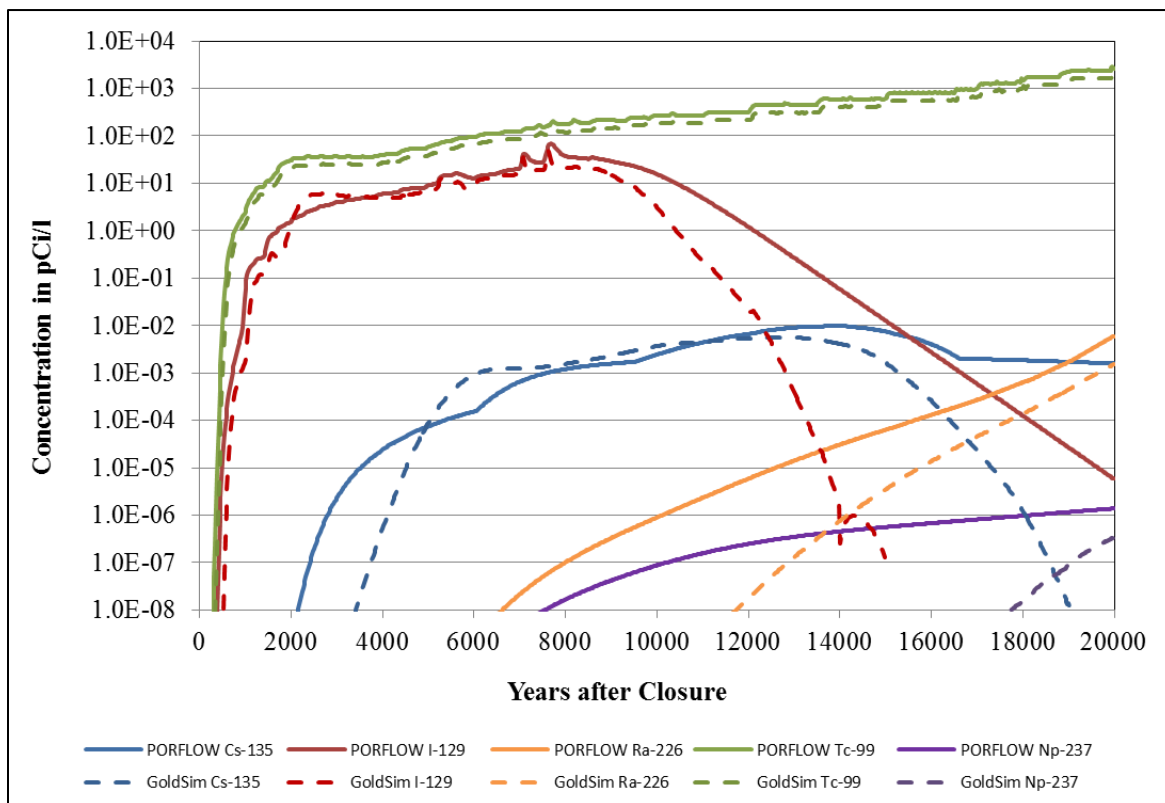
Radionuclide concentrations at the 100-meter boundary are presented here for Sector H because the concentrations in Sectors H and I are very similar in the PORFLOW runs. This is not true for the GoldSim runs because the simpler analytical solutions used in the GoldSim model do not fully capture the influence of the groundwater divide on the 100-meter boundary concentrations in Sector I.

An examination of PORFLOW- and GoldSim-generated radionuclide concentrations presented in Figure 5.1-19 indicates that the SDF GoldSim Model can also provide a computationally efficient approximation of 100-meter boundary radionuclide concentrations in northern sectors such as Sector H. This is important because of the model differences for Sector I. Similar to the Sector G comparison, there is a good consistency in the trends observed in the two sets of model results throughout the 20,000-year simulation. The basic dilution/attenuation processes in the saturated zone are similarly captured by the abstraction, but again there are also differences that have little impact on the utility of the abstraction model to evaluate peak doses.

For Tc-99, I-129, Cs-135, and Np-237, a comparison between the PORFLOW-generated and GoldSim-generated concentration breakthrough curves for Sector H is consistent with the comparison for Sector G such that the similar aspects will not be discussed here. The major difference between the Sector G and Sector H results can be seen by comparing Ra-226 curves. As can be seen in the Sector G plot (Figure 5.1-17) the GoldSim model concentrations approach the PORFLOW model concentrations at later times (higher concentrations). This is not true for Sector H where the influence of the ground water divide

increases the Ra-226 concentrations enough that the differences are perceptible and the PORFLOW breakthrough curve is to be higher.

Figure 5.1-19: Maximum Radionuclide Concentrations at 100-Meter Boundary for Sector H

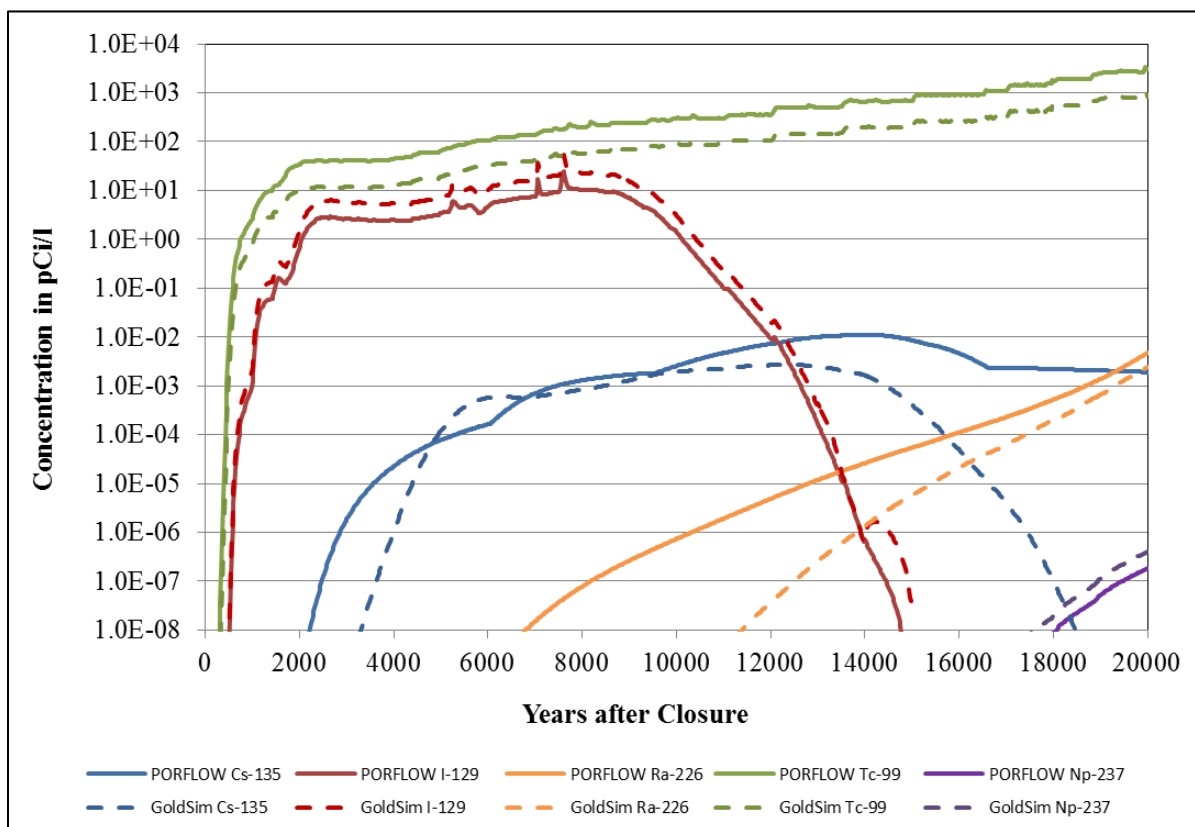


5.1.2.4 Sector I

Radionuclide concentrations at the 100-meter boundary are presented here for Sector I because the concentrations in Sector I are generally the highest in the PORFLOW runs. This is not true for the GoldSim runs because the simpler analytical solutions used in the GoldSim model do not fully capture the influence of the groundwater divide (as reflected in the streamlines presented in Figure 2.0-1) on the 100-meter boundary concentrations in Sector I.

An examination of PORFLOW- and GoldSim-generated radionuclide concentrations presented in Figure 5.1-20 indicates that the SDF GoldSim Model underestimates the concentrations at the 100-meter boundary for all the examined species. Note that despite underestimating the concentrations, the basic trends indicative of flow field and chemistry changes are captured by the GoldSim model.

Figure 5.1-20: Maximum Radionuclide Concentrations at 100-Meter Boundary for Sector I



5.1.3 MOP Dose Time Histories

The third phase of the benchmarking process focuses on examining how well the abstracted model approximates the MOP dose results. Comparisons of the maximum total MOP dose levels (in millirem per year) generated by the two models form the basis of this phase of the benchmarking effort along with a comparison of dose contributions from the major contributing radionuclides.

5.1.3.1 Total MOP Dose Time Histories

An important check on the appropriateness of the SDF GoldSim Model as a surrogate for the SDF PORFLOW Model is a comparison between the maximum total doses generated by the two models. The Evaluation Case maximum dose and sector specific dose time histories for from the GoldSim model are presented in Figure 5.1-21.

A comparison between Figure 5.1-21 and the equivalent data from the PORFLOW model simulations presented in Figure 5.1-22 shows that the GoldSim model closely approximates the maximum doses generated by the PORFLOW model and the trends in dose for most sectors. The 20,000-year maximum doses curve plotted in Figure 5.1-22 is also presented in Figure 5.1-23 along with the PORFLOW-generated maximum dose curve.

Differences do arise due to the influence of the groundwater divide as discussed in Section 5.1.1.4. For the PORFLOW model, the Evaluation Case has a peak dose of 11.6 mrem/yr

occurring in Sector I at 7,700 years. For the GoldSim model, the Evaluation Case has a peak dose of 8.3 mrem/yr occurring in Sector G at 7,600 years. In addition to the influence of the groundwater divide, other simplifications in the GoldSim model that influence how well individual sector results from both models match include the nature of the spatial and temporal discretization of the models. Because the PORFLOW results are generated at each node in a finely discretized grid, for a given time, sector results are based upon the maximum concentration of any node within the sector, including nodes from the Upper-UTR, the Lower-UTR, or the Gordon Aquifers. In contrast, the GoldSim model results are based on the concentrations generated at the center of each sector resulting from the superposition of plume concentrations from the various SDU releases. This center-point analysis may potentially underestimate the GoldSim peak doses relative to the PORFLOW results. The PORFLOW maximum point analysis will add a degree of numerical dispersion to the PORFLOW breakthrough curves since the point of analysis can shift in time.

The one sector that shows a large degree of variance between the two models due to the center-point analysis is Sector F. This difference is associated with the GoldSim model evaluating the results at the center of the sector and PORFLOW consistently choosing the results near the contact between Sectors E and F, picking up more of the mass from SDU 4. Since the GoldSim model also bases maximum dose results for the southern sectors on Sectors A through E, the model differences in Sector F calculations are unimportant.

In addition, the GoldSim simulations use larger time steps (20 years versus two years) to reduce the simulation run times. This will also slightly underestimate the maximum dose results for spike-type releases. Despite the GoldSim model simplifications, the similarity between GoldSim model results and PORFLOW model results justifies the use of the GoldSim model for evaluating parameter sensitivity and the influence of parameter uncertainty on the system.

Figure 5.1-21: GoldSim Total Maximum MOP Dose Evaluation Case Results by Sector over 20,000 years

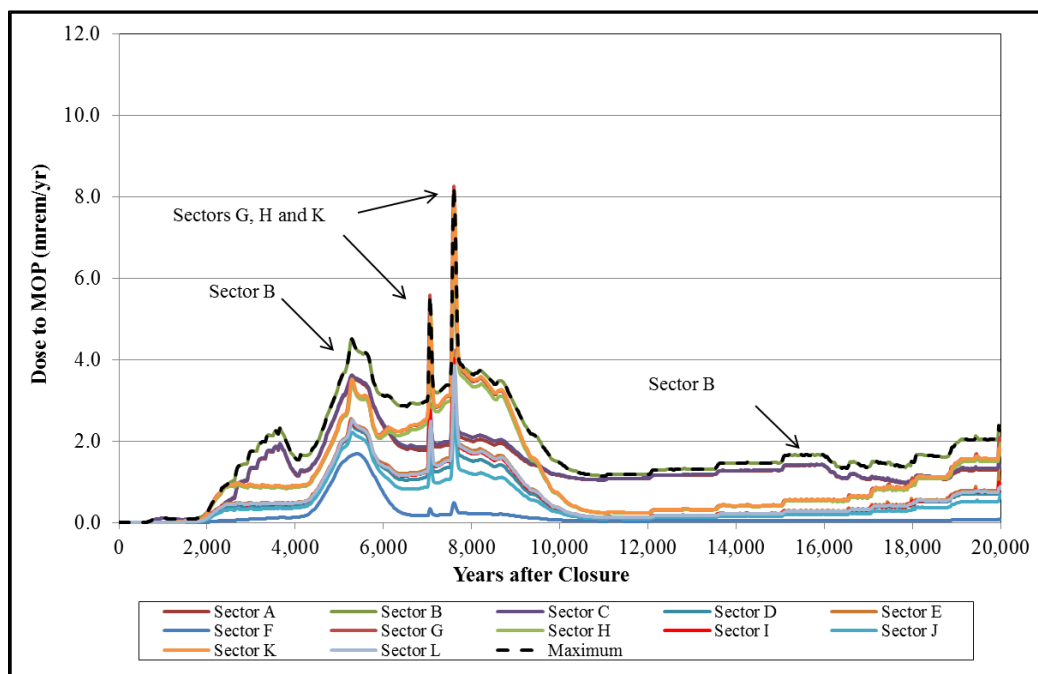


Figure 5.1-22: PORFLOW Total Maximum MOP Dose Evaluation Case Results by Sector over 20,000 years

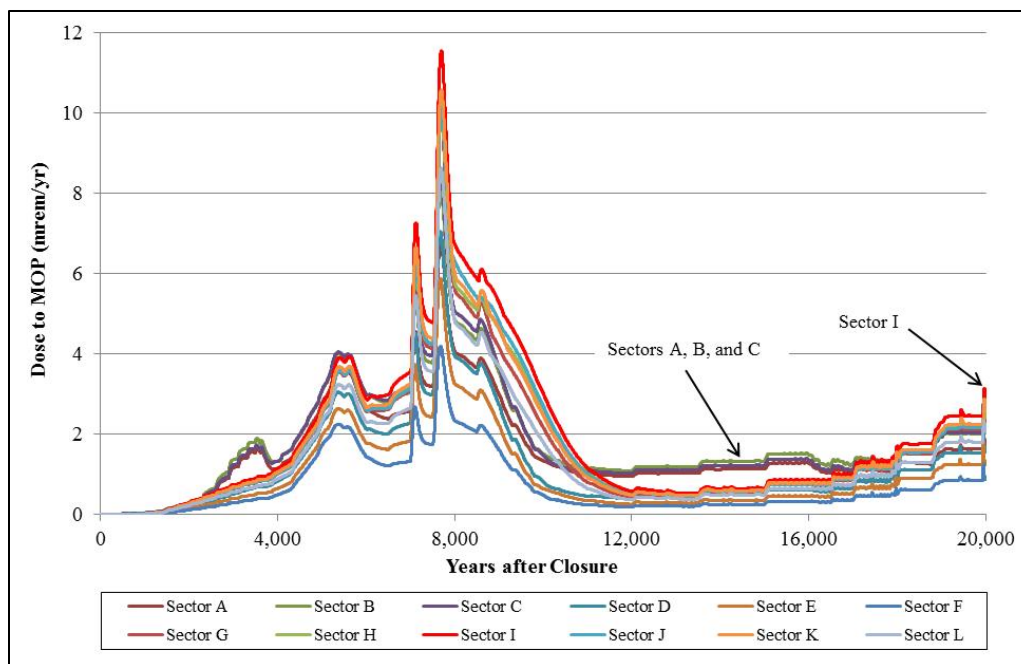
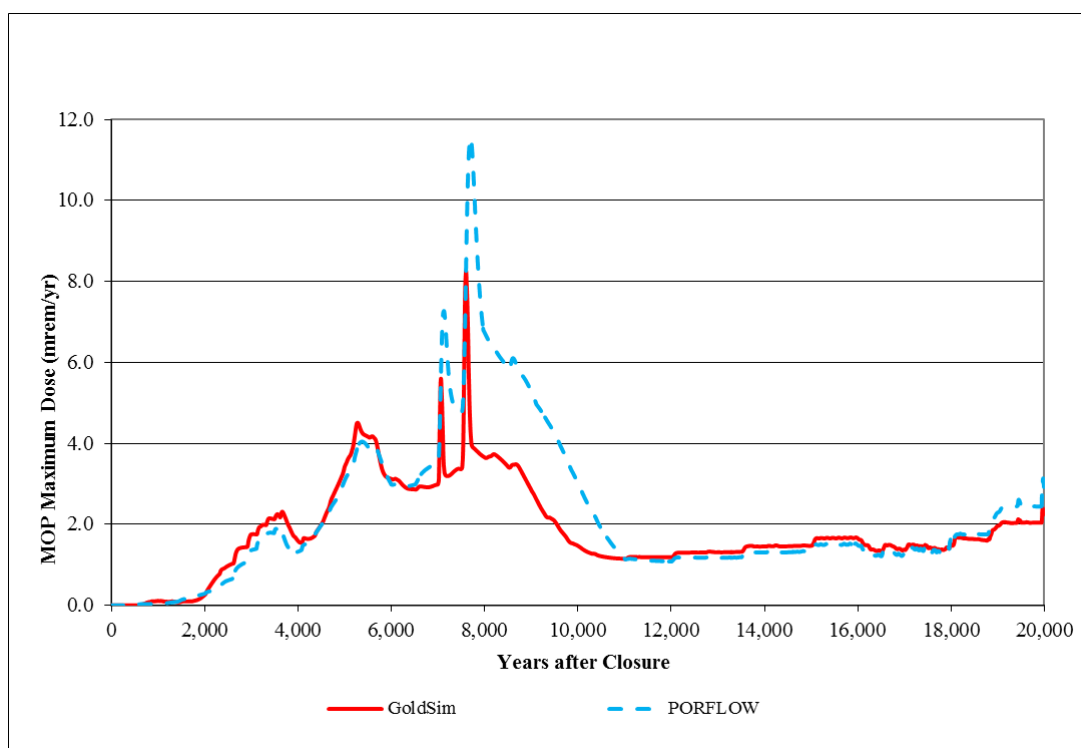


Figure 5.1-23: Comparison of Maximum MOP Dose Evaluation Case Results over 20,000 years



5.1.3.2 Radionuclide Contributions to Total MOP Dose Time Histories

This section presents a comparison of the SDF GoldSim Model and SDF PORFLOW Model dose breakthrough curves for the major contributing species to MOP dose, I-129, Cs-135, Tc-99, and Ra-226. The MOP dose breakthrough curves are presented for Sectors B, G, and H.

5.1.3.2.1 Sector B

As can be seen by comparing the GoldSim-generated species dose contributions presented in Figures 5.1-23 to the comparable results from PORFLOW presented in Figure 5.1-24, the SDF GoldSim Model closely approximates the PORFLOW-generated results for Sector B for all species. The peak dose from the GoldSim model over the 20,000 year analysis period is 7.4 mrem/yr, occurring at 7,600 years. For the PORFLOW model the peak dose over the same period is 8.1 mrem/yr, occurring at 7,682 years. The GoldSim-generated Sector B peak dose is therefore 8.6 % lower. As can be readily seen, the release of I-129 dominates the peak dose results over the 20,000 year period.

Figure 5.1-23: Individual Radionuclide Contributions to the GoldSim Sector B 100-meter Peak Groundwater Pathway Dose Results at 20,000 Years

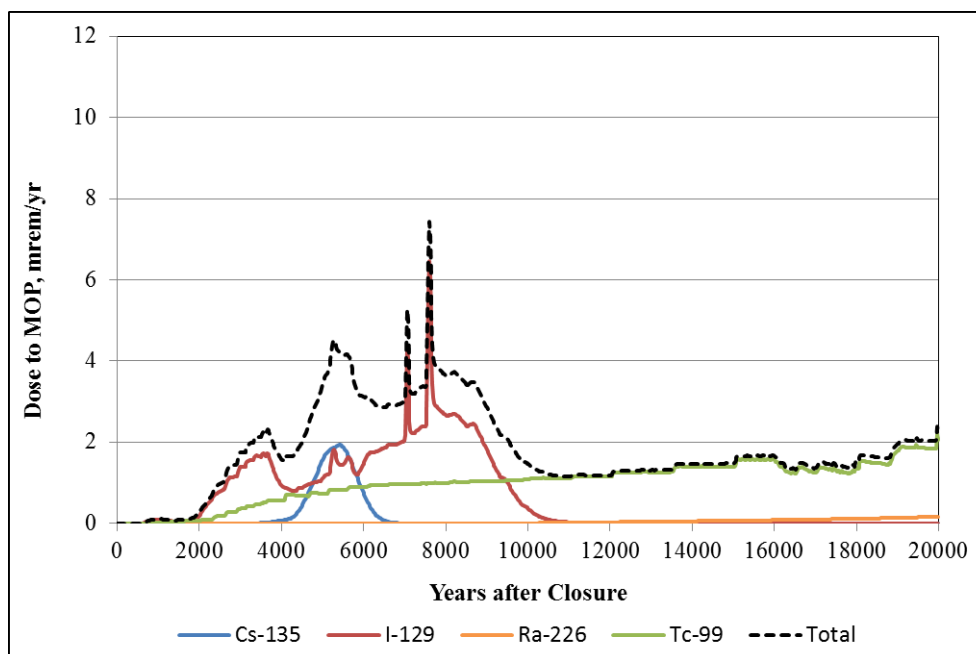
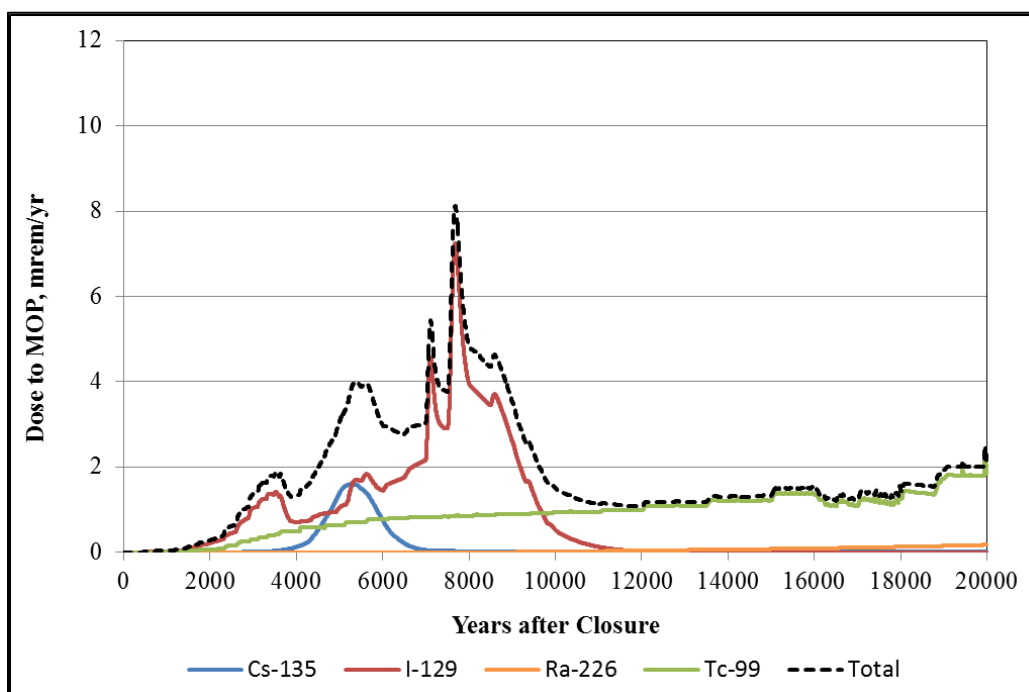


Figure 5.1-24 Individual Radionuclide Contributions to the PORFLOW Sector B 100-meter Peak Groundwater Pathway Dose Results at 20,000 Years



5.1.3.2.1 Sector G

By comparing the GoldSim-generated species dose contributions presented in Figures 5.1-25 to the comparable results from PORFLOW presented in Figure 5.1-26, it can be seen that the SDF GoldSim Model closely approximates the PORFLOW-generated results in Sector G for all species, although not quite as good as in Sector B. The peak dose for Sector G, from the GoldSim model over the 20,000 year analysis period is 8.3 mrem/yr, occurring at 7,600 years. For the PORFLOW model the peak dose over the same period is 10.0 mrem/yr, occurring at 7,688 years. The GoldSim-generated Sector B peak dose is therefore 17 % lower. As with Sector B, the release of I-129 dominates the peak dose results in Sector G over the 20,000 year period.

Figure 5.1-25: Individual Radionuclide Contributions to the GoldSim Sector G 100-meter Peak Groundwater Pathway Dose Results at 20,000 Years

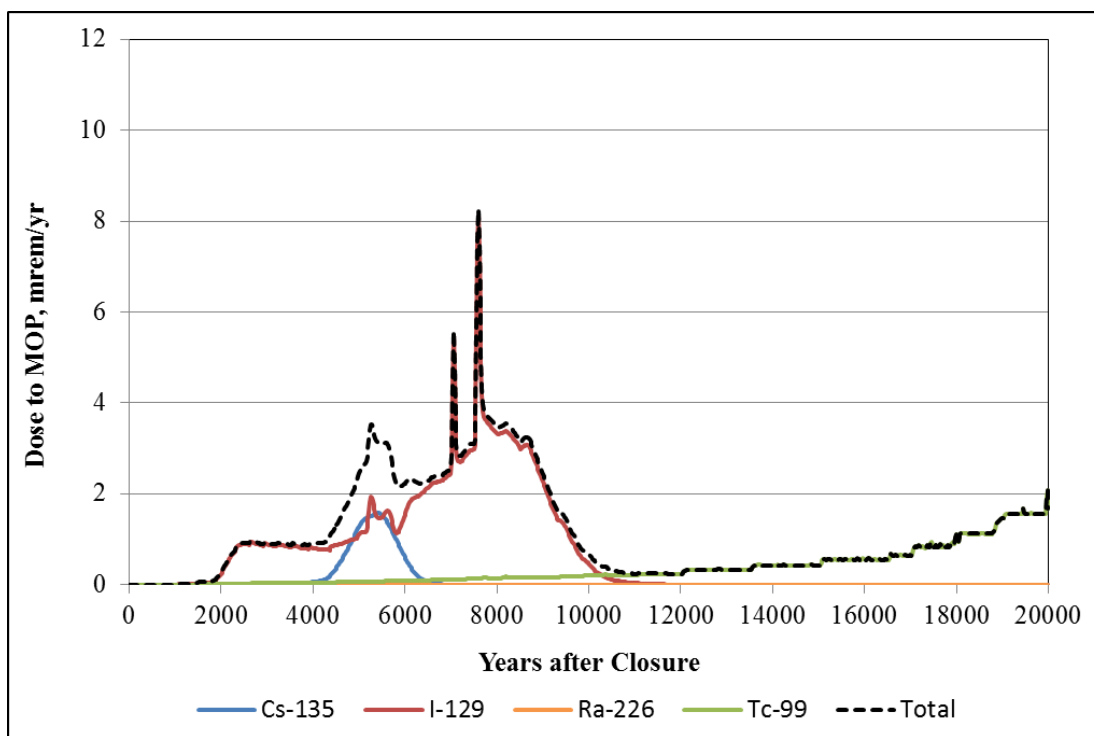
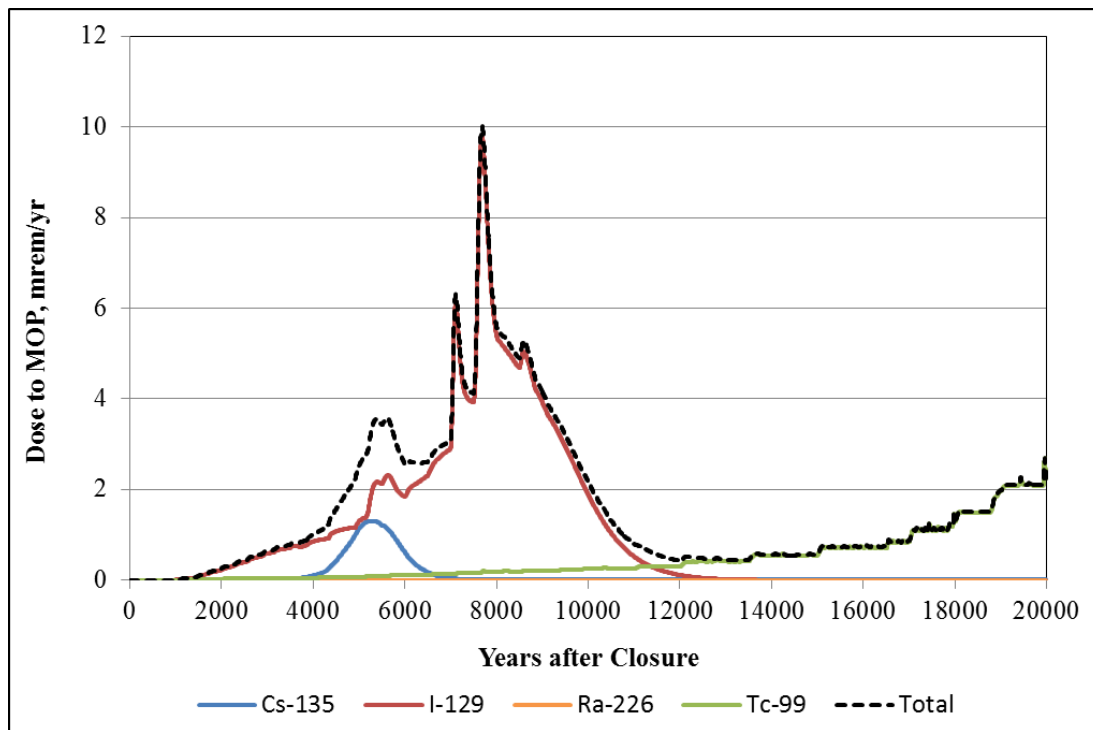


Figure 5.1-26 Individual Radionuclide Contributions to the PORFLOW Sector G 100-meter Peak Groundwater Pathway Dose Results at 20,000 Years



5.1.3.2.3 Sector H

By comparing the GoldSim-generated species dose contributions presented in Figures 5.1-27 to the comparable results from PORFLOW as presented in Figure 5.1-28, it can be seen the SDF GoldSim Model closely approximates the PORFLOW-generated results for Sector H for all species, but again not quite as good as in Sector B. The peak total dose for Sector H, from the GoldSim model over the 20,000-year analysis period is 7.8 mrem/yr, occurring at 7,620 years. For the PORFLOW model the peak dose over the same period is 10.3 mrem/yr, occurring at 7,688 years. The GoldSim-generated Sector B peak dose is therefore 24 % lower. As with Sectors B and G, the release of I-129 dominates the peak dose results in Sector H over the 20,000-year period.

Figure 5.1-27: Individual Radionuclide Contributions to the GoldSim Sector H 100-meter Peak Groundwater Pathway Dose Results at 20,000 Years

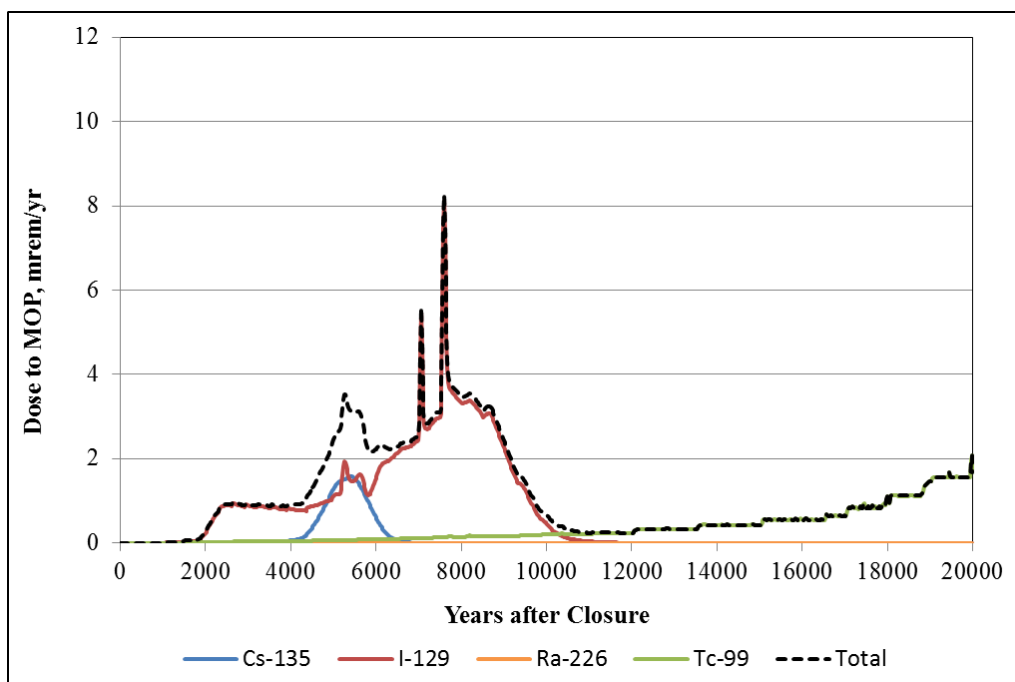
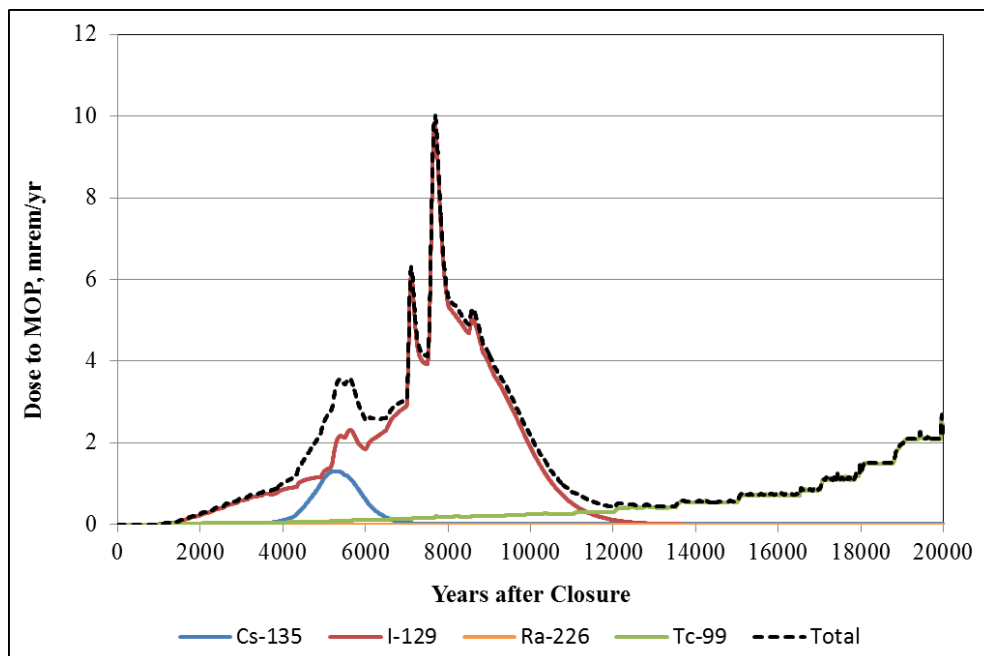


Figure 5.1-28 Individual Radionuclide Contributions to the PORFLOW Sector H 100-meter Peak Groundwater Pathway Dose Results at 20,000 Years



5.1.4 IHI Well Dose Time Histories

The fourth phase of the benchmarking process focuses on examining how well the abstracted model approximates the IHI dose results at the seven well analyzed in the GoldSim and PORFLOW Models. Comparisons of the maximum total dose results (in millirem per year) and individual well dose levels generated by the two models for the IHI are the basis for the fourth phase.

5.1.4.1 Total IHI Dose Time Histories

In this section, the IHI analysis for the SDF PORFLOW and SDF GoldSim Models are compared to demonstrate how closely the GoldSim model approximates the PORFLOW IHI dose time histories. The results are presented in the form of dose time histories for the seven wells (Well #1 through Well #7) whose locations are shown in Figure 3.3-3. An additional time history representing the maximum value from all wells for each time step is also presented.

The results of the IHI dose history analyses for the two models are presented in Figures 5.1-29 (for the GoldSim model) and 5.1-30 (for the PORFLOW model). As a group, it can be seen that the trends predicted by the GoldSim model are quite similar to the trends predicted by the PORFLOW model. For the GoldSim model, the maximum peak value for all wells is 36.3 mrem/yr and occurs at 7,600 years. For the PORFLOW model, the maximum peak value for all wells generated by the PORFLOW model is 32.2 mrem/yr and occurs at 7,668 years.

A closer look at the curves does shows that though trends are always similar, there are differences with respect to which of the individual wells has the higher peak value and differences in the peak values. Figures 5.1-31 (for the GoldSim model) and 5.1-32 (for the PORFLOW model) show the dose time histories for the northern wells. The peak values tend to be around twice as high for the GoldSim results, although, the GoldSim and PORFLOW model results are similar for Well #1. The peak exposure levels for Well #1 are 19.1 mrem/yr for the GoldSim results and 24.3 for the PORFLOW results, a difference of 21 %.

Figures 5.1-33 (for the GoldSim model) and 5.1-34 (for the PORFLOW model) show the dose time histories for the southern wells (#6 and #7). Although showing similar trends, the peak values for Well #6 are 17.6 mrem/yr and 32.2 mrem/yr for the GoldSim and PORFLOW simulations, respectively. Note that the peak exposure levels for Well #7 are quite close, 7.5 mrem/yr and 7.4 mrem/yr for the GoldSim and PORFLOW simulations, respectively. The differences between the individual well results are not surprising because of the proximity of the wells to the SDUs and differences in the effects on dispersion over short distances. It should be noted that the GoldSim concentrations are taken at depth level of the centerline of the source as opposed to over an element thickness, which may explain the generally higher GoldSim results. On the other hand, when taking into account the maximum exposure levels from all wells as depicted in Figure 5.1-35, the two models generate quite similar results.

Figure 5.1-29: GoldSim Model IHI Well Dose Time Histories

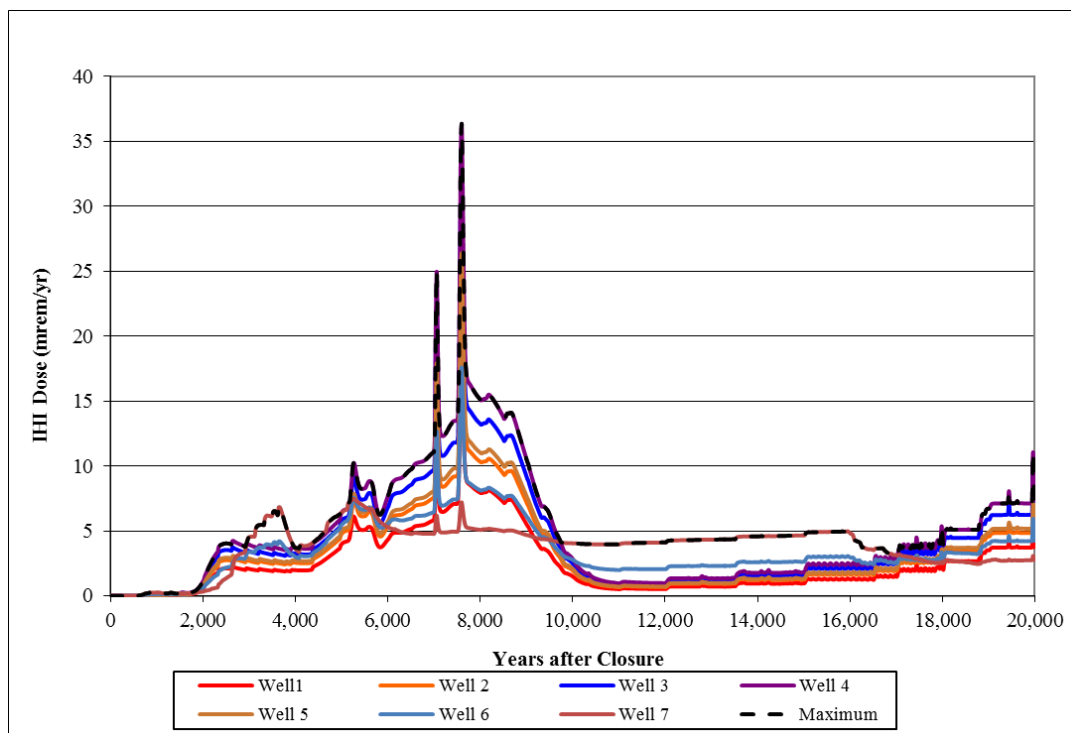


Figure 5.1-30: PORFLOW Model IHI Well Dose Time Histories

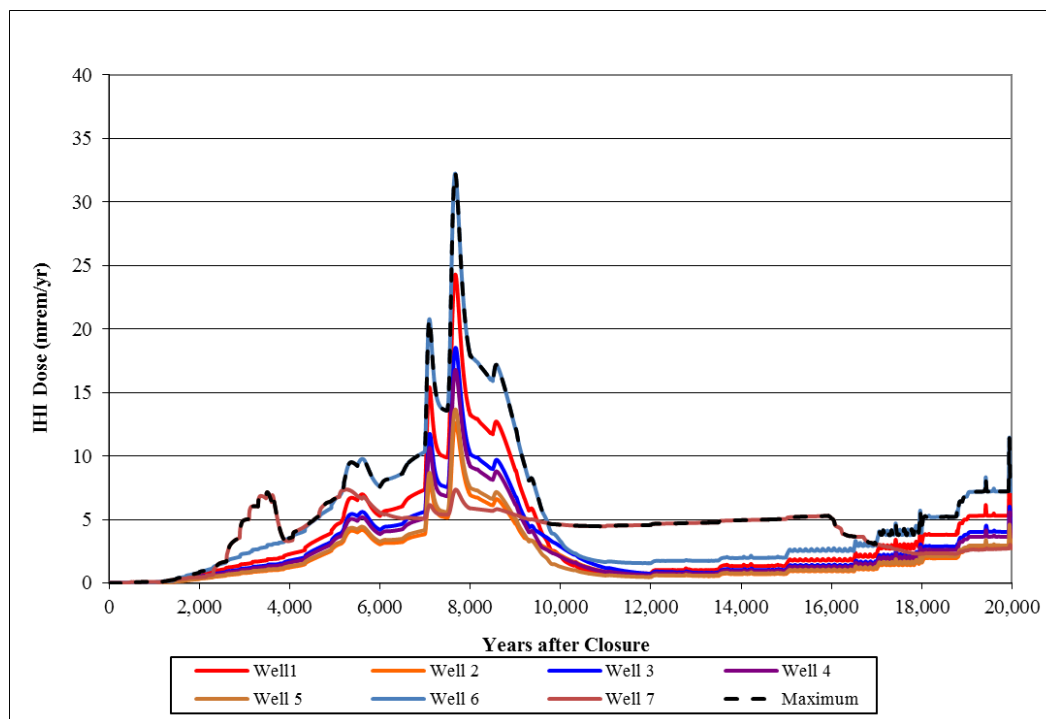


Figure 5.1-31: GoldSim Model IHI Well Dose Time Histories for the Northern Wells

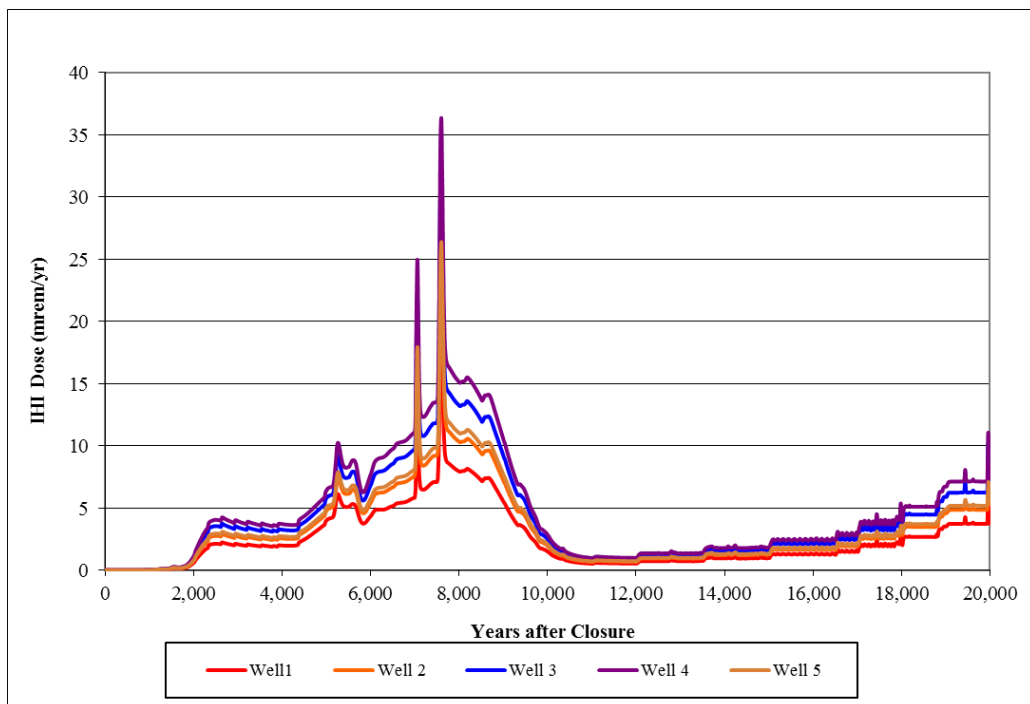


Figure 5.1-32: PORFLOW Model IHI Well Dose Time Histories for the Northern Wells

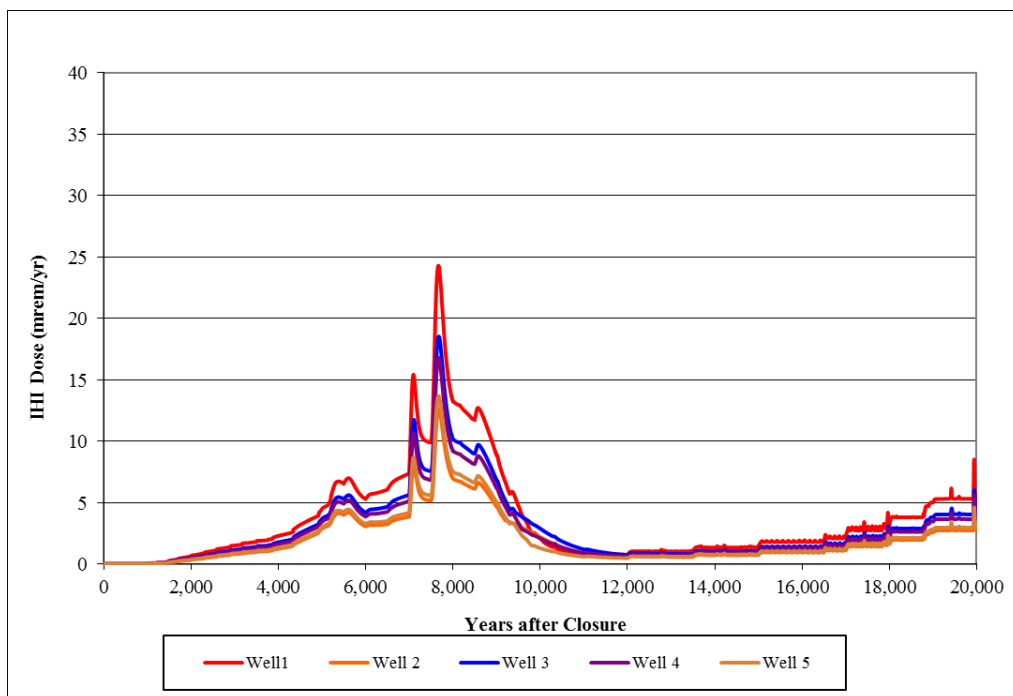


Figure 5.1-33: GoldSim Model IHI Well Dose Time Histories for the Southern Wells

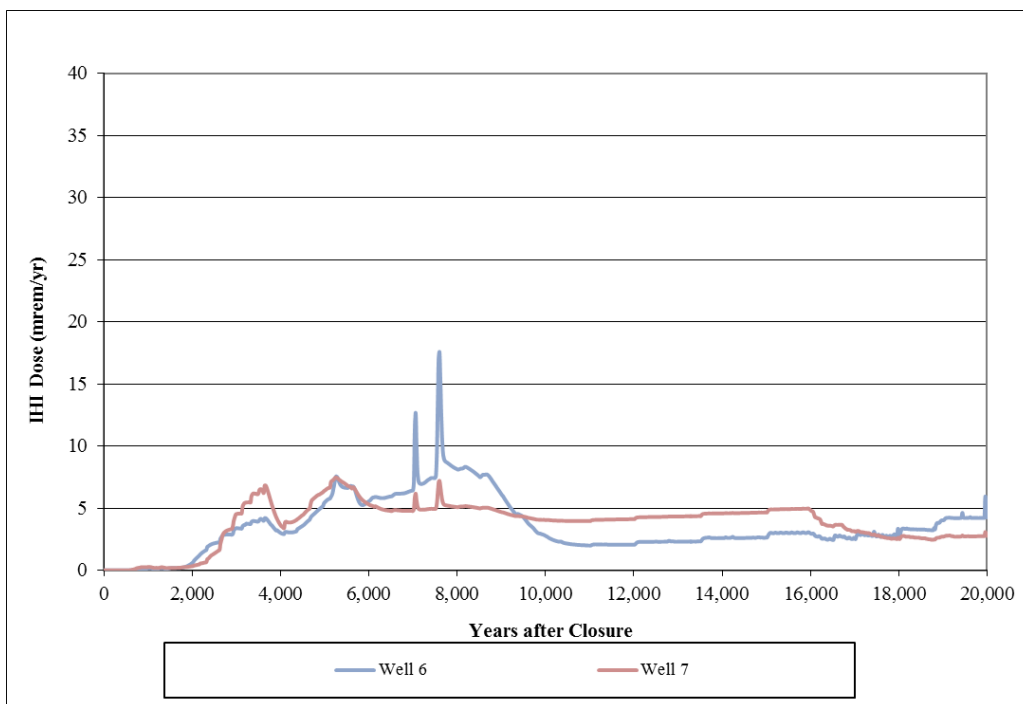


Figure 5.1-34: PORFLOW Model IHI Well Dose Time Histories for the Southern Wells

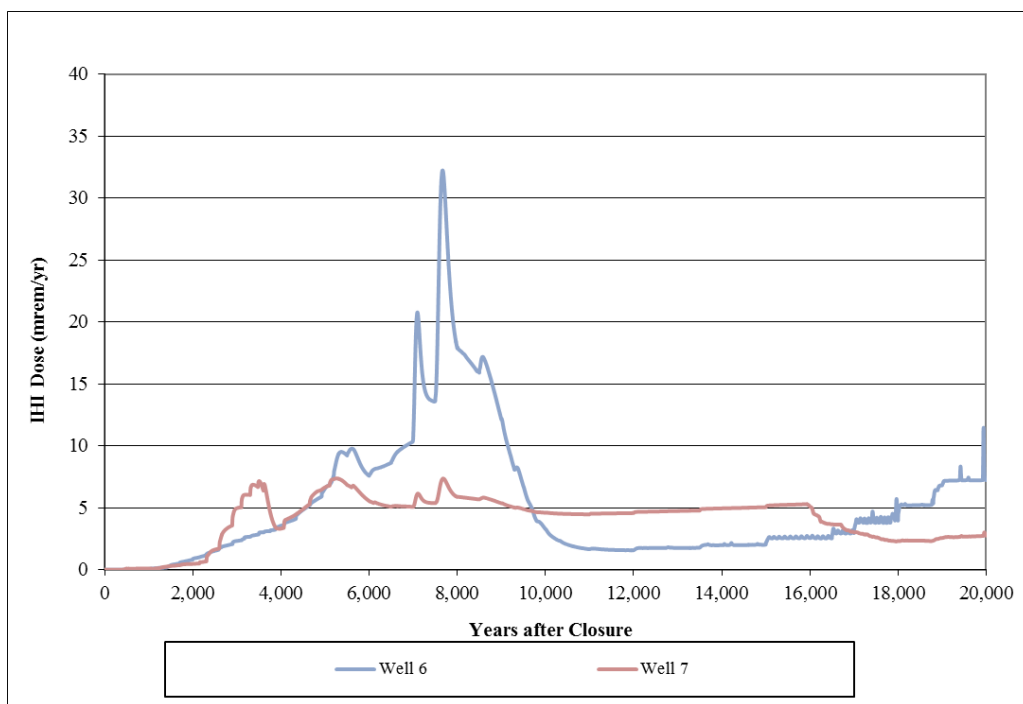
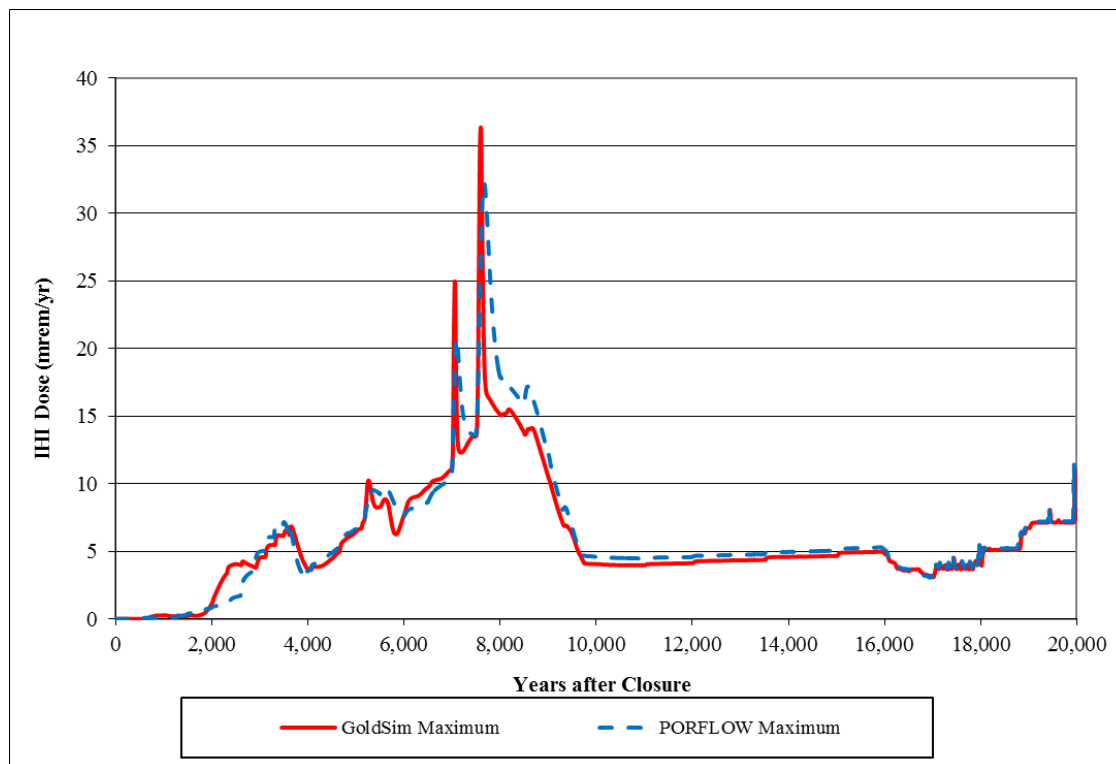


Figure 5.1-35: GoldSim and PORFLOW Model Maximum IHI Well Dose Time Histories



5.2 Benchmarking Conclusion

The benchmarking analysis described in Section 5.1, presents comparisons between SDF PORFLOW Model radionuclide releases to the saturated zone and releases produced by the GoldSim-based abstraction of the PORFLOW model. The comparisons show similarities in trends that indicate that the SDF GoldSim Model mixing-cell network that simulates the engineered barrier and unsaturated zone can provide a good approximation of the SDU radionuclide releases to the saturated zone. In the SDF GoldSim Model, the releases of radionuclides from the SDU abstraction model are applied as boundary conditions to the saturated zone abstraction model. The saturated zone abstraction model is based on a one-dimensional analytical solution (GoldSim pipe-model element) used in conjunction with a Green's Function based GoldSim plume function that evaluates the influence horizontal and vertical transverse dispersion on plume attenuation. The product of the pipe-element solution and the plume function define the concentrations at the 100-meter boundary.

A comparison of the 100-meter boundary concentrations produced by the SDF GoldSim Model with the concentrations generated by the SDF PORFLOW Model, as presented in Section 5.1.2, show that the SDF GoldSim model reproduces the trends found in the PORFLOW model results. The concentrations generated at the 100-meter boundary, are used by the GoldSim model dose-calculator to evaluate dose-based exposure to the MOP. The comparisons between GoldSim and PORFLOW model generated total-dose levels and the radionuclide dose contributions from species dominating the results, presented in Section 5.1.3, show a good match in trends, A

similar comparison of dose results for the IHI analysis, presented in Section 5.1.4 also show a good match in trends for the maximum total dose. Results for individual IHI wells are not as consistent as the maximum dose (from any well) values, but the trends are still similar (see Section 5.1.4). Based upon these assessments it is concluded that uncertainty and sensitivity analyses conducted using Version 4.101 of the SDF GoldSim Model are expected to be representative of the SDF conceptual model for the SA Evaluation Case.

6.0 REFERENCES

Note: References identified as (Copyright) were used in the development of this SDF GoldSim Model Document, but are protected by copyright laws. No part of the publication may be reproduced in any form or by any means, including photocopying or electronic transmittal, without permission in writing from the copyright owner.

B-SQP-C-00002, Hommel, S., *Software Quality Assurance Plan for GoldSim© for the Savannah River Site's Liquid Waste Program*, Savannah River Site, Aiken, SC, Rev. 0, April 23, 2012.

B-SQP-C-00003, Lester, B., *Software Quality Assurance Plan for ReadPORFLOWData.dll for the Savannah River Site's Liquid Waste Program*, Savannah River Site, Aiken, SC, Rev. 2, June 2013.

GTG-2010c (Copyright), *GoldSim User's Guide, Volumes 1 & 2*, GoldSim Technology Group LLC, Issaquah, WA, January 2010.

GTG-2010d, (Copyright), *User's Guide, Probabilistic Simulation Environment, Version 10.5, Volumes 1 & 2*, GoldSim Technology Group LLC, Issaquah, WA, December 2010.

GTG-2010e, (Copyright), *GoldSim User's Guide, GoldSim Containment Transport Module, Version 6.0*, GoldSim Technology Group LLC, Issaquah, WA, December 2010.

ML073510127, *Recommended Site-Specific Sorption Coefficients for Reviewing Non-High-Level Waste Determinations at the Savannah River Site and Idaho National Laboratory*, U.S. Nuclear Regulatory Commission, Washington DC, October 2007.

SRNL-STI-2009-00473, Kaplan, D.I., *Geochemical Data Package for Performance Assessment Calculations Related to the Savannah River Site*, Savannah River Site, Aiken, SC, Rev. 0, March 15, 2010.

SRNL-STI-2010-00493, Seaman, J.C. and Kaplan, D.I., *Chloride, Chromate, Silver, Thallium, and Uranium Sorption to SRS Soils, Sediments, and Cementitious Materials*, Savannah River Site, Aiken, SC, Rev. 0, September 29, 2010.

SRNL-STI-2010-00667, Almond, P.M., and Kaplan, D.I., *Distribution Coefficients (K_d) Generated from a Core Sample Collected from the Saltstone Disposal Facility*, Savannah River Site, Aiken, SC, Rev. 0, April 29, 2011.

SRNL-STI-2011-00011, Kaplan, D.I., *Estimated Neptunium Sediment Sorption Values as a Function of pH and Measured Barium and Radium K_d Values*, Savannah River Site, Aiken, SC, Rev. 0, January 23, 2011.

SRNL-STI-2011-00672, Almond, P.M., et al., *Variability of K_d Values in Cementitious Materials and Sediments*, Savannah River Site, Aiken, SC, Rev. 0, February 2012.

SRNL-STI-2012-00769, Kaplan, D.I. and Dien, L., *Solubility of Technetium Dioxides (TcO₂-c, TcO₂·1.6H₂O and TcO₂·2H₂O) in Reducing Cementitious Material Leachates: A Thermodynamic Calculation*, Savannah River Site, Aiken, SC, Rev. 1, February 1, 2013.

SRNL-STI-2013-00280, Jordan, J.M. and Flach, G.P., *PORFLOW Modeling Supporting the FY13 Saltstone Special Analysis*, Savannah River Site, Aiken, SC, Rev. 0, September 29, 2010.

SRR-CWDA-2009-00017, *Performance Assessment for the Saltstone Disposal Facility at the Savannah River Site*, Savannah River Site, Aiken, SC, Rev. 0, October 29, 2009.

SRR-CWDA-2011-00178, *Saltstone Disposal Facility Stochastic Fate and Transport Model*, Savannah River Site, Rev. 1, Aiken, SC, January 10, 2012.

SRR-CWDA-2013-00058, Hommel, S., *Dose Calculation Methodology for Liquid Waste Performance Assessments at the Savannah River Site*, Savannah River Site, Aiken, SC, Rev. 0, May 2013.